Universidade de Brasília – UnB
Instituto de Geociências – IG
Pós-Graduação em Geologia

Dissertação de Mestrado
Área de Concentração: Geologia Regional

PETROLOGIA E GEOQUÍMICA DOS BASALTOS DA FORMAÇÃO PARAUAPEBAS: IMPLICAÇÕES PARA O AMBIENTE TECTÔNICO DA BACIA GRÃO PARÁ, PROVÍNCIA DE CARAJÁS.

Discente: Pedro Luiz Gomes Martins

Orientadora: Profa: Dra. Catarina Labouré Bemfica Toledo

Co – orientadora: Profa: Dra. Adalene Moreira Silva

Brasília, 2017

Pedro Luiz Gomes Martins

PETROLOGIA E GEOQUÍMICA DOS BASALTOS DA FORMAÇÃO PARAUAPEBAS: IMPLICAÇÕES PARA O AMBIENTE TECTÔNICO DA BACIA GRÃO PARÁ, PROVÍNCIA DE CARAJÁS.

Dissertação de mestrado elaborada junto ao curso de Pós-Graduação em Geologia (Área de concentração em Geologia Regional), Instituto de Geociências, Universidade de Brasília, como requisito parcial para a obtenção do título de Mestre em Geologia.

Orientadora: Prof. Dra. Catarina L.B. Toledo

Co-orientadora: Profa. Dra. Adalene Moreira Silva

Banca examinadora:

Prof. Dra. Catarina L.B. Toledo (Presidente)

Prof. Dr. Gergely Andrés Julio Szabó (IGC-USP)

Prof. Dr. César Fonseca Ferreira Filho (IG-UnB)

Prof. Dr. Elton Luiz Dantas (IG-UnB) (Suplente)

Brasília, 2017

FICHA CATALOGRÁFICA

Martins, Pedro Luiz Gomes

Petrologia e geoquímica dos basaltos da Formação Parauapebas: Implicações para o ambiente tectônico da Bacia Grão Pará, Província de Carajás, 2016.

Nº de páginas: 105

Área de concentrção: Geologia Regional

Orientadora: Catarina Labouré Bemfica Toledo

"*There are only two ways to live your life. One is as though nothing is a miracle. The other is a though everything is a miracle"*

Albert Einstein

AGRADECIMENTOS

Agradeço inicialmente ao Instituto de Geociências representado aqui pelos professores e funcionários e à Universidade de Brasília pela oportunidade de realizar este trabalho, bem como o apoio ao longo de todo o curso de mestrado.

Agradeço em especial às Profas. Dr. Catarina L. B. Toledo e Adalene Moreira Silva (minhas orientadoras e amigas) pela convivência, orientação, apoio e dedicação ao meu aprendizado nos últimos anos, horas de discussões geológicas e conversas casuais que possibilitaram a criação de uma relação de amizade, respeito e companheirismo.

Aos Profs. Dr. Farid Chemale Jr e João Orestes S. Santos pelas contribuições a este trabalho e pelas enriquecedoras discussões geológicas.

Ao CNPQ pela concessão da Bolsa de mestrado e pelos auxílios à pesquisa concedidos tanto durante as etapas e usos de laboratórios, a Vale. S.A pelo apoio nas etapas de campo, coleta de material e no custeio das análises químicas.

Não esquecendo ainda dos amigos, especialmente Darielton, Thiago Ribeiro, Marcones Michel, Cleiton Neves, Jader Alves, Victor Garcia, Eduardo Mansur, Rafaela Roma e Alisson que aturaram semanas de ausência, dias de sono e noites de insônia durante todos esses últimos anos e puderam impulsionar e motivar a conclusão desta fase de minha vida.

Finalmente agradeço a minha mãe (Ana Maria), meu sobrinho (Kauã Lucas) e minha noiva (Thássia Castro) pelo apoio e amor incondicional, respeito, confiança e amizade que tornaram a jornada mais leve e sem os quais não seria possível a realização de mais esta etapa de minha vida. Dedico a vocês, juntamente com meu falecido pai (Luciano Martins), meu eterno amigo (Gabriel Portela) e minha orientadora (Catarina), esta dissertação de mestrado.

Resumo A Formação Parauapebas constitui uma unidade extrusiva neoarqueana e representa uma importante atividade vulcânica, predominantemente máfica, do distrito Serra Norte na Província Mineral de Carajás, Pará. Inserida na sequência metavulcanossedimentar do Grupo Grão Pará (Domínio Carajás), os basaltos e basaltos andesíticos, tipos mais abundantes da Formação Parauapebas, ocorrem em sucessões de extensos derrames de lavas maciças e amigdaloidais. O estudo dos testemunhos de sondagem de nove furos estratigráficos que interceptam rochas basálticas no corpo N4WS (Serra Norte) demonstrou que estas rochas atingem pelo menos 369 m de espessura, nos quais foram identificados 11 ciclos marcados por bases maciças e topos com amígdalas e zonas de espilitização. Os basaltos são verde escuros, afaníticos, finos, hipocristalinos ou hipovítreos. Apresentam textura ígnea preservada sendo comumente intergranular ou intersetal e, em alguns domínios, microporfiríticos. Seus constituintes primários essenciais são plagioclásio (An $_{40\text{-}55}$) e augita ($WO_{média}$ = 37,7 %; $EN_{média}$ = 41,3 %; $FS_{média}$ = 21,0 %) e os acessórios são titanita, ilmenita, pirita e magnetita. A albita (An $_{0,5\text{-}8,4}$), Mg- clorita (brunsvigita), Fe-epidoto, quartzo e calcita ocorrem como fases secundárias, sendo interpretadas como produto de alteração hidrotermal de fundo oceânico e/ou metamorfismo incipiente. Em geral, as rochas vulcânicas estudadas destacam-se pelo conteúdo de SiO_2 entre 51,12 e 55,26 %, teores elevados de álcalis (4,70 – 7,50 %) com teores de K_2O entre 1,23 e 2,81%, TiO_2 (<1,0 %) e MgO e FeO entre 4,38 – 7,38 % e 7,02 - 12,35 %, respectivamente. Nos diagramas classificatórios, as amostras situam-se no campo dos basaltos andesíticos, na transição da série toleítica e calcialcalina. Apresentam, relativo aos valores do condrito e manto primitivo, anomalias negativas acentuadas de Nb (Nb/Nb* = 0,05 – 0,69) e Ti (Ti/Ti* = 0,31 – 0,51), enriquecimento em elementos terras-raras leves (La/Yb_{cn} = 4,00 - 7,58; La/Sm_{cn} = 2,83 – 4,09), distribuição plana de elementos terras-raras pesados (Gd/Yb_{cn} = 1,14 – 1,54) e anomalias negativas discretas de Eu (Eu/Eu* = 0,58 – 0,97). Os dados obtidos para o sistema Sm-Nd demonstram idades-modelo entre 3,02 e 3,36 Ga, com $\varepsilon Nd_{(t)}$ negativo variando entre -1,53 a -4,11, indicando que a contaminação crustal tem papel fundamental na composição química das rochas estudadas. Os dados de SHRIMP U-Pb em zircão demonstram idades de cristalização magmática de 2749 ± 6,5 e 2745 ± 5 Ma para as rochas vulcânicas máficas. Os basaltos da Formação Parauapebas foram formados, provavelmente, em um ambiente intraplaca continental sem influência de zonas de subducção. Embora este vulcanismo possa ter sido originado pela abertura de uma bacia *back-arc* continental, a inexistência de rochas plutônicas típicas de ambiente de arcos magmáticos, contemporâneas com o magmatismo da Bacia Grão-Pará, não favorecem esta interpretação. Portanto, a Bacia Grão-Pará provavelmente foi formada em regime divergente relacionado a um ambiente do tipo *rift* intracontinental por volta de 2,75

Ga, fechado posteriormente por processos colisionais ocorridos, provavelmente, no Neoarqueano. Este processo de rifteamento pode ser associado a um *slab breakoff* relacionado a um relaxamento da orogênese mesoarqueana (Colisão Rio Maria-Carajás).

Palavras-chave: Província Mineral de Carajás; Assinatura geoquímica e isotópica de basaltos arqueanos; Formação Parauapebas.

Abstract *The Parauapebas Formation constitutes a neoarquean extrusive unit and represents an important predominantly mafic, volcanic activity of the Serra Norte district in the Carajás Mineral Province, Pará. The basalts and basaltic-andesites of the Grão Pará Group (Carajás Domain) occur in extensive succession of massive or amygdaloidal lava flows with at least 370 m in thickness. The study of nine drill cores showed that basaltic rocks reached at least 369 m in thickness, in which 11 cycles marked by massive bases and tops with amygdaloidal and spilitization zones. The basalts are grayish green amygdaloidal, porphyritic, aphanitic or fine-grained, and hypocrystalline. The primary igneous textures are largely amygdaloidal, intergranular and intersertal and rarely microporphyritic. The primary mineral assemblages consist predominantly of plagioclase (An $_{40-55}$) and augite ($WO_{average}$ = 37.7 %; $EN_{average}$ = 41.3 %; $FS_{average}$ = 21.0 %), and the mineral accessories are titanite, ilmenite, pyrite and magnetite. Albite, chlorite (brunsvigite), Fe-epidote, quartz and calcite are the main secondary minerals, being interpreted as products of seafloor hydrothermal alteration and/or sub-greenschist metamorphism. Generally, the studied volcanic rocks are characterized by SiO_2 contents between 51.12 and 55.26%, high alkali contents (4.70 - 7.50%) with K_2O contents between 1.23 and 2.81 %, TiO_2 (<1.0%) and MgO and FeO between 4.38 - 7.38% and 7.02 - 12.35%, respectively. In the classificatory diagrams, the samples plot into the basaltic andesite field, and the transitional and calc-alkaline fields. The primitive mantle normalized multi-element spiderdiagram of major and trace, and chondrite normalized rare earth elements diagrams, showed negative anomalies of Nb (Nb / Nb * = 0,05 - 0,69) and Ti (Ti / Ti * = 0,31 - 0,51), enrichment in rare earth elements (La / Yb_{cn} = 4.00 - 7.58; La / Sm_{cn} = 2.83 - 4.09), flat distribution of heavy rare earth elements (Gd / Yb_{cn} = 1,14 - 1,54) and moderate negative Eu anomalies (Eu / Eu * = 0.58 - 0.97). The data obtained for the Sm-Nd system demonstrate model ages between 3.02 and 3.36 Ga, with negative ℇNd (t) ranging from -1.53 to -4.11, indicating that crustal contamination plays a fundamental role in the geochemistry of the studied rocks. SHRIMP zircon U–Pb dating indicates the crystallization ages of 2749 ± 6.5 and 2745 ± 5 Ma for volcanic mafic rocks. The Parauapebas Formation basalts were most likely produced within an intraplate tectonic setting, rather than in a subduction environment. Although this volcanism could be originated by the opening of a back-arc continental basin, a rift continental setting is more plausible on the basis of regional geology. Therefore, the Carajás Basin likely formed in an extensional regime related to the continental rift setting at ca. 2.75 Ga and later closed possibly by colisional process at the Neoarchean. The rifting process could be associated to a slab breakoff related to the Rio Maria-Carajás Collision.*

Keywords: *Carajás Mineral Province, geochemical and isotopic fingerprints of archean basalts; Parauapebas Formation.*

SUMÁRIO

ÍNDICE DE FIGURAS

ÍNDICE DE TABELAS

CAPÍTULO I – INTRODUÇÃO

1.1. Apresentação e justificativa

As investigações em terrenos arqueanos antigos fornecem importantes informações a respeitos da evolução da litosfera, atmosfera, hidrosfera e biosfera da Terra primitiva. Os avanços no conhecimento dos terrenos arqueanos também têm sido fundamentais para o estudo da gênese dos depósitos minerais a eles associados e fornecem subsídios para a exploração mineral nestes terrenos. (Huston *et al*. 2010).

Existem cerca de 35 crátons arqueanos espalhados pelo mundo (p. ex., Bleeker, 2003) e para compreender como estes crátons foram construídos e amalgamados é fundamental entender o ambiente tectônico no qual as sequências vulcanossedimentares arqueanas se desenvolveram. Embora existem muitas dúvidas na compreensão do ambiente geodinâmico atuante nos primórdios da evolução do planeta, há atualmente consenso de que a tectônica de placas atuou desde o neo-mesoarqueano (Dilek & Polat, 2008; Furnes *et al*., 2015; Smithies *et al*. 2005). Apesar das diferenças litológicas existentes entre os terrenos arqueanos e fanerozóicos, tais como abundância de komatiitos e formações ferríferas nos terrenos mais antigos, as assinaturas dos processos tectônicos ainda estão bem preservadas no arqueano. As diferenças litológicas observadas resultam provavelmente do elevado gradiente geotérmico e do baixo conteúdo de oxigênio atmosférico durante o Arqueano. Desta forma, o ambiente geodinâmico das sequências vulcanossedimentares arqueanas pode ser interpretado em um contexto de tectônica de placas moderna com auxílio da assinatura geoquímica e isotópica das rochas vulcânicas (Dilek & Furnes, 2011, Furnes *et al*., 2015).

Neste contexto, o maior e o mais bem preservado segmento arqueano do Cráton Amazônico, a Província Mineral de Carajás, se torna uma área de grande interesse de estudo para a compreensão geodinâmica da formação e amalgamação deste importante cráton arqueano com os demais adjacentes.

Inserida no Domínio Carajás, porção norte da Província Mineral de Carajás, a sequência vulcanossedimentar neoarqueana do Grupo Grão Pará é composta pela Formação Parauapebas na base, constituída por rochas vulcânicas máficas e intercalações de rochas vulcânicas félsicas, seguida pelos jaspilitos da Formação Carajás, sobrepostos pelas rochas vulcânicas, sedimentares clásticas e químicas da Formação Igarapé Cigarra. O topo desta sequência é formado por sedimentos clásticos metamorfizados em baixo grau da Formação Águas Claras, também conhecida como Grupo Rio Fresco (Macambira, 2003).

Nas últimas décadas, os aspectos estratigráficos, estruturais e geocronológicos do Grupo Grão Pará foram investigados por vários pesquisadores (Gibbs *et al*., 1986, Dardenne *et al*., 1988, Zuchetti, 2007). Entretanto, poucos trabalhos foram dedicados ao estudo dos aspectos petrogenéticos e à investigação do ambiente tectônico de formação das sequências vulcânicas basais do Grupo Grão Pará.

O enfoque principal desta dissertação consiste, portanto, na utilização de dados geológicos, geoquímicos e isotópicos de alta precisão para propor o ambiente tectônico de formação das rochas vulcânicas da Formação Parauapebas. Pretende-se assim contribuir para a compreensão do magmatismo e dos processos geológicos envolvidos na evolução da Bacia Grão-Pará.

1.2. Localização da área e acesso

A área de estudo localiza-se no distrito mineiro Serra Norte, província mineral de Carajás – PA, especificamente nos depósitos de ferro N4WS e N5S. O município de Parauapebas, localizado a aproximadamente 550 km a sudoeste de Belém (Fig. I), serve como referência e apoio logístico. Os depósitos de ferro N4 e N5 fazem parte dos depósitos pertencentes à Companhia Vale do Rio Doce (CVRD), situados na parte norte da serra dos Carajás e nomeados de N1 a N9. O acesso pode ser feito pela rodovia PA-150, que liga Belém a Marabá e Cuiabá (MT), seguindo-se pela Trans-Carajás (PA-275) até o núcleo urbano de Carajás e, depois, para os depósitos de ferro, numa extensão de aproximadamente 700 km (Fig. II). O aeroporto de Carajás (CKS) é servido diariamente por voos diretos de/para Belém, Brasília, Belo Horizonte e para cidades menores do sul e do sudeste do Pará.

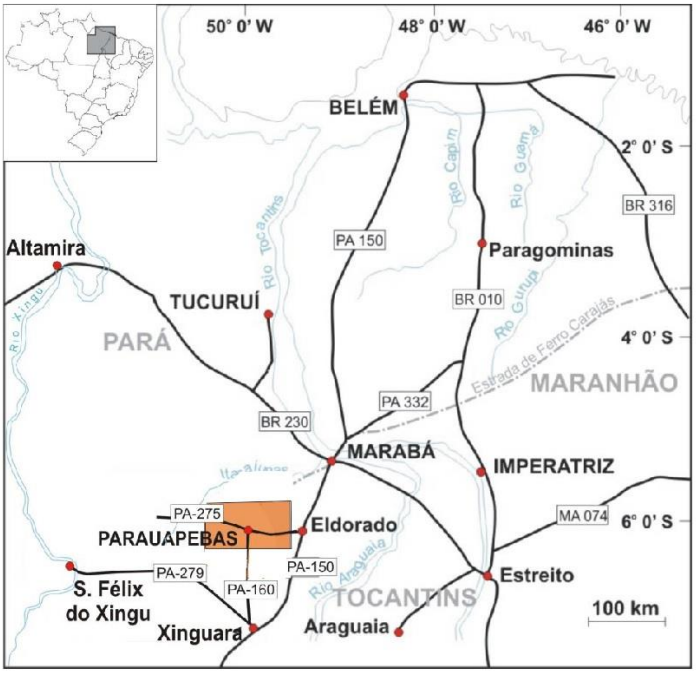

***Figura I**. Mapa de localização e principais vias de acesso terrestre da região da Serra de Carajás, marcada pelo polígono de preenchimento laranja (modificado da carta do Brasil ao Milionésimo, IBGE, 1999).*

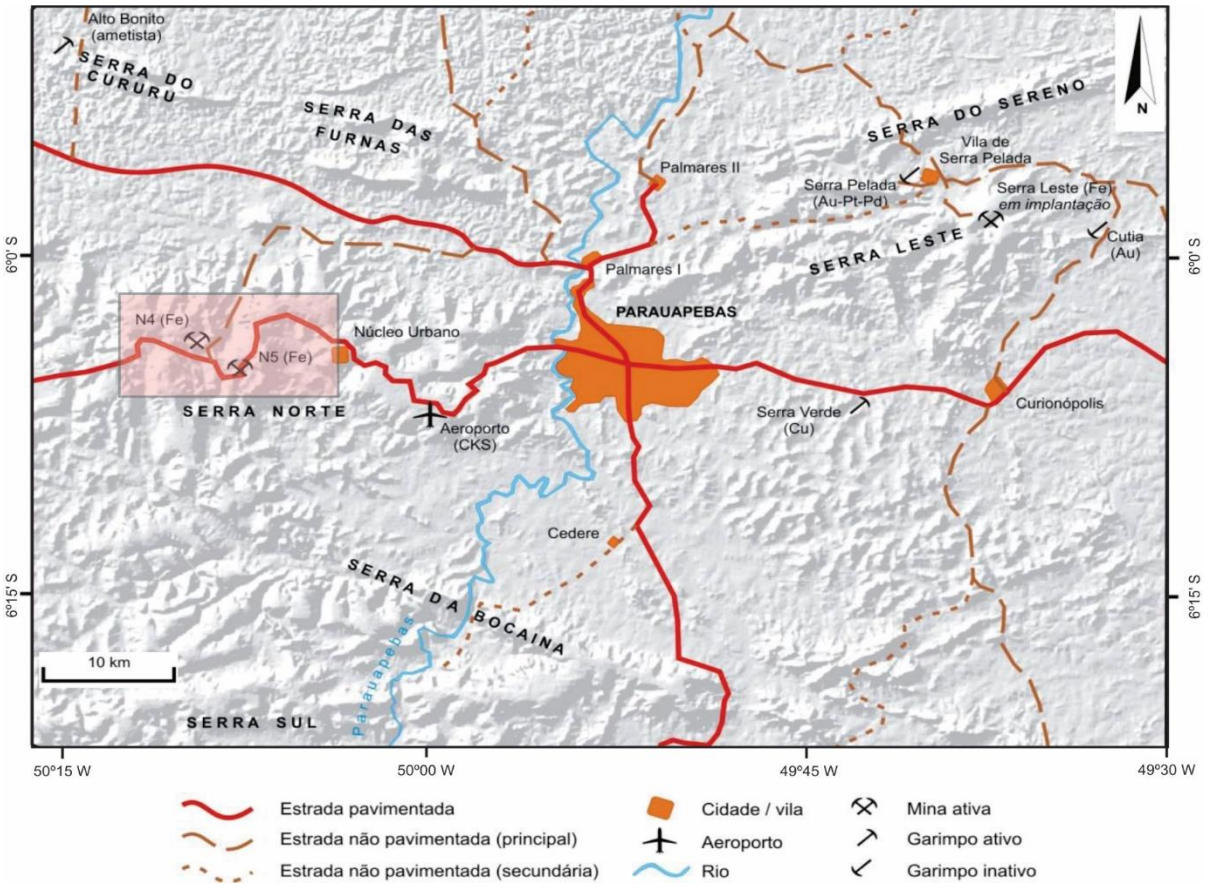

***Figura II**. Fusão do mapa planimétrico de parte da Serra de Carajás com imagem de relevo sombreado (SRTM), mostrando as principais feições geomorfológicas, acessos e localidades (modificado de Tavares, 2015). O polígono marcado representa as regiões da área de estudo, especificamente sobre os corpos N4 e N5.*

1.3. Objetivos

O propósito do presente trabalho está centrado na caracterização das rochas vulcânicas máficas da Formação Parauapebas e no estudo do ambiente tectônico de formação da Bacia Carajás, a partir da integração de dados geológicos, geoquímicos e isotópicos das rochas vulcânicas, base do Grupo Grão Pará. Os objetivos específicos incluem:

i. Estudo das relações de contato entre os diferentes tipos de rochas vulcânicas e sedimentares do Grupo Grão Pará, buscando estabelecer as relações estratigráficas originais, a partir da descrição de 9 furos de sondagem nos corpos N4WS e N5S;

ii. Caracterização petrográfica das rochas vulcânicas e plutônicas com o intuito de identificar as estruturas e a mineralogia primária, bem como caracterizar as assembleias metamórficas/hidrotermais secundárias;

iii. Estudo da assinatura geoquímica das rochas vulcânicas, visando o entendimento do ambiente tectônico de deposição dessa sequência vulcanossedimentar;

iv. Identificação, caracterização e datação dos diferentes episódios de geração de magmas na bacia, por meio da geoquímica isotópica U-Pb, Sm-Nd e Sr-Sr.

1.4. Materiais e métodos de trabalho

Inicialmente, manteve-se um enfoque em revisões bibliográficas e estudos complementares a fim de aprofundar o conhecimento concernente ao contexto geológico da Província Carajás, à geodinâmica presente no arqueano e diferentes aspectos relacionados as sequências vulcanossedimentares arqueanas de Carajás. A caracterização das rochas vulcânicas e sedimentares do Grupo Grão-Pará, assembleias primárias e secundárias, foi efetuada por meio da descrição sistemática de 9 furos de sondagem, assim como estudos petrográficos por microscópio petrográfico, em luz transmitida e refletida, e análises químicas.

O trabalho de campo foi realizado em duas etapas (julho de 2012 e maio de 2013) e consistiu na descrição de testemunhos de sondagem e coleta de amostras de furos de sondagens dos Corpos N4WS e N5S e arredores. O trabalho contou com o apoio da VALE, incluindo discussões sobre o contexto geológico regional e deslocamentos na área.

As amostras deste estudo foram coletadas em testemunhos correspondentes a nove furos de sondagens, distribuídas em três seções na direção EW que seccionam o depósito de N4WS (vide Fig. 2 do artigo em anexo). A amostragem foi realizada sistematicamente a cada dois metros, com amostras representativas de 15 cm, totalizando 1766 amostras (1051 amostras de

jaspilitos, 346 amostras de minério e 369 amostras de basaltos). As amostras foram seccionadas ao meio na laminação para facilitar a análise, sendo que uma parte foi separada para análise geoquímica (XRF, ICP-MS, ICP-AES e Titulação) e a outra metade foi utilizada para medições e aquisição de dados geofísicos. As análises litogeoquímicas foram efetuadas no laboratório ALS Chemex (Canadá). A descrição das técnicas utilizadas nas amostras máficas utilizadas encontram-se no item "3.3. *Whole-rock geochemistry analyses*" do artigo em anexo e os dados analíticos são expressos na Tabela 1 do mesmo.

Algumas amostras foram selecionadas para a confecção de lâminas delgadas e polidas, totalizando 151 lâminas. Este estudo permitiu o reconhecimento das diversas estruturas e texturas, bem como da assembleia mineral primária e secundária, nas rochas da sequência vulcanossedimentar do Grupo Grão-Pará no corpo N4WS e N5S, e inclui lâminas de basalto, gabro (*sill*) e jaspilito. A partir da análise petrográfica foram selecionadas 8 lâminas de seções representativas das rochas máficas para o estudo da química dos minerais. Fichas petrográficas representativas do basalto são apresentadas no Anexo.

As análises de química mineral foram efetuadas por microssonda eletrônica JEOL JXA-8230, em modo de dispersão por comprimentos de onda (WDS – Wavelength-Dispersive Spectrosmetry), no Laboratório de Microssonda Eletrônica da Universidade de Brasília. Os minerais selecionados correspondem a anfibólio, plagioclásio, clinopiroxênio, clorita, magnetita, feldspato potássico, epidoto, calcita. As composições dos minerais primários foram obtidas com a seleção de domínios preservados contendo os minerais ígneos definidos por clinopiroxênio, plagioclásio e feldspato potássico. O tratamento dos dados foi feito por meio de planilha eletrônica Excel e os resultados analíticos encontram-se no Apêndice do artigo. Análises de química mineral em grãos de zircão foram realizadas no *CMCA – Centre for Microscopy, Characterization and Analyses da University of Western Australia*. Os métodos analíticos usados e os resultados encontrados estão expostos, respectivamente, no item 3.2 e na tabela 3 do artigo em anexo.

As análises isotópicas foram desenvolvidas pelo Laboratório de Geocronologia do Instituto de Geociências (IG) da Universidade de Brasília (Sr-Nd) e da *University of Western Australia, UWA*, Austrália (SHRIMP U-Pb). Análises Sm-Nd em rocha total foram desenvolvidas segundo o método descrito por Gioia and Pimentel (2000), obtendo-se três análises (Tabela 4 do artigo). Foram também realizadas duas análises por SHRIMP U-Pb em zircão, e os resultados estão sumarizados na tabela 2. As técnicas utilizadas são descritas nos itens 3.4. "*U-Pb SHRIMP analyses* e 3.5. "*Sr-Nd isotopic analyses*" do artigo em anexo.

1.5. Estrutura da dissertação

Conforme previsto no regulamento do Curso de Pós-graduação em Geologia da Universidade de Brasília, os principais resultados da presente dissertação de mestrado apresentam-se estruturados na forma de artigo intitulado "*Neoarchean continental magmatism in southeastern Amazonian Craton, Brazil: petrography, geochemistry and tectonic significance of basalts from Carajás Basin*", a ser submetido para publicação em periódico com corpo editorial. O artigo é apresentado na forma em que será submetido à revista *Precambrian Research*, mantendo o estilo e formato previstos no periódico. Além disso, a dissertação apresenta uma parte inicial que engloba a apresentação, justificativa, objetivos e materiais e métodos, e uma síntese do conhecimento atual da geologia da Província Mineral de Carajás. Por fim, a última parte da dissertação, é voltada para as considerações finais do trabalho.

CAPÍTULO II – CONTEXTO REGIONAL

2.1. Introdução

Inserido na Plataforma Sul-Americana, o Cráton Amazônico representa uma das mais expressivas áreas no mundo de idade do Arqueano/Proterozóico, estabilizada tectonicamente por volta de 1Ga (Brito Neves & Cordani, 1991). Contido predominantemente no Brasil, estende-se ao norte para os países vizinhos (Venezuela, Guiana Suriname e Guiana Francesa), onde os limites estão encobertos por sedimentos fanerozóicos. A oeste limita-se pela Cadeia Andina e a leste e sudeste limita-se pela Faixa Araguaia, de idade neoproterozóico e relacionada à Orogênese Brasiliana (Fig. III).

A compartimentação tectônica do Cráton Amazônico ainda é tema de amplo debate. Existem duas principais correntes para os modelos evolutivos propostos para o Cráton Amazônico: uma baseada principalmente em geologia estrutural e geofísica, implicando em retrabalhamento crustal das massas continentais aglutinadas no Arqueano e Paleoproterozóico através de orogenias predominantemente ensiálicas (Hasui *et al.* 1984; Costa & Hasui, 1997), a outra baseada em geocronologia e geoquímica isotópica, além da reciclagem de blocos crustais arqueanos que envolve processo de acresção juvenil (Cordani & Brito Neves, 1982; Teixeira *et al*. 1989; Tassinari & Macambira, 2004; Tassinari *et al*. 2000). No entanto, apesar de divergências quanto à posição exata dos seus limites, existe certo consenso quanto à existência de dois blocos tectônicos/geocronológicos distintos na porção oriental do cráton. Um núcleo cratônico majoritariamente arqueano chamado de Província Carajás (ou Amazônia Central), a sul, e a província Transamazonas (ou Maroni-Itacaiúnas), a norte, qual representa uma colagem paleoproterozoica (p.ex. Cordani *et al*, 1984; Teixeira *et al*., 1989; Santos, 2003; Vásquez *et al*., 2008) (Fig. III e IV a).

2.2. Província Mineral de Carajás

A Província Mineral de Carajás (Fig. IV b) é subdividida em dois domínios tectônicos distintos: Domínio Rio Maria ao sul e o Domínio Carajás ao norte, também conhecido como Domínio Itacaiúnas (Araújo *et al*., 1988; Huhn and Santos, 1988; Vasquez *et al*., 2008). Uma zona pouco definida e estudada, conhecida como Subdomínio Transicional, separa o domínio Mesoarqueano Rio Maria e o domínio Neoarqueano formado pelas sequências vulcanossedimentares do Domínio Carajás (Dall'Agnol *et al*., 2006; Feio *et al*., 2013).

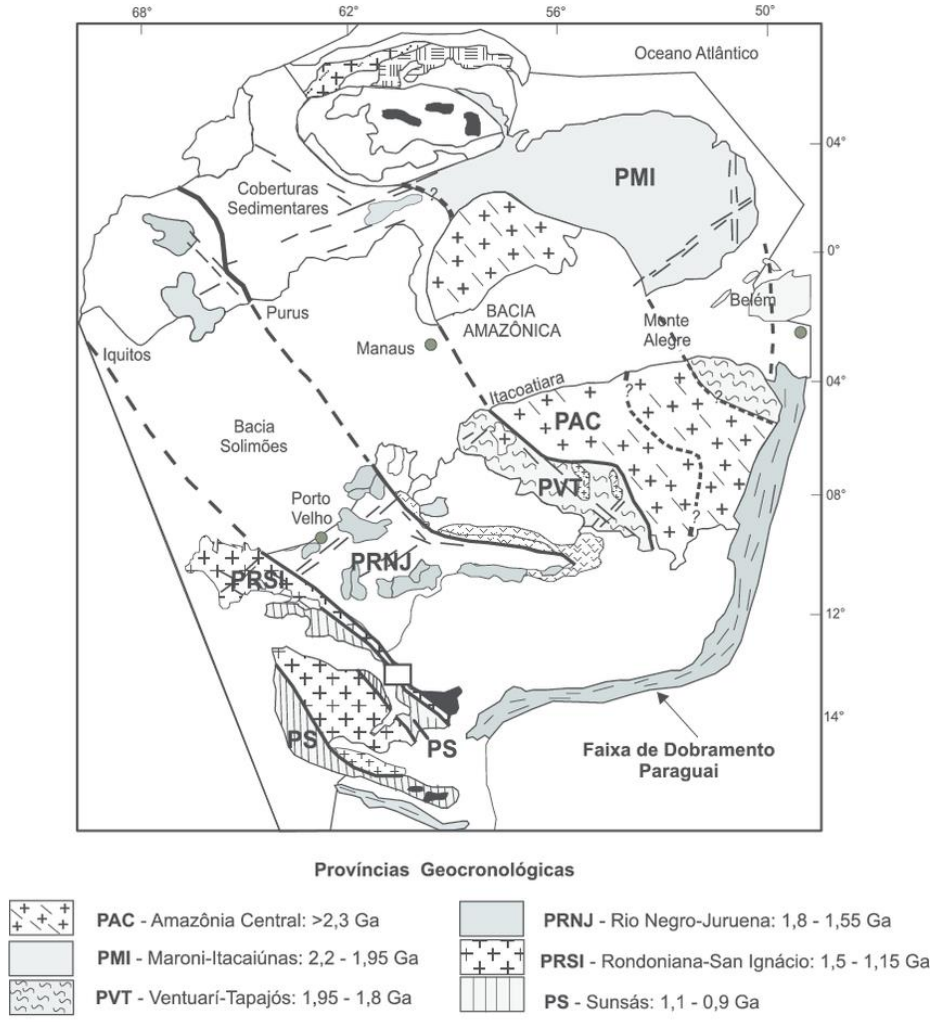

Figura III. *Mapa simplificado o do Cráton Amazônico, destacando sua compartimentação tectônica e a Província Mineral de Carajás dentro da Província Amazônia Central (extraído de Tassinari & Macambira, 2004).*

O Domínio Rio Maria (ou Terreno Granito-*Greenstone* Rio Maria) possui evolução mesoarqueana, caracterizada por uma amálgama de terrenos tipo granito-*greenstone* juvenis, com idades de formação entre 3,05 Ga e 2,82 Ga (DOCEGEO, 1988, Althoff *et al*., 2000; Souza *et al*., 2001; Dall'Agnol *et al*., 2006, dentre outros), constituídos por *greenstone belts*, assembleias do tipo TTG, leucogranodioritos, granitoides de alto Mg e granitos potássicos (Althoff *et al*., 2000; Souza *et al*., 2001; Dall'Agnol *et al*., 2006; Oliveira, *et al.*, 2011; Almeida *et al*., 2011, 2013). Hirata *et al*. (1982) incluíram os *greenstone belts* da região de Rio Maria no Supergrupo Andorinhas, constituído por metabasaltos, intercalações de talco xistos, metatufos, meta*cherts*, formações ferríferas do Grupo Babaçu (unidade inferior), e metapelitos, metapsamitos e metariodacitos do Grupo Lagoa Seca (unidade superior), considerando-os como parte do Complexo Xingu. Posteriormente, o Supergrupo Andorinhas foi individualizado do Complexo Xingu (DOCEGEO 1988, Huhn *et al*. 1988) e datado, fornecendo idades mesoarqueanas (p.ex., 2904 ± 29 Ma; Macambira & Lancelot, 1996). A recente caracterização

de komatiitos com textura spinifex em uma sequência *greenstone belt* dentro do Subdomínio Transicional (Siepierski & Ferreira Filho, 2016) sugere que os terrenos granito-*greenstone* se estendem mais para o norte do que indicado nos mapas regionais anteriores. A estruturação principal do Domínio Rio Maria é um resultado de encurtamento N-S durante processo acrescionário/colisional mesoarqueano, porém influenciado por tectonismo vertical do tipo domos-e-quilhas (Althoff *et al*., 2000).

Já a Domínio Carajás, também conhecido como Cinturão Itacaiúnas (Araújo *et al.*, 1988), é constituído por gnaisses graníticos, granodioríticos e tonalíticos do Complexo Xingu; por granulitos máficos derivados de gabros, piroxenitos, noritos, dioritos e monzodioritos diferenciados e estratificados do Complexo Pium; pelas rochas da sequência vulcanossedimentar do Supergrupo Itacaiúnas, além de complexos máfico-ultramáficos arqueanos, como o Complexo Luanga e Lago Grande (Fig. IV c).

Recentemente, Dall'Agnol *et al*. (2013) propuseram a subdivisão do Domínio Carajás em Bacia Carajás e nos subdomínios Canaã dos Carajás e Sapucaia (conhecido informalmente como Subdomínio Transicional). Os subdomínios de Canaã dos Carajás e Sapucaia compreendem uma região pouco conhecida, intensamente deformada, constituída por rochas granitoides e gnáissicas neoarqueanas, geralmente reunidas no Complexo Xingu (Fig. IV b).

Várias gerações de granitos, com idades e composição distintas, intrudem a Província de Carajás (Fig. IV b, c) e são correlacionados a quatro eventos magmáticos principais. O evento mais antigo é marcado por intrusões graníticas mesoarqueanas (~ 2.96-2.93 Ga e 2.87-2.83 Ga) (Feio & Dall'Agnol, 2012; Feio *et al*., 2013) encontradas no embasamento da Bacia Carajás e interpretadas anteriormente como parte do Complexo Xingu. O magmatismo neoarqueano é marcado por corpos graníticos subalcalinos do tipo A (~2.76-2.73 Ga), contemporâneos à sedimentação do Supergrupo Itacaiúnas, representado pelas suítes Plaquê e Planalto, Complexo Estrela e granito Serra do Rabo (Avelar *et al.* 1999; Barros *et al*., 2009; Dall'Agnol *et al*. 2005; Feio e Dall'Agnol, 2012; Feio *et al.*, 2013; Huhn *et al*. 1999). Intrusões mais novas (~ 2.56 Ga), como os granitos peralcalinos a metaluminosos Old Salobo e Itacaiúnas (Machado *et al*. 1991), estão associadas a magmatismo pouco esxpressivo, também do tipo A, aparentemente concentrado no extremo norte da Província Carajás, ao longo do Cinturão Norte do Cobre; o último evento magmático promoveu a formação de vários plútons graníticos anorogênicos paleoproterozoicos, dentre eles, o Central de Carajás, Young Salobo e Cigano (p.ex. Dall'Agnol *et al*., 2006).

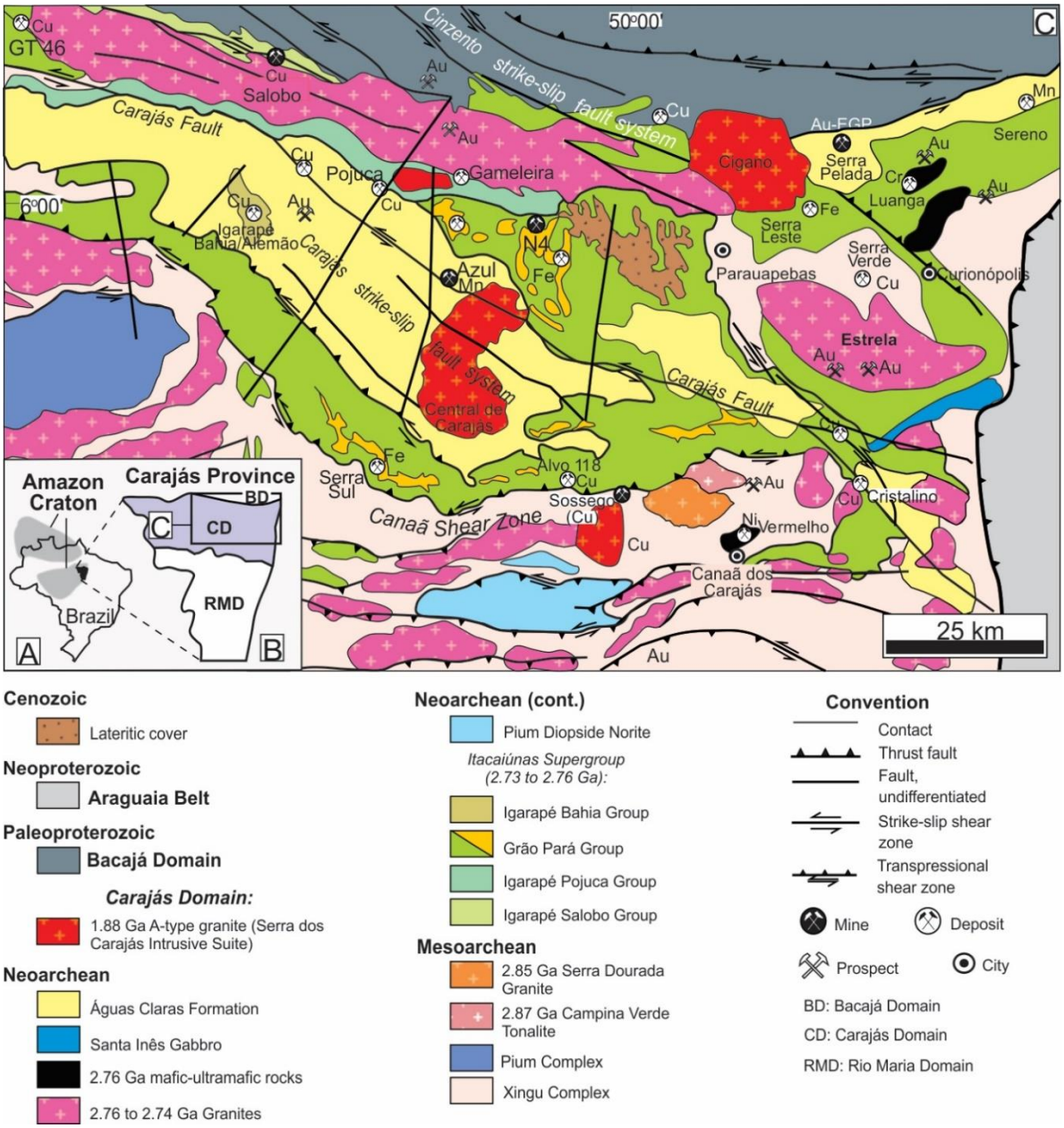

***Figura IV**. a) Localização da Província Carajás no Brasil; b) Localização do Domínio Carajás dentro da Província Carajás; c) Mapa geológico da porção norte, Domínio Carajás, da Província de Carajás (modificado de Vasquez et al., 2008)*

A estrutura dominante da Serra dos Carajás é definida por Beisegel *et al*. (1973) como um sinclinório de aproximadamente 1000 km de comprimento e 100 km de largura, com eixo WNW-ESE. O Cinturão Itacaiúnas (Araújo et al., 1988) é uma faixa de deformação com direção média E-W, que ocorre no extremo norte da Província Carajás, coincidente com o Domínio Carajás (Santos, 2003), e paralelo ao limite com o Domínio Rio Maria, formado na porção norte pelos sistemas transcorrentes Carajás e Cinzento. A Falha de Carajás representa a descontinuidade mais destacada, com cerca de 130 km de comprimento (Pinheiro e Holdsworth 2000), com indicação cinemática predominantemente sinistral.

2.3. Grupo Grão-Pará

A sequência vulcanossedimentar neoarqueana do Grupo Grão Pará (~2.76 Ga; Gibbs *et al*., 1986; Olszewski *et al*., 1989; Machado *et al*., 1991; Trendall *et al*., 1998), localizada na porção norte do Domínio Carajás, é a principal sequência da Bacia Carajás. O Grupo Grão-Pará possui aproximadamente 260 km de comprimento e 70 km de largura, com as rochas vulcânicas cobrindo uma área extensa de aproximadamente 11.000 km^2 (Macambira, 2003). Esta sequência é composta pela Formação Parauapebas na base, constituída por rochas vulcânicas máficas e intercalações de vulcânicas félsicas; seguida pelos jaspilitos da Formação Carajás (Lindenmayer *et al*. 2001; Macambira, 2003; Meirelles, 1986). Existem dúvidas quanto à estratigrafia completa do Grupo Grão Pará: alguns autores defendem a existência de mais duas unidades, uma, essencialmente vulcânica, acima da Formação Carajás, denominada de Igarapé Cigarra (Gibbs *et al*., 1986; Macambira, 2003) e outra no topo do grupo, denominada de Formação Igarapé Boa Sorte (Macambira, 2003). Entretanto, outros autores (Meirelles, 1986, Meirelles e Dardenne, 1991 e Lindenmayer *et al*., 2001) consideram as relações de topo e base das rochas vulcânicas com os jaspilitos como de caráter estrutural, questionando o valor estratigráfico da Formação Igarapé Cigarra, e posicionam o pacote sedimentar, chamado de Igarapé Boa Sorte, na base da Formação Águas Claras, depositada discordantemente sobre o Grupo Grão Pará (Nogueira *et al*., 1994).

Sobre a Formação Parauapebas, há desacordos na literatura (Beisiegel *et al*., 1973; Gibbs *et al*., 1986; Wirth *et al*., 1986; Teixeira & Eaggler, 1994) quanto à terminologia de classificação das rochas (espilitos, basaltos, andesitos, andesitos metabasálticos) e grau de metamorfismo, desde ausente (Lemos e Villas, 1983) até fácies anfibolito (Meireles *et al*., 1984). Essa discrepância existe por conta dos diversos eventos que atuaram nessas rochas em diferentes intensidades, e também por poucas amostras não alteradas analisadas. Entretanto, de forma geral, a Formação Parauapebas é representada por derrames basálticos e basalto andesíticos maciços, amigdaloidas e porfiríticos, associados a riolitos, brechas e tufos vulcânicos (Macambira, 2003). Estudos geoquímicos nas rochas vulcânicas máficas (p.ex. Lemos & Villas,1983; Gibbs *et al*., 1986; Meirelles, 1986; Teixeira & Eggler, 1994) propõem algumas gêneses para este magmatismo: vulcanismo toleítico continental que sofreu contaminação crustal e provavelmente se originou em uma bacia de *rift* continental (Gibbs *et al*., 1986; Olszewski *et al*., 1989), vulcanismo basáltico principalmente shoshonítico que possivelmente ascendeu por um sistema de *rift* em ambiente de crosta continental associado a subducção (Dardenne *et al*., 1988; Zuchetti, 2007), e ainda vulcanismo de andesitos basálticos

cálcio alcalinos em ambiente de arco de ilha associados à zona de subducção (Teixeira & Eggler 1994).

Já a Formação Carajás é constituída por formações ferríferas bandadas de fácies óxidos (jaspilito) quase totalmente transformadas em minério hematítico de até algumas centenas de metros. Está em contato com a Formação Parauapebas e mostra intercalações com as rochas vulcânicas máficas (Macambira, 2003). A formação ferrífera bandada é descrita como jaspilito meso- e microbandado formado por bandas de jaspe e óxidos de ferro, sendo o jaspe caracterizado como um *chert* impregnado por hematita microcristalina (Lindenmayer *et al*., 2001; Macambira, 2003; Figueiredo e Silva, 2004). Além do bandamento composicional, os jaspilitos de Carajás preservam outras estruturas deposicionais, tais como estruturas de escavação e preenchimento (*scour-and-fill*), laminação interna plano-paralela e esferulitos/grânulos de provável origem orgânica (Macambira, 2003). Lindenmayer *et al*. (2001) concluem que os jaspilitos formaram-se por precipitação química em plataformas marginais de águas rasas, em período de calma tectônica e perto de fumarolas com ampla distribuição areal.

Diques e *sills* de gabro e diabásio cortam as unidades anteriormente descritas (Beisiegel *et al*. 1973; Meirelles 1986; Lindenmayer *et al*. 2001; Macambira 2003). A Figura V apresenta uma seção geológica esquemática do corpo N4, da Serra dos Carajás.

A idade do vulcanismo do Grupo Grão Pará é determinada em 2758 ± 39 Ma, por meio de análises U-Pb em zircões de riolitos pertencentes à Formação Parauapebas, feitas por Wirth *et al*. (1986). Esta idade (~2,76 Ga) é ratificada por análises isotópicas por diversos autores (p. ex. Olszewski *et al*., (1989); Machado *et al*., 1991; Trendall *et al*., 1998).

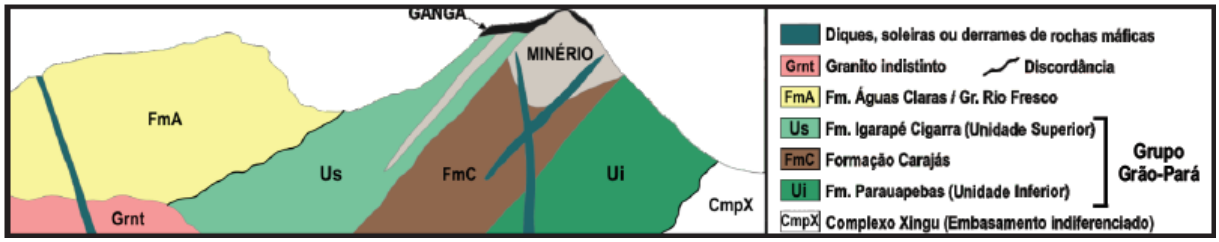

Figura V. *Seção geológica esquemática geral do corpo N4, Serra Norte (modificado de Macambira, 2003).*

2.4. Evolução geotectônico arqueana do nordeste da Província Carajás

A evolução estrutural do Domínio Carajás é atribuída, por muitos autores, ao desenvolvimento de importantes transcorrências e empurrões oblíquos, geradas a partir de encurtamento na direção NE-SW e agrupadas no Cinturão Itacaiúnas (Rosière *et al*., 2006; Tavares, 2015). A formação destas estruturas regionais está relacionada a um suposto orógeno colisional ocorrido entre o final do Neoarqueano e/ou no início do Paleoproterozoico, com reativações tardias por até centenas de milhões de anos após o estágio principal de deformação (Araújo *et al*., 1988, Pinheiro & Holdsworth, 2000). Entretanto, Tavares (2015) sugere que o Cinturão Itacaiúnas se constituiu pela superposição de quatro eventos arqueanos, sendo dois compressivos (Colisão Rio Maria-Carajás, entre 2,87 e 2,83 Ga; inversão da Bacia Carajás, entre 2,68 e 2.63 Ga) e dois extensionais (instalação da Bacia Carajás, por volta de 2,76 Ga; fragmentação do paleocontinente Carajás, entre 2,61 e 2,54 Ga) que produziram e/ou reativaram estruturas subparalelas, na direção média E-W.

A colisão Rio Maria-Carajás se deu entre 2,87 e 2,83 Ga (p. ex. Machado *et al*., 1991; Feio *et al*., 2013), representando a colisão das associações juvenis do Domínio Rio Maria com a margem ativa do paleocontinente ao qual a região do Domínio Carajás pertencia à época. A aglutinação dessas duas porções se tornou estável por volta de 2,83 Ga, idade a partir da qual cessam as atividades tectonotermais mesoarqueanas. Tavares (2015) considera esta colisão como o principal evento mesoarqueno e responsável pela estruturação principal na direção E-W das associações e estruturas mesoarqueanas. Entretanto, este assunto ainda está aberto. Dall'Agnol *et al*. (2013) defendem que parte do extremo sul do Domínio Carajás é composto por litotipos que apresentam diversas características geoquímicas e isotópicas correlacionáveis ao Domínio Rio Maria, porém tectonicamente retrabalhados. Para estes autores, entretanto, a deformação principal naquelas unidades é do Neoarqueano, pois consideram as zonas de cisalhamento contemporâneas à granitogênese do tipo A de 2,76 a 2,71 Ga, como proposto por Barros *et al*. (2009).

Entre 2,76 e 2,70 Ga, o Domínio Carajás passou por um novo período de atividade geotectônica, marcado pela deposição do Supergrupo Itacaiúnas, denominado assim por DOCEGEO (1988) e por magmatismo bimodal (máfico-ultramáfico e félsico, semelhante ao tipo-A). Ainda não há consenso sobre a tectônica de abertura da bacia que proporcionou a deposição do Supergrupo Itacaiúnas. Sabe-se que a deposição das sequências vulcanossedimentares se deu em ambiente dominantemente marinho, entretanto é discutido se a tectônica de abertura da bacia foi relacionada a um *rift* intracontinental (p. ex., Gibbs *et* al.,

1986 e Tavares, 2015) ou associada a um arco magmático ativo (p. ex. Meirelles & Dardenne, 1991; Lobato *et al*., 2005; Zucchetti, 2007).

Tavares (2015) sugere que, após esta fase extensional, ocorre a inversão da bacia. Em seu trabalho, o autor atribui o intervalo entre 2,68 e 2,63 Ga como o período de duração deste evento, relacionado ao fechamento da bacia, o que representaria uma segunda colisão entre os domínios Carajás e Rio Maria, porém de menor intensidade e de caráter intracontinental, sem desenvolvimento de arco ou de granitogênese sin-colisional. Outra proposta de evolução tectônica é feita por Rosière *et al.* (2006). Estes autores estudaram a região da Serra dos Carajás e indicaram a possibilidade de evolução tectônica em dois estágios, sendo um relacionado a tectônica vertical do tipo domos-e-quilhas, seguido de fase transcorrente.

O estágio final da evolução arqueana no Cinturão Itacaiúnas é considerada como mais um evento extensivo, relacionado à fragmentação do paleocontinente Carajás. Tavares (2015) considera que tal evento ocorreu entre 2,61 e 2,54 Ga e está associado a magmatismo granítico pouco expressivo, também do tipo A e aparentemente concentrado no extremo norte da PC, ao longo do Cinturão Norte do Cobre e cronocorrelato à intrusão do Granito Velho Salobo.

CAPÍTULO III – *NEOARCHEAN MAGMATISM IN SOUTHEASTERN AMAZONIAN CRATON, BRAZIL: PETROGRAPHY, GEOCHEMISTRY AND TECTONIC SIGNIFICANCE OF BASALTS FROM CARAJÁS BASIN*

ARTIGO:

"NEOARCHEAN MAGMATISM IN SOUTHEASTERN AMAZONIAN CRATON, BRAZIL: PETROGRAPHY, GEOCHEMISTRY AND TECTONIC SIGNIFICANCE OF BASALTS FROM CARAJÁS BASIN"

ABSTRACT The Neoarchean Carajás Basin is situated in the northern part of the Carajás Mineral Province. The main assemblages of this basin consists of volcano-sedimentary sequences composed predominantly of mafic volcanic rocks, and banded iron formations that have experienced a sub-greenschist to greenschist facies metamorphism, which the Grão Pará Group (GGP) is the dominant sequence. The mafic rocks of GGP (Parauapebas Formation) occur in extensive succession of massive or amygdaloidal lava flows with at least 370 m in thickness, which eleven cycles were identified by massive structure on the bottom and amygdaloidal and spilitization zones on the top. The basalts are grayish green amygdaloidal, porphyritic, aphanitic or fine-grained, and hypocrystalline. The primary igneous textures are mainly amygdaloidal, intergranular and intersertal and rarely microporphyritic. The primary mineral assemblages consist predominantly of clinopyroxene and plagioclase. On the other hand, the secondary mineral assemblages consists mainly of chlorite, albite, Fe-epidote, quartz and calcite, and are interpreted as product of seafloor hydrothermal alteration and/or sub-greenschist facies metamorphism. Geochemical investigations on volcanic rocks of the Parauapebas Formation show 51.12–55.26 wt.% SiO2, 0.69-0.92 wt.% TiO2, 7.02-12.35 wt.% FeO, and MgO ranging from 4.38 to 7.38 wt.%. The rocks are sub-alkaline and plot in the transitional and calc-alkaline fields. The primitive mantle-normalized multi-element spider diagram of major and trace elements shows typical features of arc-like trace element patterns and similar to those of the upper continental crust. These features include LILE enrichment, Nb and Ti depletion. The chondrite-normalized REE diagram shows a fractionated pattern, strongly enriched LREE patterns, flat HREE patterns, moderately negative Eu anomalies and minor Ce anomalies. SHRIMP zircon U–Pb dating constrains the Early Neoarchean crystallization ages of 2749 ± 6.5 and 2745 ± 5 Ma for volcanic mafic rocks. The geochemistry and Nd isotopic features indicate that the basaltic rocks were derived from the subcontinental lithospheric mantle affected by upper continental crustal components. The arc-like signatures observed, such as HFSE depletion, may have originated from crustal contamination during the migration of the basaltic magma rather than a subduction-modified magma source. The Parauapebas Formation basalts were most likely produced within an intraplate tectonic setting, rather than a subduction environment. Although this volcanism could be originated by the opening of a back-arc continental basin, a rift continental setting is more plausible on the basis of regional geology. Therefore, the Carajás Basin was likely formed in an extensional regime related to a continental rift setting at ca. 2.75 Ga and later closed possibly by colisional process in the Neoarchean. The rifting process could be associated to a slab breakoff related to the Rio Maria-Carajás Collision

and subsequent upwelling asthenosphere that provided heat leading to partial melting of the lithospheric mantle.

Keywords: Amazonian Craton, Carajás Mineral Province, Carajás basin, contaminated intracontinental basalts, rift-related basin.

1. Introduction

The Archean-Paleoproterozoic terranes within the cratonic provinces of the Earth are composed of a wide variety of volcanic and sedimentary rocks that record various magmatic and tectonic episodes, evolutionary conditions, and different stages of metamorphism, metasomatism and mineralization (Bédard et al., 2003; Furnes et al., 2015; Jenner et al., 2013). Understanding the petrogenesis and geodynamic setting of Archean volcano-sedimentary successions is of fundamental importance because they provide invaluable information of the tectonic evolution of the early Earth.

The Carajás Mineral Province (CMP), located in the southeastern sector of the Amazonian Craton in Brazil (Fig. 1a), is the largest and best-preserved Archean segment of this important craton. It is famous for hosting several world-class mineral deposits (DOCEGEO, 1988; Vasquez et al., 2008), including the largest iron ore deposit of the world, as well as several Cu-Au and Ni world-class deposits. The province consists mainly of many well-preserved Mesoarchean granitoid–greenstone terrains further south (Rio Maria Domain), and Neoarchean volcanic-sedimentary sequences and granitic-gneissic-granulite rocks (Carajás Domain) (Souza et al., 1996; Vasquez et al., 2008) (Fig. 1b). Given its well-preserved diverse rock types, the Carajás Province provides an excellent opportunity for studying the petrogenetic and geodynamic origins of Archean crust (e.g., Gibbs et al., 1986; Lobato et al., 2005; Vasquez et al., 2008).

In order to understand the nature and evolution of the CMP and especially for its northern part (Carajás Domain), we focus on the large sequence of basalts of the Parauapebas Formation, the lowermost unit of the Grão Pará Group (GPG) volcanic-sedimentary sequence in the Serra dos Carajás (Fig. 1c). Deciphering their genesis harbor critical information for providing constraints on the tectonic setting of the Carajás Basin during the Neoarchean. The tectonic setting of the Grão-Pará Group is still hotly debated. Some authors (Gibbs et al., 1986; Macambira, 2003; Olszewski et al., 1989; Tavares, 2015) argue that this extensive basaltic volcanism is result of an intra-plate rifting of older continental crust, whereas others (e.g. Dardenne et al., 1988; Teixeira and Eggler, 1994; Zuchetti, 2007) propose a subduction-related environment for its formation.

Accordingly, in order to decipher the nature and tectonic setting of GPG, the geochemical characteristics of the volcanic rocks had been investigated by several authors (Gibbs et al., 1986; Dardenne et al., 1988; Olszewski et al., 1989; Teixeira and Eggler, 1994 and Zuchetti, 2007), but no modern geochemical studies have been conducted in those

supracrustal rocks. In this contribution, we present systematic chemical study, including new high-precision major and trace element data, Sr–Nd isotopes and zircon U–Pb geochronology, of the Neoarchean basalts of the Grão-Pará Group, northern Carajás Province. The principal objectives are: (i) to determine the eruption ages of the basalts; (ii) to investigate the potential role of crustal contamination on the geochemistry of rocks from the Parauapebas Formation; (iii) to examine the tectonic setting of the basalts; and (iv) to constraint the geodynamic evolution of the Carajás Basin during the early Archean.

2. Regional setting

2.1. The Carajás Mineral Province

The Carajás Mineral Province (CMP), located in the southeastern portion of the Amazonian Craton (Fig. 1a), contains world-class deposits of Fe and Cu, as well as Mn and Ni mines (Beisiegel et al., 1973; DOCEGEO, 1988; Monteiro et al., 2014; Moreto et al., 2015), and represents one of the largest cratonic areas in the Earth. It is divided into two Archean domains: the Neoarchean Carajás domain in the North and the Mesoarchean Rio Maria domain (RMD) in the South (Fig. 1b) A regional E-W deformed zone, informally named "Transition" subdomains (Feio and Dall'Agnoll 2012; Feio et al., 2013), separates the Rio Maria and Carajás domains.

The Rio Maria domain is constituted of greenstone belts, tonalitic-trondhjemitic assemblages (TTG), leucogranodiorites, high-Mg granitoids and potassic granites. It is evolved in a context of amalgamation of granite-greenstone terranes, with formation ages between 3.05 Ga and 2.82 Ga (Almeida et al., 2011, 2013; Althoff et al., 2000; Dall'Agnol et al., 2006; Oliveira et al., 2011; Souza et al., 2001). Moreover, some geological and geophysical data indicate that the RMD collided with the northern domain (Carajás Domain) and, consequently, the units of the latter were strongly deformed and flattened. Even though the age of this colisional event is poorly constrained, it could be coeval with the formation of the abundant granite magmatism of the Canaã dos Carajás region (~2870 to 2830 Ma, Feio et al., 2013), as proposed by Tavares (2015).

On the other hand, the Carajás domain presents a more complex geological evolution than the Rio Maria Domain. Apart from the strongly deformed granitoids and gneissic rocks of the "Transition" subdomain, Carajás domain is composed essentially of the Neoarchean Carajás basin (Vasquez et al., 2008). In the Carajás Basin, excluding the basement granitoids of the Xingu Complex (similar in age and lithological content to those found in the "Transitional"

subdomain), the main assemblages are of Neoarchean age (~2.76 Ga; Gibbs et al., 1986; Machado et al., 1991; Wirth et al. 1986) and are grouped in the Itacaiúnas Supergroup. It is formed dominantly by banded iron formations, accompanied by a bimodal volcanism metamorphosed in sub-greenschist or greenschist conditions. The Itacaiúnas Supergroup consists of several volcano-sedimentary sequences named: Igarapé Salobo (~2.76 Ga; Machado et al. 1991), Grão Pará (~2.76 Ga; Machado et al. 1991; Wirth et al. 1986), Igarapé Bahia (~2.74 Ga; Galarza and Macambira 2002), and Igarapé Pojuca groups (~2.73 Ga; Machado et al. 1991). These volcano-sedimentary sequences are covered by the fluvial to marine siliciclastic deposits of the Águas Claras formation (Araújo et al., 1988; DOCEGEO, 1988; Nogueira et al., 1994, 2000). Dating of syndepositional volcanism at 2681 ± 5 Ma (Trendall et al., 1998) and intrusive mafic dikes and sills at 2645 ± 12 Ma and 2708 ± 37 Ma (Dias et al., 1996; Mougeot et al., 1996) constrains the age of the Águas Claras Formation to the Archean.

Near the borders of the Carajás basin (Fig. 1c) several Neoarchean mafic-ultramafic layered complexes are exposed (Vasquez et al., 2008 and references therein). These layered complexes intrude rocks of the Xingu Complex and the Itacaiúnas Supergroup (DOCEGEO, 1988; Ferreira Filho et al., 2007), and include large Ni-laterite mineralized layered intrusions of the Cateté Suite (e.g., Vermelho, Serra da Onça, Serra do Puma and Serra do Jacaré complexes) and the PGE-mineralized Luanga and Lago Grande complexes. These intrusions are Neoarchean (e.g., 2766 ± 6Ma Serra da Onça Complex: Lafon et al., 2000; 2763 ±6Ma Luanga Complex: Machado et al., 1991) and represent a major magmatic event coeval with the extensive basaltic volcanism of the Grão Pará Group (Machado et al., 1991; Ferreira Filho et al., 2007).

The evolution of the Carajás Basin is widely discussed. It is known that the depositional site of these sequences occurred in a marine environment, but different models have been proposed to explain the evolution of the Archean volcano-sedimentary sequences, which includes the large sequence of basalts of the Grão Pará Group, object of this study. Although subduction-related settings have also been proposed (e.g., Dardenne et al., 1988, Meirelles & Dardenne, 1991, Teixeira and Eggler, 1994; Zucchetti, 2007), the Carajás basin is generally interpreted as a rift-related continental basin formed at ~2760 Ma (e.g., Dall'Agnol et al., 2006; DOCEGEO, 1988; Gibbs et al., 1986; Tavares, 2015) and later closed by collisional processes.

Three main episodes of granite plutons occur in the Carajás Basin or in adjacent areas (Fig. 1c) and are intrusive into the Itacaiúnas Supergroup: (i) Neoarchean (ca. 2.76-2.73 Ga; Feio and Dall'Agnol, 2012; Feio et al., 2013) A-type subalkaline granitic magmatism

represented by Planalto and Vila Jussara suites, Estrela Complex and Serra do Rabo Granite; (ii) Neoarchean younger peralkaline to meta-aluminous granites such as Old Salobo (2,573 ± 3 Ma, Machado et al. 1991) and Itacaiúnas (2,560 ± 37 Ma, Souza et al. 1996) granites; and (iii) Paleoproterozoic (ca. 1.88 Ga) intrusions include several anorogenic granitic plutons like the Serra dos Carajás, Young Salobo, and Cigano that belong to an extensive A-type Proterozoic province of the Amazon Craton (e.g., Dall'Agnol et al., 2006).

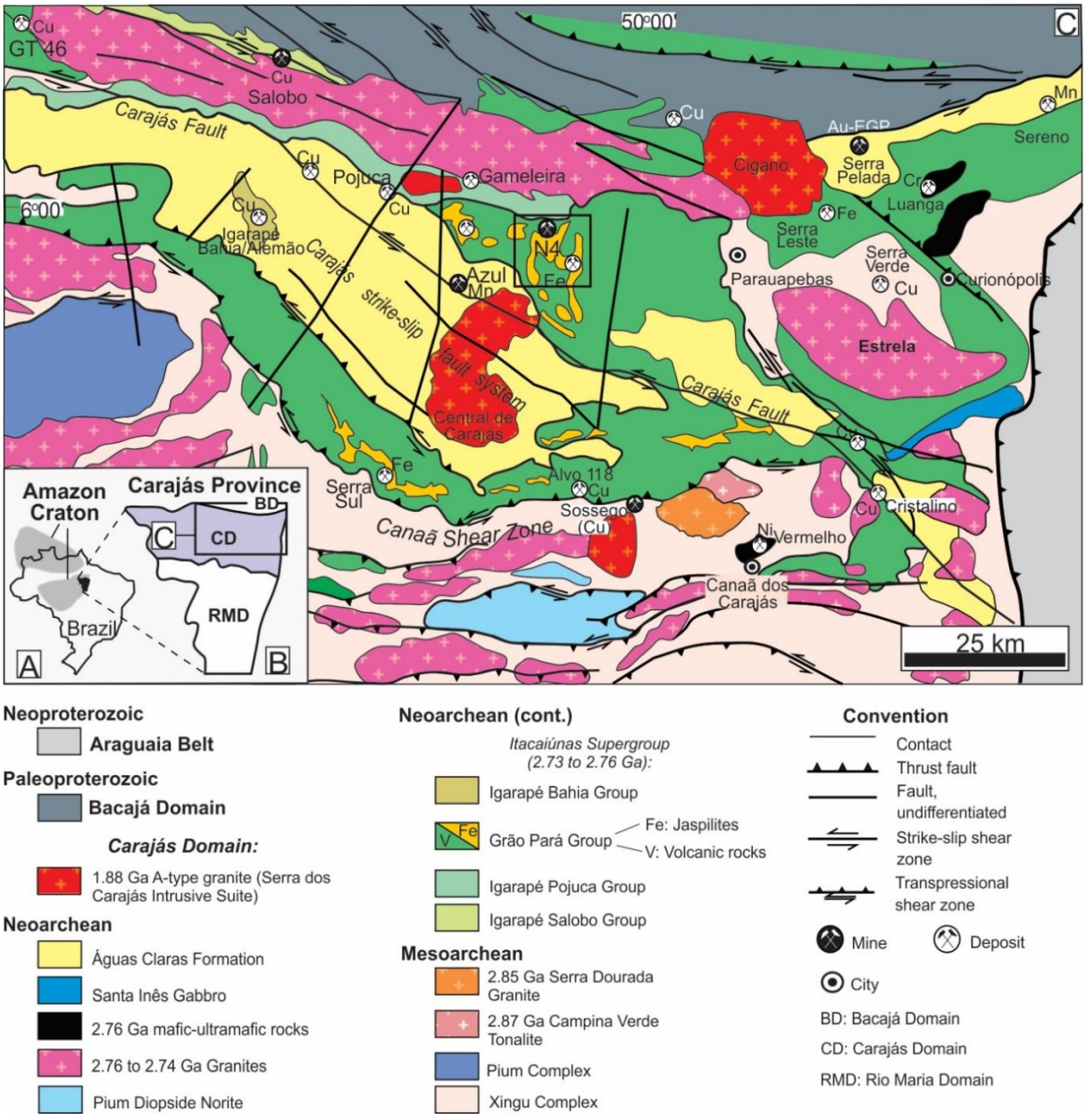

Figure 1. *a) Location of the Carajás Province in Brazil; b) Location of the Carajás Domain into the Carajás Mineral Province; the rectangle corresponds approximately to the area detailed in figure c; c) Simplified geological map of the northeast part of Carajás Province, Carajás Domain (modified after Vasquez et al., 2008 and Moreto et al., 2015); the black rectangle indicates approximately the location of N4 deposit (Fig. 2a).*

2.2. *Grão-Pará Group*

The Neoarchean Grão Pará Group (~2.76 Ga; Gibbs et al., 1986; Olszewski et al., (1989); Machado et al., 1991; Trendall et al., 1998, Wirth et al., 1996), located in the northern part of the CMP, is the main volcano-sedimentary sequence of the Carajás Basin, and is bordered by the "Transitional" subdomain to the south, and the Bacajá Domain to the north (Fig. 1c). The volcano-sedimentary sequence of the Grão Pará Group is approximately 260 km long by 70 km wide, with its rocks covering an area of approximately 18000 km2 (Macambira, 2003). This sequence comprises an extensive volcanism, dominantly mafic, which is assigned to the Parauapebas Formation, footwall to the Carajás Formation that consists of jaspilite-hosted giant iron deposits of Carajás. There are doubts regarding the complete stratigraphy of the Grão Pará group. Some authors defend the existence of more two units: one, essentially volcanic, above the Carajás Formation, denominated Igarapé Cigarra Formation (Gibbs et al., 1986; Macambira, 2003), and other, at the top of the group, composed of sedimentary rocks of the Igarapé Boa Sorte Formation (Macambira, 2003). However, other authors (Meirelles, 1986, Meirelles; Dardenne, 1991; Lindenmayer et al., 2001) consider the top and base relations of the volcanic rocks and jaspilites as of structural character, questioning the stratigraphic value of the Igarapé Cigarra Formation, and positioning the sedimentary package, denominated Igarapé Boa Sorte, at the base of the Águas Claras Formation, deposited above the Grão Pará Group with an unconformity (Nogueira et al., 1994).

The Parauapebas Formation is the lowermost unit of the Grão Pará Group and contains mainly basalts and basaltic andesites, and minor basic to intermediate pyroclastic rocks and rhyolites (Gibbs et al., 1986; Macambira, 2003; Meirelles & Dardenne, 1991, Teixeira and Eggler, 1994; Zucchetti, 2007), which occur concurrently beneath the Carajás Formation and reflect the contemporaneity of the two formations (Beisiegel et al., 1973; Macambira, 2003). This extensive volcanism, essentiality basaltic, is usually considered to be the result of an intra-plate rifting of older continental crust (e.g., DOCEGEO, 1988; Gibbs et al., 1986; Macambira, 2003; Olszewski et al., 1989; Tavares, 2015), but some authors (e.g., Lobato et al., 2005; Meirelles & Dardenne, 1991, Teixeira and Eggler, 1994; Zucchetti, 2007) have suggested a subduction-related environments. The age of the volcanism of the Grão Pará Group is determined as 2758 ± 39 Ma, using U-Pb analysis in zircon from rhyolites of the Parauapebas Formation by Wirth et al. (1986). This age (~ 2.76 Ga) is ratified by isotopic analyzes of several authors (e.g., Olszewski et al., 1989; Machado et al., 1991; Trendall et al., 1998).

The Carajás Formation is constituted by layers and discontinuous lenses of banded iron formations (jaspilites) and iron ore, intruded by sills and mafic dikes. The jaspilites host one of the largest high-grade (over 60 wt% Fe) iron ore deposits and resources in the world (Figueiredo e Silva et al. 2008; Lobato et al. 2005) and have centimeter-thick intercalations of iron oxide, jasper and chert and are heavily weathered, with textures and primary structures preserved (Macambira, 2003). Lindenmayer et al. (2001) have concluded that the Carajás iron formations were possibly deposited on shallow and stable platforms, below the wave base level and near to hydrothermal vents. The use of SHRIMP dating of zircon grains in a mafic sill that cuts the Carajás Formation, along with data from U-Pb zircon dating, suggests a minimum age of 2740 ± 8 Ma for the deposition of the Carajás BIFs (Trendall et al., 1998).

3. Sampling and analytical procedures

3.1 Sampling

Representative samples from drilling cores of six boreholes over three E-W trending sections across the N4WS deposit were collected (Fig. 2a, b; 3). Samples of 15 cm were collected at every 2 m in each drilling core (~370 mafic samples in total). Approximately 60 basalt samples were selected for petrographic description. From the bottom to the top, the lithotypes observed in the core samples include mafic rock (MS), jaspilite (JP), less altered mafic rock (MSD), more altered mafic rock (MD), iron ore layer of weathered hematite (HF), chemical laterite (CQ) and hematite laterite (CM) (Fig. 2c). The lithotype classification is the same used by Vale mining company. For this study, after petrographic screening for preserved igneous textures and minimal alteration, forty five (45) least altered samples of basalts were selected for analyses of whole-rock major and trace elements, four were further selected for Sm–Nd isotope analyses, and two basalt samples were collected for U-Pb dating, and zircon mineral chemistry analyses. Moreover, the samples used in the whole rock geochemistry and isotopic studies were collected away from fractures and shear zones, and are devoid of secondary quartz, carbonates, sulphides and any evidence of weathering. The criteria for their selection was the spatial distribution, petrographic variety, and included a complete set of samples with preserved primary features. Samples with evident hydrothermal alterations, such as those associated to spilitization zone, were not considered.

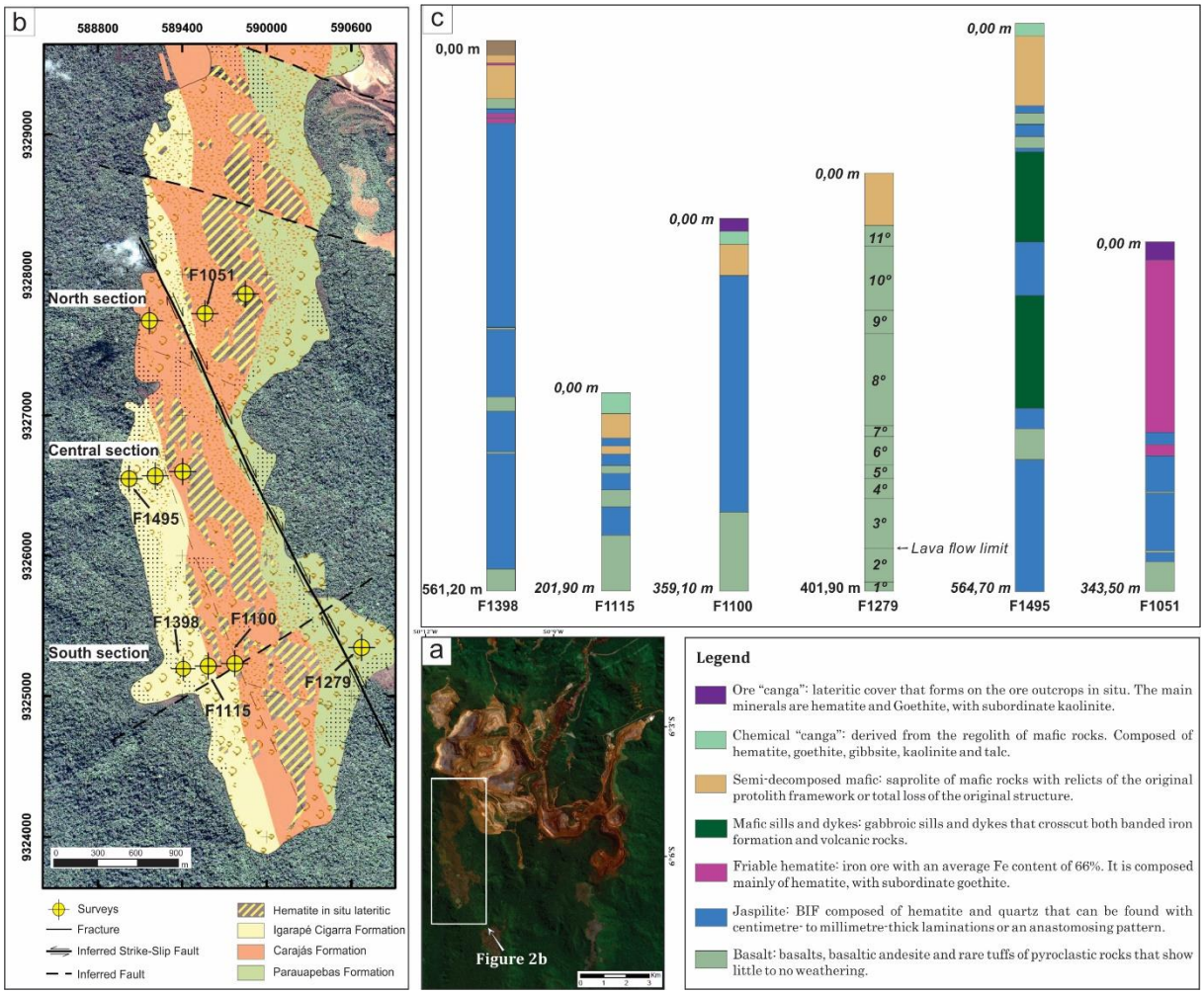

Figure 2. *a) Landsat 8 Operational Land Imager (OLI) sensor satellite image showing the open pit of the N4 mine; the rectangle corresponds to the area of the N4WS body (Fig. 2b); b) Geological map of the N4WS body, showing the position of each sampled drill hole (modified after Resende and Barbosa, 1972); c) Detailed drill core log from the sampled drill holes; limits between lava flows is shown on the F1279 drill hole.*

3.2. Microprobe analyses

Electron microprobe analyses were carried out on clinopyroxene, plagioclase and chlorite, on the 5-spectrometer JEOL JXA-8230 SuperProbe at the Electron Microprobe Laboratory of the Universidade de Brasília (Brazil), using an accelerating voltage of 15 kV at beam current of 10 nA. Both synthetic and natural mineral standards were used for the analyses and the same standards and procedure were retained throughout the analytical work.

Additionally, backscattering electron (BSE) images (not shown) and punctual qualitative analyses by energy-dispersive spectrometry (EDS) and quantitative analyses by WDS for zircon crystals of two basalt samples were acquired on an electron microprobe at the CMCA – Centre for Microscopy, Characterization and Analyses of University of Western Australia. The instrument is a JEOL JXA8530F microprobe which is a high-vacuum only, field-

emission gun electron probe micro-analyzer (EPMA). Operating conditions were 40 degrees takeoff angle, and a beam energy of 20 kV. The beam current was of 130 nA, and the beam diameter was fully focused. Natural minerals and synthetic pure oxides were used as standards. Analytical results of the analyzed zircon crystals are found in Table 3.

3.3. Whole-rock geochemistry analyses

Sample preparation and lithogeochemical analyses were performed at the ALS Chemex (Canada), following standard laboratory procedures. Major elements were determined by X-Ray Fluorescence (XRF) and are presented in oxides weight percentages. The rare earth elements (REE), high field strength elements (HFSE) and large ion lithophile elements (LILE) were determined by ICP-MS and the metals Ag, As, Cd, Co, Cu, Li, Mo, Ni, Pb, Sc, Tl and Zn were determined by ICP-AES. A complete description of analytical methods is available in the ALS Chemex Home Page (www.alsglobal.com). Some of the geochemical diagrams were produced using the GCDkit program (Janousek et al., 2006, 2011). Eu (Eu/Eu*), Ce (Ce/Ce*), Nb (Nb/Nb*), Ti (Ti/ Ti*), and Zr (Zr/Zr*) anomalies were calculated with respect to the neighboring immobile elements, following the method of Taylor and McLennan (1985).

3.4 U-Pb SHRIMP analyses

Zircon concentrates were extracted from ca. 10 kg rock samples using conventional gravimetric and magnetic techniques at the Geochronology Laboratory of the Universidade de Brasília. Mineral fractions were handpicked under a binocular stereo microscope to obtain fractions of similar size, shape and color. Before every micro-analytical procedure, mounts were cleaned with dilute (2%) HNO_3. Cathodoluminescence (CL) images were taken to examine the internal structure of individual grains.

Zircon U–Pb analyses were performed on the Sensitive High-mass Resolution Ion MicroProbe (SHRIMP II) housed at the John de Later Centre at Curtin University of Technology, Perth, Australia, using an analytical circular spot size of 20 to 25 □m in diameter. About two minutes of rasterization was used to remove the gold coating, which contains common lead in small amounts (ppbs). Individual analyses are composed of nine measurements for zircon ($^{196}Zr_2O$, ^{204}Pb, background, ^{206}Pb, ^{207}Pb, ^{208}Pb, ^{238}U, ^{248}ThO, ^{254}UO), repeated in five scans. The standards zircon D23 and glass NBS611 were used to identify the position of the peak of mass ^{204}Pb, whereas the calibration of the U content and the Pb/U ratio were done using the zircon standard BR266 (559 Ma, 903 ppm U). The age calculations and plotting of Concordia diagram were done using ISOPLOT 3.0 (Ludwig, 2003). The presented ages are

mean average $^{207}Pb/^{206}Pb$ and are calculated at 2σ level. Individual analyses are quoted at 1σ level (Table 2).

3.5. Sr and Nd isotopic analyses

The isotopic composition of selected samples was determined using a Thermo Scientific TRITON™ Plus Thermal Ionization Mass Spectrometer (TIMS) operating in the multi-dynamic mode and were carried out at the Geochronology Laboratory of the Universidade de Brasília.

Rb concentration of whole-rock powders could not be determined during this work. The average $^{87}Sr/^{86}Sr$ obtained for the NBS-987 standard was 0.710257 ± 0.000007 (2SD; n = 9) during the course of this study. This value agrees well, within the analytical error, with the most typically recommended value of 0.71025 (Faure, 2001; Machado, 2013).

Nd isotopic analyses followed the method described by Gioia and Pimentel (2000). Whole-rock powders (~300 mg) were mixed with ^{149}Sm-^{150}Nd spike solution and dissolved in Savillex bombs. Sm and Nd extraction of whole-rock samples followed conventional cation exchange techniques. The $^{143}Nd/^{144}Nd$ ratios were normalized to $^{146}Nd/^{144}Nd$ of 0.7219 and the decay constant used was 6.54 x 10-12 yr-1. The TDM values were calculated using the model of DePaolo (1981). Nd procedure blanks were better than 100 pg. Sr and Nd data of four samples are shown in Table 4.

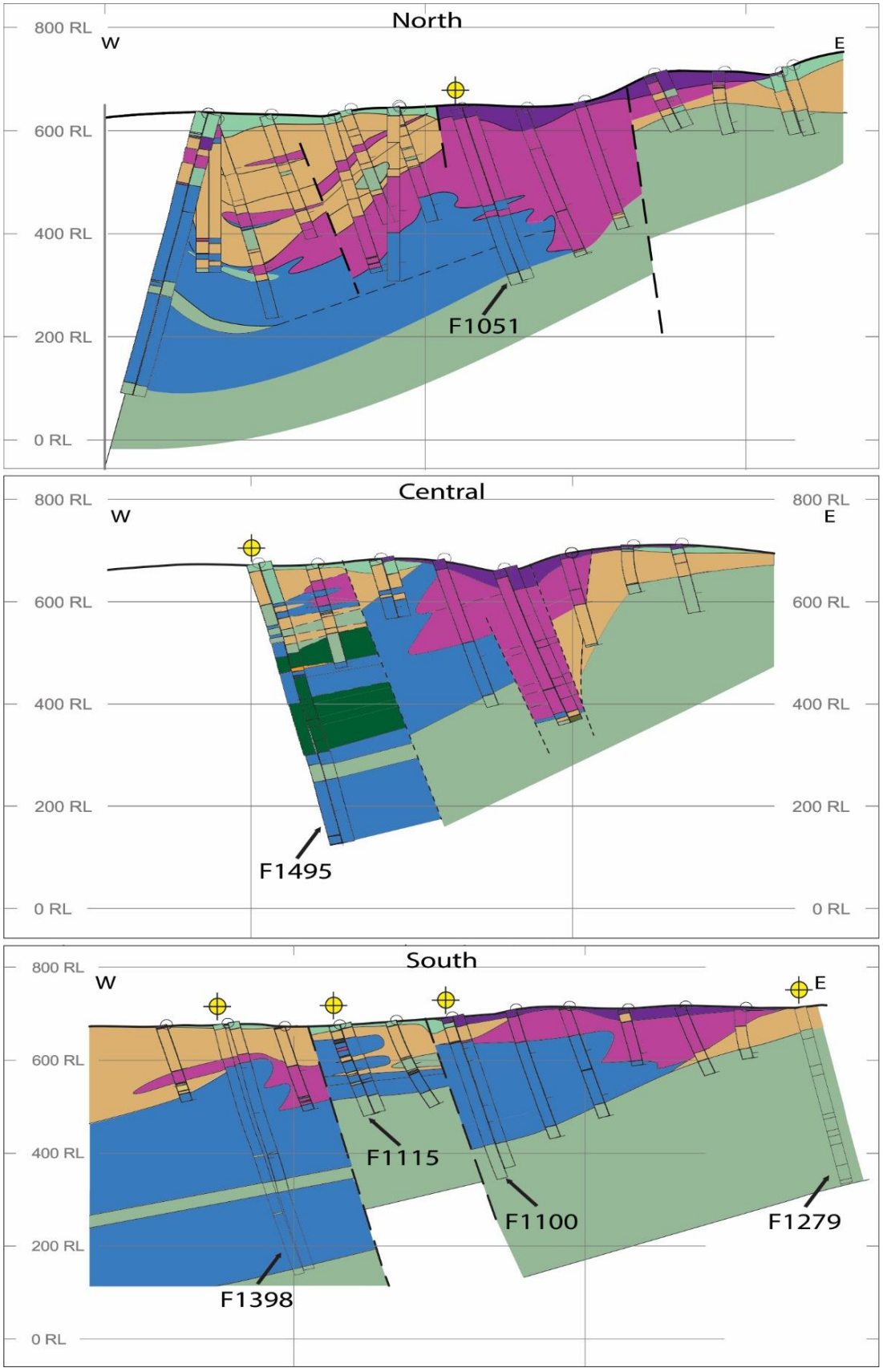

Figure 3. *E-W geological sections interpreted from the N4WS deposit running through sampled drill holes (sections and legend is indicated in Figure 2).The unidentified cores were added to elaborate the geological sections and the dotted lines indicate a possible fault.*

4. Field aspects and petrography

The basalts of the Parauapebas Formation occur stratigraphically below the Carajás Formation that consists of jaspillites, which host iron mineralization and are conformably intercalated with basaltic rocks (Fig. 3; 4a). The jaspillites are characterized by micro- and mesobanding imposed by alternating jasper and iron oxides (mainly hematite) (Fig. 4b, c). The mafic rocks occur in extensive successions of massive or amygdaloidal lava flows with at least 370 m in thickness (Fig. 2c), with eleven cycles identified by massive texture at the bottom and amygdaloidal and spilitization (seawater metasomatic alteration) zones at the top (Fig. 4a, c). Sills and dykes of gabbros, most of them hydrothermalized, crosscut all these rocks (Fig. 4d).

The basalts are grayish green (Fig. 5a, b, c), and sometimes greenish, depending on the degree of chloritization, whether aphanitic or fine-grained, or hypocrystalline. They still preserve their primary mineral assemblage and igneous textures. The primary igneous textures are largely amygdaloidal, intergranular and intersertal and rarely microporphyritic (Fig. 6a, b, c). The primary mineral assemblages consist predominantly of clinopyroxene and plagioclase with minor quartz; K-feldspar, ilmenite, magnetite and rare pirite, titanite and zircon are present as accessory minerals (Fig. 6a, b).

Clinopyroxene (0.5–1.5 mm) is pale brown in color (Fig. 6a). It occurs as anhedral to subhedral crystals and is partially or totally replaced by chlorite and/or epidote. The compositional ranges of Cpx show variations of $En_{(25–50)}$, $Fs_{(13–36)}$, $Wo_{(24–49)}$ and display diopsidic to augitic compositions (Suplementary Table 2). Plagioclase grains are either phenocrysts or interstitial. Phenocrysts are subhedral to euhedral (~3.0 mm), and interstitial grains are long, prismatic in shape (Fig. 6e, f), and exhibit swallowtail texture. They have been divided into two types: primary and secondary. Primary plagioclases are mostly labradorite-andesine and secondary plagioclases display albitic composition (Suplementary Table 1).

Seafloor hydrothermal alteration and/or sub-greenschist facies metamorphism is evident by the replacement of calcic plagioclase (labradorite – andesine An_{40-55}) to sodic plagioclase (albite $An_{0.5-8.4}$), presence of Fe-epidote, quartz, calcite, and major replacement of glass and augite by chlorite (Fig.6a, e). The secondary mineral assemblages are predominantly found in spilitization and amygdaloidal zones at the top of the lava flows, while the preserved igneous minerals and textures are restricted to the central/basal portion of the flows.

The basaltic lavas display different textures (amygdaloidal, massive, aphanitic, fine-grained and porphyritic; Fig.7). The base and central portions of lava flows are characterized

by massive and coarse-grained, respectively. However, amygdaloidal (Fig. 5b) and spilitization (Fig. 5c) zones are common in the boundary between the lava flows. Amygdules have lenticular or subcircular forms and are typically filled with assemblages of one or more of the minerals chlorite (brunsvigite), quartz, calcite, and Fe-epidote (Fig. 5b; 6c, d, e).

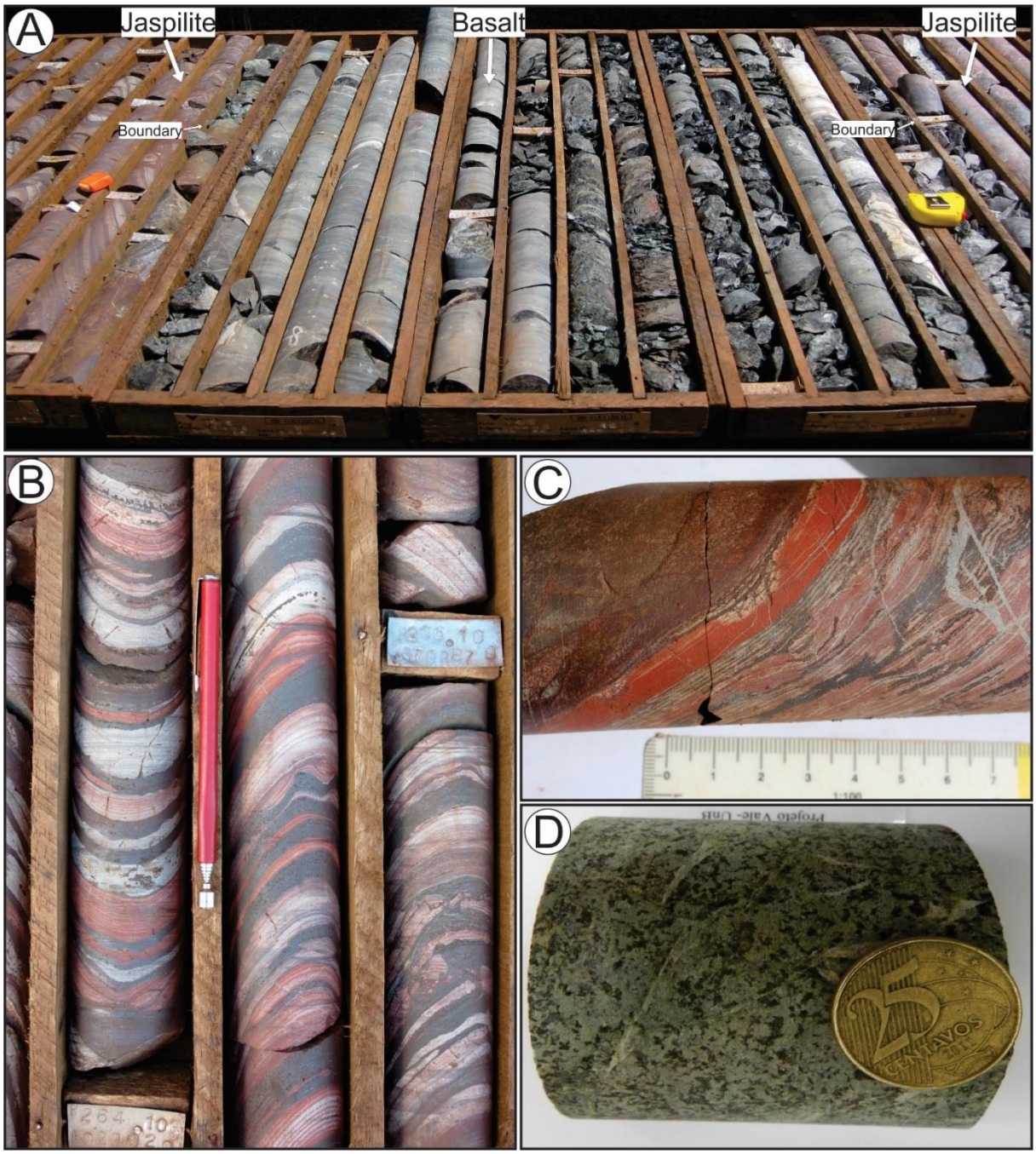

Figure 4. *Macroscopic aspects of the rocks from the Grão Pará Group: a) Overview of sampled drilling cores showing the basaltic rocks intercalated with jaspillites; b) Jaspillites with centimeter-thick intercalations of iron oxide (mainly hematite), jasper and chert; c) Contact between metric lava flows and jaspillites; d) Hydrothermally-altered gabbro that crosscuts both jaspillites and basalts.*

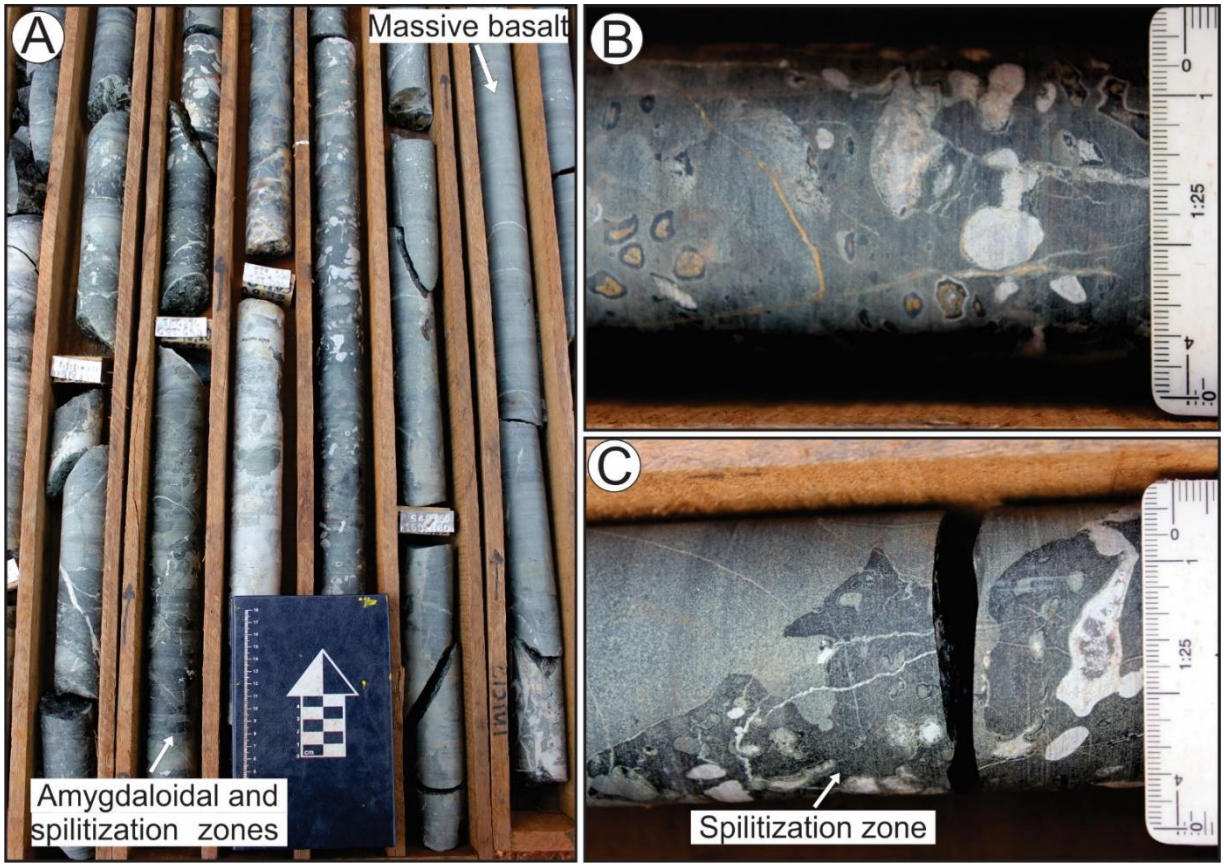

Figure 5. *Macroscopic aspects of the basalts from Grão Pará Group: a) Overview of basaltic lava flow, characterized by massive texture on the bottom and amygdaloidal and spilitization zones on the top; b) Amygdaloidal zone; amygdules are mainly filled with calcite and chlorite; c) Spilitization zone; amygdules are very common in this zones.*

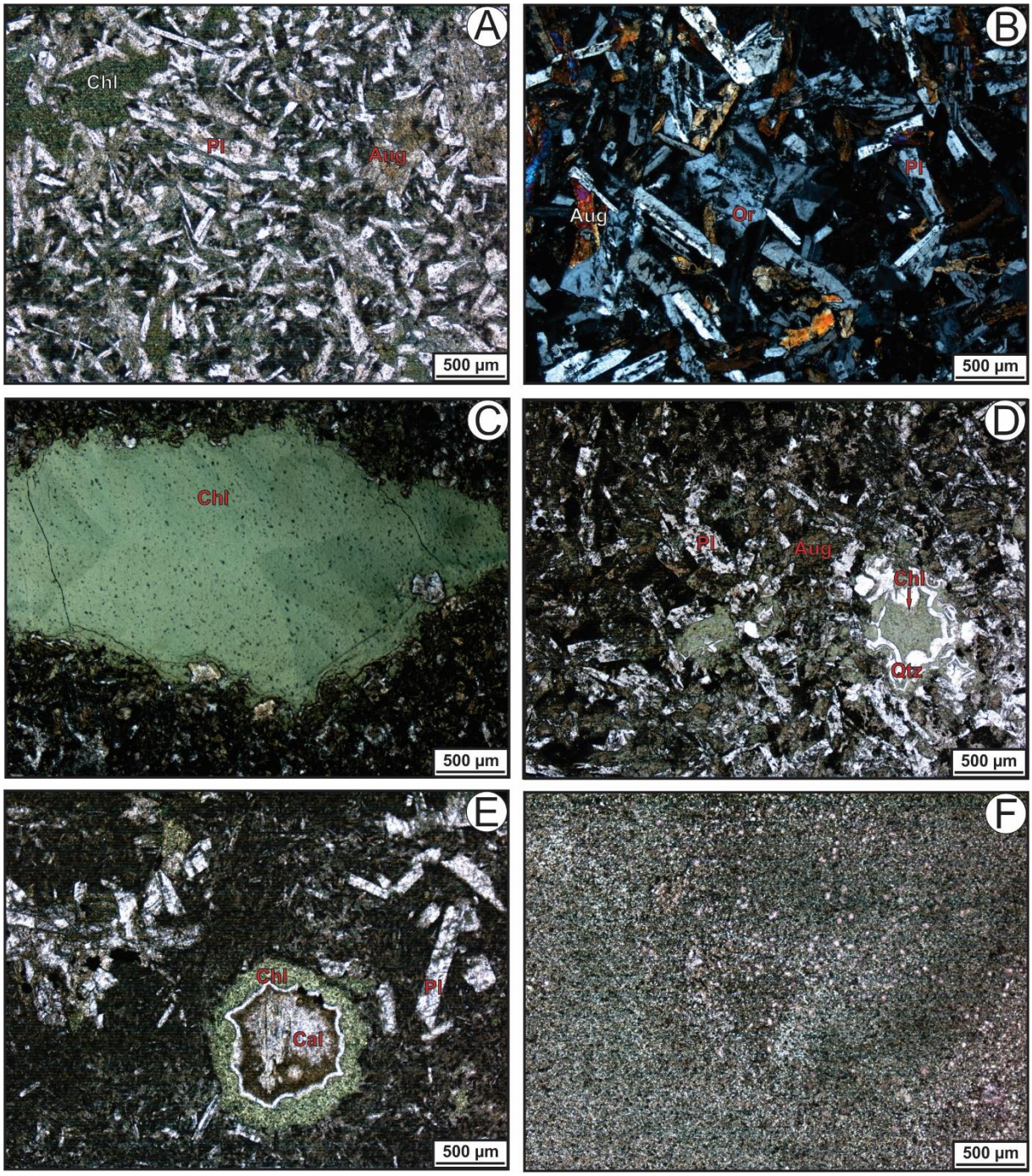

***Figure 6**. Photomicrographs of representative basalts of Paraopebas Formation: a) Basalt exhibits preserved primary igneous texture (intergranular/intersertal) and primary mineral assemblage, composed mainly of plagioclase and augite; b) Intergranular texture and interstitial orthoclase; c) Amygdule with subcircular form filled with chlorite in a fine-grained groundmass of augite, plagioclase and glass (replaced by chlorite); d) Intergranular and amygdaloidal texture; e) Subhedral plagioclase and amygdule filled with calcite, quartz and chlorite in a spilitization zone; f) Fine-grained basalt. Mineral abbreviations: (Aug) augite, (Cal) calcite, (Chl) chlorite, (Or) orthoclase, (Pl) plagioclase and (Qtz) quartz.*

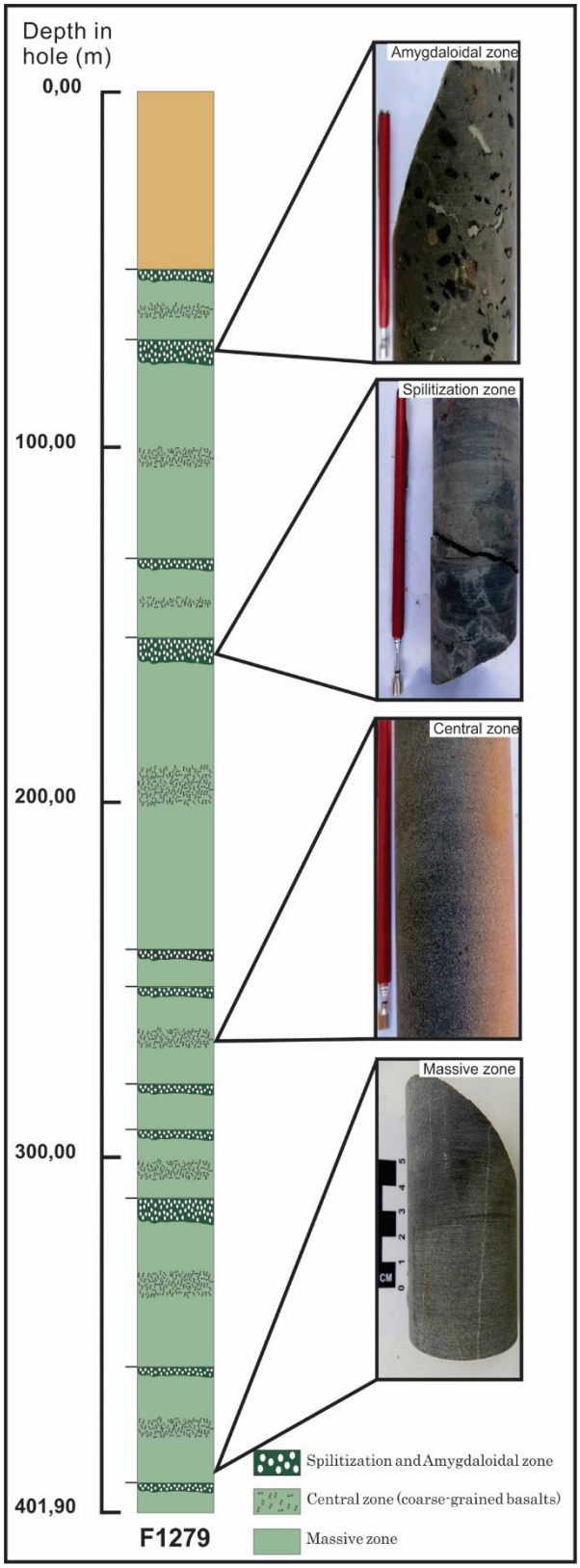

Figure 7*. Schematic sections and detailed core photographs of different textures presents in the lava flows. Amygdaloidal and spilitization zones are common in the boundary between the lava flows. Base and central regions are characterized by massive and coarse-grained, respectively.*

5. Whole rock geochemistry

Major (wt. %) and trace element (ppm) compositions of the volcanic rocks of the Parauapebas Formation are shown in Table 1. Due to the moderate LOI contents in most samples (LOI > 2.0 wt.%), major element analyses were recalculated to 100 wt.% on anhydrous basis for presentation in plots. These rocks have high SiO_2 contents ranging from 51.12 to 55.26 wt.%, low TiO_2 (0.69-0.92 wt. %), and Fe_2O_3 = 1.17-2.88 wt.%, and FeO = 7.02%-12.35 wt.%. The total alkali contents (Na_2O+K_2O) range from 3.93 to 6.17 wt.% (Fig. 8a) and transitional metals (Cr and Ni) reach an average of 90.89 ppm and 47.40 ppm, respectively. The MgO has low values that range from 4.38 to 7.38 wt.% (Table 1).

Although considerable mobile components, such as the alkalis (K_2O and Na_2O), undergo redistribution during post-magmatic processes, in some cases their relation with the SiO_2 content can be reliably adopted for classification. Thus, we decided to use the SiO_2 vs. total alkali diagram (TAS) plot as a reference, and the Zr/TiO_2 versus Nb/Y classification diagram for comparison. According to the TAS diagram (Fig.8a), the samples are subalkaline and mainly plot coherently within or near the basaltic andesite field, which only four samples plotting in the basaltic trachy-andesite and andesite fields. In the Zr/TiO_2 vs. Nb/Y classification diagram (Fig. 8b), the volcanic rocks are classified as basaltic andesite, andesite and basalt with most samples plotting in the former category. In additional, the samples plot in the transitional and calc-alkaline field (Zr/Y = 4.16 – 5.21) and in the transition between tholeiitic and calc-alkaline fields on the Y vs. Zr and alkali–FeO*–MgO diagrams, respectively (Fig. 8c, d).

The primitive mantle-normalized multi-element spiderdiagram of major and trace elements (Fig. 9a) shows features that are typical of arc-like trace element patterns (e.g., Pearce and Peate, 1995) and similar to those of the upper continental crust (Rudnick and Gao, 2003). These features include enrichment of large-ion lithophile elements (LILE) (e.g., Ba/La* ≅ 6.34) and variable degrees of depletion in some high field strength elements (HFSE) (Nb and Ti). Consequently these diagram show remarkable negative Nb anomalies with Nb/Nb* ranging from 0.12 to 0.33, and small negative Ti anomalies with Ti/Ti* varying from 0.31 to 0.51. Additionally, the primitive mantle-normalized trace element distributions do not show a common feature observed in arc lavas, prominent Zr depletion and Sr enrichment (Fig. 9a). These signatures are common in contaminated lavas (arc-like continental basalts) and are attributed to the incorporation of crustal material (Taylor and McLennan, 1985; Xia et al., 2014; Wang et al., 2015).

The chondrite-normalized rare earth element diagram shows a fractionated pattern with high REE abundances (Fig. 9b). The analyzed rocks exhibit strong enriched light rare earth elements (LREE) patterns (La/Yb_{CN} = 4.00-7.58; La/Sm_{CN} = 2.83–4.09), flat heavy rare earth elements (HREE) patterns (Gd/Yb_{CN} = 1.14–1.84), moderately negative Eu anomalies (Eu/Eu* = 0.58–0.97) and minor Ce anomalies (Ce/Ce* = 0.94–1.06) (Fig. 9b). The strong enrichment of LREE relative to HREE that is shown by all samples is a characteristic feature of contaminated volcanic rocks (Xia et al., 2014; Wang et al., 2015) and correlates well with the average of upper continental crust (Rudnick and Gao, 2003), as shown on Fig. 9b.

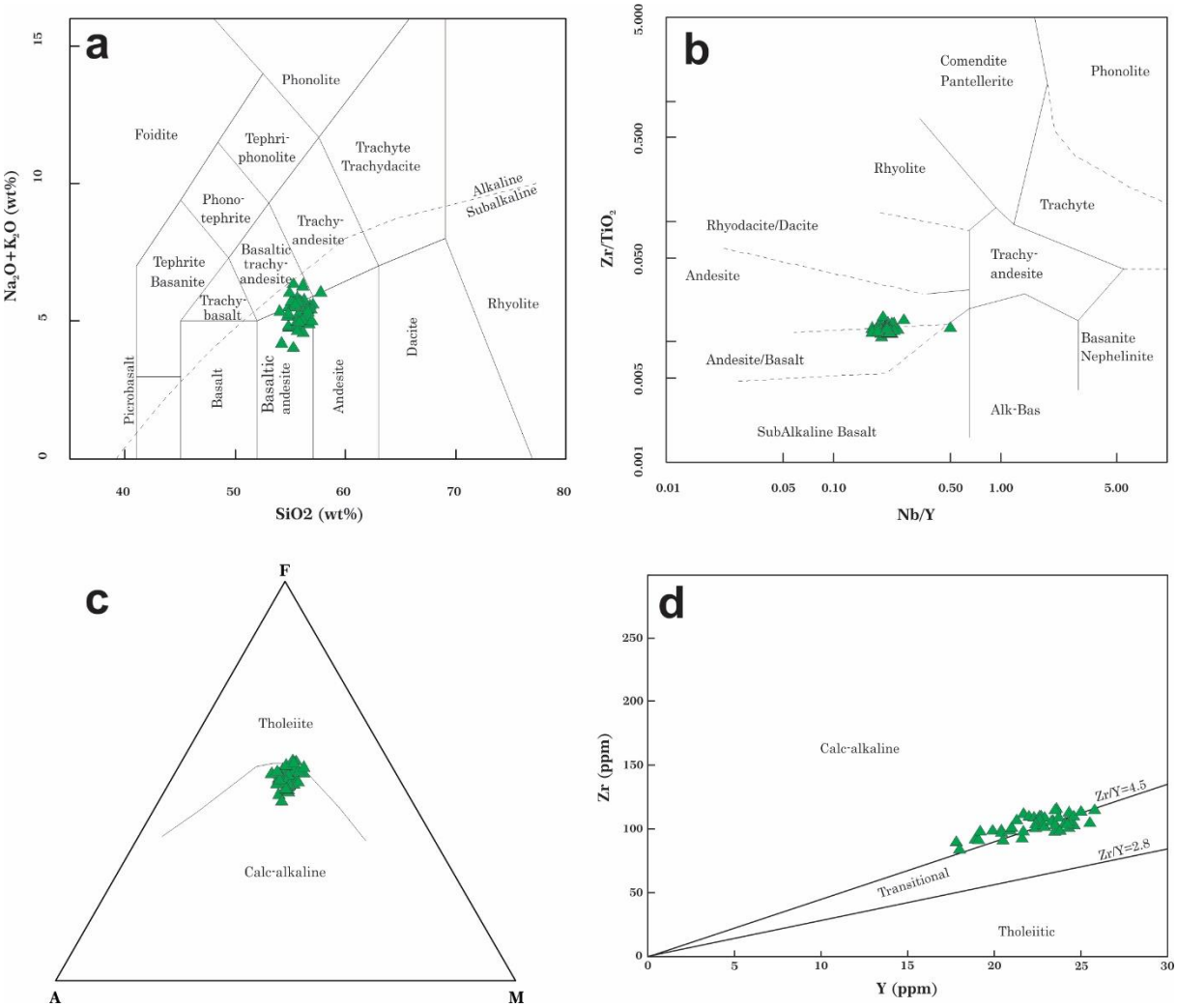

***Figure 8**. Classification of the Parauapebas Formation basalts: a) SiO2 vs. total alkali diagram (Le Bas et al., 1986); b) Nb/Y vs Zr/TiO2 diagram (Winchester and Floyd, 1977); c) AFM diagram (Irvine and Baragar, 1971); d) Zr vs. Y plot showing the transitional to calc-alkaline affinity (after Ross and Bedard, 2009).*

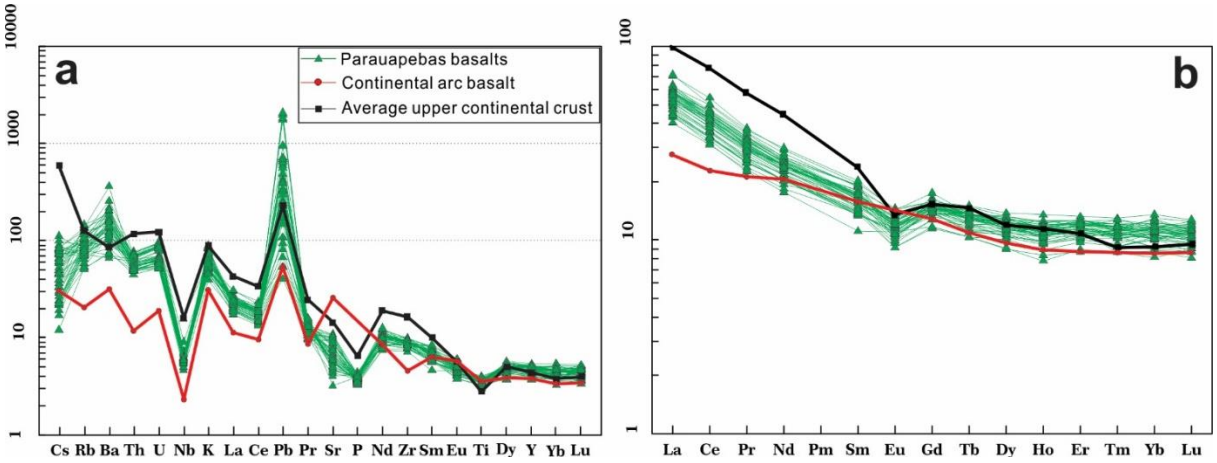

Figure 9. *a) Primitive mantle-normalized spidergram of the Parauapebas basalts; b) Chondrite-normalized REE distributions for the basaltic rocks of the Parauapebas Formation. Chondrite and primitive mantle values for normalization are from Sun and McDonough (1989). Data for the continental arc (e.g. Vanuatu arc) and average upper continental crust are from Peate et al. (1997) and Rudnick and Gao (2003).*

Table 1

Major (wt.%) and trace element (ppm) compositions and significant element ratios for representative samples of metabasalts from Grão-Pará basin.

Sample	F1051/01	F1051/173	F1065/43	F1065/45	F1065/47	F1065/48	F1065/49	F1065/51	F1065/54	F1065/56	F1065/57	F1065/58	F1100/172	F1100/173	F1100/174
Depth	351.89	344.00	84.00	88.00	92.00	94.00	96.00	100.00	106.00	110.00	112.00	114.00	342.00	344.00	346.00
SiO_2	54.37	53.33	55.19	55.07	55.26	54.82	53.63	55.05	52.75	53.24	53.69	54.79	52.90	52.93	52.56
TiO_2	0.77	0.79	0.83	0.82	0.80	0.80	0.81	0.82	0.80	0.78	0.79	0.80	0.77	0.69	0.73
Al_2O_3	13.40	13.63	13.84	13.68	13.51	13.51	13.48	13.66	13.09	13.61	13.37	13.42	13.61	13.29	13.51
Fe_2O_3	1.86	1.69	2.82	1.69	1.72	1.62	2.00	1.64	1.84	2.25	1.77	1.86	2.79	1.40	2.13
FeO	8.59	9.23	7.02	8.93	8.98	9.54	8.08	8.88	8.74	8.55	8.73	9.28	7.50	8.64	8.60
MnO	0.28	0.36	0.30	0.27	0.26	0.24	0.23	0.31	0.19	0.20	0.20	0.22	0.33	0.32	0.34
MgO	4.67	4.92	5.21	5.68	5.38	5.38	4.53	5.37	4.95	4.65	4.48	4.76	5.59	5.66	5.26
CaO	7.19	6.96	4.46	4.96	5.94	5.80	7.86	5.79	7.65	8.27	7.98	6.82	7.65	6.25	8.04
Na_2O	2.76	2.34	3.96	3.23	3.12	2.86	2.90	3.29	2.92	2.96	3.21	2.98	4.07	3.55	2.91
K_2O	1.95	2.12	1.82	2.18	2.31	2.00	2.24	1.97	1.54	1.65	1.89	1.97	1.24	1.84	1.67
P_2O_5	0.09	0.09	0.09	0.09	0.09	0.09	0.09	0.09	0.08	0.08	0.09	0.09	0.08	0.10	0.08
LOI	2.95	3.43	3.93	3.36	2.70	2.69	3.46	2.58	3.82	3.60	2.97	2.60	2.95	3.31	2.77
Total	98.88	98.89	99.47	99.95	100.07	99.34	99.31	99.45	98.37	99.84	99.16	99.58	99.48	97.97	98.60
S	4	7.00	16.00	7.00	4.00	4.00	3.00	3.00	3.00	2.00	3.00	3.00	4.00	4.00	3.00
V	252	238.00	237.00	234.00	231.00	235.00	236.00	244.00	244.00	244.00	240.00	242.00	266.00	192.00	253.00
Cr	100	90.00	80.00	80.00	80.00	80.00	80.00	90.00	90.00	90.00	90.00	90.00	100.00	110.00	100.00
Co	50.5	45.40	43.70	45.90	45.50	47.10	42.90	44.10	43.90	44.20	45.00	47.40	48.70	61.60	45.30
Ni	48	55.00	54.00	47.00	42.00	43.00	45.00	45.00	44.00	48.00	47.00	44.00	56.00	52.00	48.00
Rb	58.8	60.40	58.90	70.60	82.20	72.00	69.90	71.50	48.40	53.40	64.10	64.40	33.70	55.50	51.40
Sr	124.5	125.50	104.50	122.50	140.50	156.00	179.00	147.50	122.00	179.50	126.00	141.00	210.00	153.00	241.00
Y	24.6	20.90	23.40	24.20	22.80	22.40	23.50	23.30	23.50	25.50	24.10	22.90	18.00	22.60	21.60
Zr	111	100.00	107.00	105.00	104.00	105.00	104.00	107.00	99.00	106.00	106.00	103.00	85.00	111.00	94.00
Nb	4.7	4.50	4.80	4.80	4.60	4.70	4.60	11.70	4.50	4.80	4.70	4.60	3.50	4.50	3.70
Cs	0.2	0.20	0.27	0.55	0.54	0.51	0.38	0.41	0.18	0.20	0.24	0.41	0.18	0.19	0.19
Ba	672	838.00	1030.00	1195.00	1085.00	903.00	889.00	1215.00	486.00	517.00	654.00	667.00	558.00	851.00	744.00
Ta	0.5	0.50	0.50	3.30	0.50	0.50	0.50	0.90	0.50	0.50	0.50	0.60	0.40	0.40	0.40
Pb	24	13.00	147.00	13.00	53.00	36.00	130.00	15.00	25.00	19.00	49.00	17.00	18.00	44.00	31.00
Th	6.2	5.38	6.23	6.24	5.90	6.21	5.99	6.18	5.46	5.72	5.82	5.88	3.98	5.32	4.45
U	1.84	1.70	1.98	1.91	1.91	1.89	1.87	1.97	1.74	1.91	1.83	1.95	1.15	1.52	1.31
La	17.7	16.60	19.60	18.80	17.30	18.00	17.90	17.40	17.90	19.00	18.60	18.20	13.70	16.80	15.90
Ce	35.3	32.10	36.20	36.80	34.30	35.40	36.10	34.40	35.20	37.80	36.90	36.10	25.50	33.60	30.90
Pr	3.81	3.65	4.14	4.15	3.86	3.99	4.05	3.95	4.07	4.32	4.14	3.92	2.76	3.65	3.44
Nd	14.9	13.90	16.20	15.40	14.60	15.20	15.80	15.20	15.50	16.00	15.60	15.30	10.60	14.50	13.10
Sm	3.05	2.87	3.70	3.35	3.50	3.28	3.28	3.24	3.33	3.34	3.74	3.29	2.16	3.20	2.92
Eu	0.92	0.84	0.85	0.87	0.79	0.77	1.01	0.87	0.90	0.92	0.80	0.85	0.81	0.98	0.98
Gd	4.04	4.06	3.82	3.88	3.57	3.63	4.04	3.74	3.84	4.27	4.01	3.82	3.03	4.05	3.73
Tb	0.64	0.57	0.65	0.65	0.65	0.57	0.61	0.67	0.61	0.64	0.62	0.64	0.49	0.64	0.57
Dy	4.15	3.61	3.99	4.06	3.66	3.86	3.94	4.16	4.06	4.27	3.99	3.80	2.89	3.98	3.50
Ho	0.86	0.81	0.80	0.83	0.76	0.73	0.81	0.83	0.84	0.89	0.82	0.80	0.60	0.83	0.75
Er	2.6	2.39	2.69	2.60	2.31	2.55	2.52	2.45	2.54	2.63	2.68	2.38	1.83	2.61	2.31
Tm	0.38	0.37	0.36	0.36	0.36	0.39	0.38	0.41	0.37	0.38	0.36	0.34	0.28	0.39	0.33
Yb	2.42	2.20	2.70	2.45	2.59	2.48	2.46	2.43	2.34	2.26	2.32	2.44	1.70	2.37	2.24
Lu	0.35	0.33	0.40	0.39	0.37	0.37	0.37	0.40	0.37	0.36	0.36	0.36	0.29	0.38	0.32
$(La/Yb)_{cn}$	5.25	5.41	5.21	5.50	4.79	5.21	5.22	5.14	5.49	6.03	5.75	5.35	5.78	5.08	5.09
$(La/Sm)_{cn}$	3.75	3.73	3.42	3.62	3.19	3.54	3.52	3.47	3.47	3.67	3.21	3.57	4.09	3.39	3.52
$(Gd/Yb)_{cn}$	1.38	1.53	1.17	1.31	1.14	1.21	1.36	1.27	1.36	1.56	1.43	1.30	1.47	1.41	1.38
$(Ce/Ce^*)_{cn}$	1.00	0.97	0.94	0.98	0.99	0.98	1.00	0.98	0.97	0.98	0.99	1.00	0.96	1.00	0.98
$(Eu/Eu^*)_{cn}$	0.80	0.75	0.69	0.74	0.68	0.68	0.85	0.76	0.77	0.74	0.63	0.73	0.97	0.83	0.91
Zr/Y	4.51	4.78	4.57	4.34	4.56	4.69	4.43	4.59	4.21	4.16	4.40	4.50	4.72	4.91	4.35
Ti/Zr	30.63	39.00	37.38	34.29	30.77	29.52	32.69	29.91	35.35	32.08	33.02	30.10	32.94	24.32	25.53
Nb/La	0.27	0.27	0.24	0.26	0.27	0.26	0.26	0.67	0.25	0.25	0.25	0.25	0.26	0.27	0.23
Lu/Yb	0.14	0.15	0.15	0.16	0.14	0.15	0.15	0.16	0.16	0.16	0.16	0.15	0.17	0.16	0.14
$(Nb/Nb^*)_n$	0.35	0.35	0.33	0.12	0.35	0.34	0.34	0.69	0.33	0.34	0.34	0.31	0.33	0.37	0.32
$(Ti/Ti^*)_n$	0.41	0.51	0.43	0.41	0.35	0.38	0.40	0.36	0.41	0.39	0.38	0.36	0.46	0.32	0.31
$(Zr/Zr^*)_n$	0.94	0.94	0.88	0.93	0.94	0.92	0.88	0.94	0.88	0.91	0.91	0.90	0.97	1.00	0.94

cn = chondrite normalized; n = primitive mantle normalized

Table 1

Major (wt.%) and trace element (ppm) compositions and significant element ratios for representative samples of metabasalts from Grão-Pará basin. (Cont.)

Sample	F1100/175	F1100/176	F1100/178	F1100/180	F1115/92	F1115/93	F1115/94	F1115/95	F1115/96	F1115/97	F1279/A	F1279/B	F1279/C	F1279/D	F1279/G
Depth	348.00	350.00	354.00	358.00	182.00	184.00	186.00	188.00	190.00	192.00	52.75	59.5	65.9	72.05	97.23
SiO_2	53.49	52.93	52.20	52.44	53.67	52.77	53.46	51.12	53.70	53.46	54.32	54.22	54.20	53.09	52.38
TiO_2	0.78	0.79	0.81	0.83	0.81	0.84	0.81	0.76	0.82	0.84	0.87	0.86	0.84	0.86	0.85
Al_2O_3	13.95	14.11	13.76	13.68	13.35	13.76	13.57	12.57	13.60	13.64	13.72	13.43	13.67	13.64	13.63
Fe_2O_3	1.58	1.59	1.50	1.87	1.93	1.79	1.58	2.15	1.78	1.75	1.81	1.63	1.55	1.82	1.66
FeO	9.18	8.87	9.00	9.90	9.41	10.60	9.98	12.35	10.20	11.50	8.56	9.73	9.83	9.67	9.40
MnO	0.32	0.33	0.33	0.44	0.42	0.38	0.45	0.45	0.44	0.47	0.27	0.30	0.34	0.34	0.44
MgO	5.71	5.53	5.74	5.87	5.77	6.63	6.13	7.38	5.73	5.91	4.82	4.96	5.16	5.46	5.30
CaO	6.22	5.92	6.75	5.98	4.30	3.35	4.08	3.54	3.69	2.83	6.56	6.21	6.11	5.84	7.03
Na_2O	2.72	2.74	2.60	2.37	3.04	3.24	3.04	2.25	3.38	2.64	3.89	3.86	3.60	3.93	3.46
K_2O	2.62	2.68	2.33	2.25	2.10	1.50	2.30	1.71	1.53	2.16	1.69	1.65	2.09	1.60	1.52
P_2O_5	0.09	0.09	0.09	0.09	0.09	0.09	0.09	0.09	0.09	0.09	0.09	0.10	0.10	0.09	0.09
LOI	2.80	2.99	3.82	3.61	3.88	3.97	3.39	3.69	3.98	3.53	2.72	2.57	2.25	2.84	3.07
Total	99.46	98.57	98.92	99.33	98.77	98.92	98.88	98.06	98.94	98.82	99.32	99.51	99.73	99.19	98.83
S	5.00	5.00	6.00	6.00	5.00	10.00	7.00	6.00	9.00	8.00	4.00	4.00	3.00	3.00	4.00
V	261.00	254.00	267.00	223.00	241.00	249.00	241.00	230.00	243.00	229.00	247.00	252.00	256.00	250.00	269.00
Cr	100.00	100.00	120.00	110.00	90.00	100.00	90.00	90.00	100.00	90.00	90.00	90.00	90.00	90.00	100.00
Co	52.90	46.20	51.80	51.90	45.30	46.30	47.00	52.40	45.70	49.60	49.50	49.20	52.20	51.40	52.50
Ni	52.00	63.00	57.00	75.00	50.00	56.00	47.00	53.00	52.00	53.00	47.00	44.00	46.00	48.00	48.00
Rb	91.10	96.50	76.30	54.30	76.30	46.10	68.40	53.70	53.80	57.00	51.90	50.10	64.90	47.30	49.20
Sr	164.50	138.00	151.50	130.50	110.00	101.00	106.50	97.90	114.00	71.20	240.00	215.00	196.50	200.00	217.00
Y	20.40	19.90	22.40	24.30	25.00	23.60	21.00	25.80	23.50	24.30	22.90	22.00	22.30	24.30	21.70
Zr	98.00	100.00	102.00	102.00	115.00	117.00	102.00	116.00	116.00	114.00	110.00	111.00	110.00	107.00	99.00
Nb	4.00	4.40	4.30	4.20	5.30	5.40	5.10	6.80	5.30	5.10	4.70	4.80	4.70	4.40	4.20
Cs	0.41	0.30	0.28	0.16	0.48	0.61	0.44	0.67	0.60	0.51	0.25	0.33	0.62	0.74	0.37
Ba	1280.00	1380.00	1160.00	973.00	1885.00	800.00	1580.00	1010.00	1165.00	1345.00	1145.00	743.00	1030.00	786.00	890.00
Ta	0.40	0.40	0.40	0.40	0.50	0.50	0.50	0.50	0.60	0.40	0.40	0.40	0.40	0.40	0.40
Pb	42.00	22.00	30.00	14.00	11.00	47.00	6.00	4.00	13.00	8.00	135.00	153.00	70.00	18.00	16.00
Th	4.69	4.69	4.99	5.72	6.63	6.86	5.96	6.58	6.51	6.38	5.17	5.17	5.21	4.89	4.54
U	1.38	1.41	1.34	1.52	2.03	2.07	1.89	2.13	2.07	1.94	1.47	1.52	1.48	1.42	1.33
La	15.20	14.10	14.80	16.60	17.40	19.10	16.70	21.90	18.10	16.00	17.80	17.90	17.00	17.20	14.70
Ce	29.90	27.70	29.60	33.20	38.00	40.20	34.00	43.90	37.50	34.50	34.30	34.30	33.10	33.70	28.90
Pr	3.25	3.08	3.21	3.66	4.18	4.39	3.57	4.62	4.03	3.71	3.85	3.77	3.61	3.78	3.35
Nd	13.00	12.20	13.10	14.20	16.10	16.80	14.80	17.50	15.10	14.20	14.60	14.40	14.60	14.60	12.90
Sm	2.71	2.82	2.91	3.50	3.74	3.65	3.06	3.80	3.40	3.44	3.33	3.29	3.06	3.17	2.65
Eu	0.78	0.73	0.83	1.05	0.73	1.00	0.89	1.07	0.85	0.88	0.94	0.96	0.85	0.92	0.83
Gd	3.60	3.31	3.74	4.10	3.88	4.04	3.57	4.09	3.74	3.70	3.90	3.80	4.05	4.08	3.63
Tb	0.53	0.56	0.64	0.64	0.69	0.70	0.63	0.71	0.68	0.65	0.64	0.61	0.62	0.65	0.61
Dy	3.57	3.34	3.76	4.24	4.04	4.25	3.68	4.43	3.85	4.15	3.79	3.63	3.58	3.86	3.83
Ho	0.70	0.71	0.82	0.82	0.90	0.88	0.80	0.97	0.90	0.86	0.76	0.78	0.77	0.81	0.79
Er	2.10	2.28	2.32	2.36	2.63	2.67	2.18	2.77	2.48	2.56	2.37	2.26	2.32	2.50	2.47
Tm	0.31	0.30	0.30	0.28	0.39	0.37	0.35	0.42	0.38	0.38	0.35	0.35	0.34	0.38	0.34
Yb	2.27	2.16	2.09	1.84	2.56	2.68	2.14	2.83	2.63	2.30	2.38	2.21	2.14	2.34	2.27
Lu	0.34	0.31	0.35	0.28	0.38	0.36	0.30	0.41	0.36	0.34	0.32	0.32	0.34	0.34	0.34
$(La/Yb)_{cn}$	4.80	4.68	5.08	6.47	4.88	5.11	5.60	5.55	4.94	4.99	5.36	5.81	5.70	5.27	4.65
$(La/Sm)_{cn}$	3.62	3.23	3.28	3.06	3.00	3.38	3.52	3.72	3.44	3.00	3.45	3.51	3.59	3.50	3.58
$(Gd/Yb)_{cn}$	1.31	1.27	1.48	1.84	1.25	1.25	1.38	1.20	1.18	1.33	1.36	1.42	1.57	1.44	1.32
$(Ce/Ce^*)_{cn}$	0.99	0.98	1.01	1.00	1.06	1.04	1.03	1.02	1.03	1.06	0.97	0.97	0.99	0.98	0.97
$(Eu/Eu^*)_{cn}$	0.76	0.73	0.77	0.85	0.58	0.79	0.82	0.82	0.73	0.75	0.80	0.83	0.74	0.78	0.82
Zr/Y	4.80	5.03	4.55	4.20	4.60	4.96	4.86	4.50	4.94	4.69	4.80	5.05	4.93	4.40	4.56
Ti/Zr	24.49	26.00	31.37	33.33	30.43	33.33	33.33	27.59	31.03	33.33	34.55	33.33	32.73	33.64	29.29
Nb/La	0.26	0.31	0.29	0.25	0.30	0.28	0.31	0.31	0.29	0.32	0.26	0.27	0.28	0.26	0.29
Lu/Yb	0.15	0.14	0.17	0.15	0.15	0.13	0.14	0.14	0.14	0.15	0.13	0.14	0.16	0.15	0.15
$(Nb/Nb^*)_n$	0.35	0.41	0.39	0.35	0.40	0.38	0.39	0.43	0.36	0.43	0.37	0.38	0.38	0.35	0.38
$(Ti/Ti^*)_n$	0.34	0.35	0.39	0.38	0.36	0.41	0.41	0.33	0.40	0.42	0.44	0.44	0.44	0.42	0.38
$(Zr/Zr^*)_n$	0.94	1.02	1.03	0.93	0.95	0.92	0.90	0.90	0.98	0.99	0.99	0.99	1.01	0.98	1.00

cn = chondrite normalized; n = primitive mantle normalized

Table 1

Major (wt.%) and trace element (ppm) compositions and significant element ratios for representative samples of metabasalts from Grão-Pará basin. (Cont.)

Sample	F1279/H	F1279/K	F1279/L	F1279/O	F1279/Q	F1279/R	F1279/S	F1279/T	F1279/V	F1279/Y	F1279/Z	F1279/ZC	F1279/ZD	F1279/ZE	F1398/151
Depth	101.9	113.9	134.7	161.5	203.8	215.62	228.85	255.9	279.5	309	318	345.1	385.8	392.9	556.00
SiO_2	52.26	54.15	53.88	54.19	53.51	53.79	51.35	53.88	54.12	53.55	54.90	53.42	53.36	53.30	54.04
TiO_2	0.78	0.87	0.86	0.85	0.84	0.87	0.84	0.89	0.92	0.90	0.82	0.78	0.74	0.76	0.78
Al_2O_3	13.57	14.00	13.38	13.31	13.39	13.75	13.43	13.35	13.43	13.50	13.27	13.55	14.01	14.03	13.32
Fe_2O_3	1.44	1.87	1.69	1.66	1.31	2.03	1.95	2.13	2.30	1.87	2.07	1.67	1.17	1.32	2.88
FeO	8.71	8.87	9.14	8.96	10.80	9.03	9.58	10.05	9.71	9.96	9.93	8.58	8.69	9.62	7.88
MnO	0.39	0.38	0.41	0.51	0.53	0.37	0.44	0.43	0.47	0.57	0.53	0.41	0.43	0.47	0.45
MgO	5.08	4.97	5.88	5.62	6.10	5.56	6.42	5.13	5.12	5.27	4.78	5.55	5.78	5.90	4.38
CaO	8.02	6.49	4.55	5.32	4.60	7.91	5.79	5.68	5.74	6.05	5.27	6.93	6.16	5.76	6.54
Na_2O	3.38	3.10	3.04	3.55	2.69	2.31	3.16	2.71	2.73	3.04	4.36	3.92	4.72	3.06	2.45
K_2O	1.64	2.43	1.70	1.67	2.07	1.62	1.94	2.36	1.70	1.43	1.81	1.49	1.43	2.80	2.65
P_2O_5	0.08	0.10	0.09	0.10	0.09	0.10	0.09	0.10	0.10	0.10	0.09	0.08	0.08	0.08	0.09
LOI	3.11	2.07	3.77	3.13	3.57	2.00	4.40	2.84	3.08	2.86	1.77	2.54	2.38	2.46	4.30
Total	98.46	99.30	98.40	98.87	99.50	99.34	99.40	99.55	99.42	99.10	99.61	98.92	98.95	99.56	99.76
S	4.00	4.00	11.00	6.00	7.00	4.00	5.00	5.00	5.00	4.00	4.00	3.00	2.00	4.00	7.00
V	257.00	261.00	260.00	254.00	255.00	270.00	273.00	258.00	262.00	252.00	240.00	242.00	234.00	248.00	227.00
Cr	120.00	100.00	90.00	90.00	100.00	90.00	90.00	60.00	50.00	60.00	60.00	70.00	110.00	100.00	100.00
Co	47.40	46.90	50.50	49.90	57.30	47.60	51.60	51.40	50.70	47.60	43.80	43.20	43.00	46.30	40.00
Ni	47.00	48.00	55.00	48.00	49.00	40.00	51.00	34.00	37.00	42.00	28.00	28.00	38.00	32.00	47.00
Rb	50.30	83.50	52.60	52.60	62.10	47.30	60.40	70.30	48.10	36.20	42.80	39.30	34.80	90.30	53.20
Sr	230.00	228.00	196.50	89.20	171.50	131.50	144.00	185.00	141.00	167.50	111.50	131.50	129.00	165.00	200.00
Y	20.50	22.60	22.60	21.30	19.20	24.60	20.40	22.70	21.70	23.70	23.80	19.10	17.80	18.90	21.10
Zr	92.00	111.00	108.00	108.00	99.00	104.00	100.00	111.00	113.00	110.00	100.00	92.00	91.00	93.00	100.00
Nb	3.80	4.80	4.60	4.60	4.30	4.20	4.30	4.70	4.70	4.60	4.40	4.20	4.10	4.10	4.40
Cs	0.39	0.70	0.92	0.60	0.66	0.68	0.82	0.64	0.38	0.33	0.22	0.19	0.10	0.69	0.14
Ba	991.00	1505.00	1160.00	1025.00	1480.00	616.00	1045.00	1500.00	1185.00	834.00	1140.00	874.00	539.00	2650.00	1505.00
Ta	0.40	0.40	0.50	0.50	0.40	0.40	0.40	0.40	0.50	0.50	9.80	0.40	0.40	0.40	0.40
Pb	51.00	25.00	13.00	24.00	25.00	29.00	18.00	8.00	5.00	4.00	7.00	4.00	4.00	3.00	14.00
Th	4.34	5.26	4.95	4.87	4.51	4.58	4.46	5.05	5.26	4.85	4.65	4.35	4.33	4.47	6.33
U	1.19	1.44	1.37	1.35	1.22	1.30	1.22	1.41	1.45	1.42	1.42	1.32	1.14	1.25	1.85
La	13.90	18.00	15.70	13.40	15.60	16.20	14.00	16.30	16.80	16.00	22.20	14.60	12.50	13.70	17.40
Ce	27.30	36.10	31.20	26.40	29.10	32.40	27.90	32.20	32.00	30.90	40.70	27.40	25.00	27.30	34.20
Pr	3.09	3.97	3.54	2.91	3.19	3.71	3.06	3.58	3.58	3.53	4.50	3.06	2.81	3.19	3.77
Nd	12.20	15.10	13.50	11.60	12.20	14.60	12.20	14.30	13.70	13.90	17.90	12.20	11.00	12.10	14.20
Sm	2.64	3.15	3.12	3.06	2.68	3.24	2.61	3.05	2.92	3.05	3.94	2.73	2.67	2.79	3.34
Eu	0.81	1.02	0.75	0.93	0.80	0.92	0.85	0.78	0.86	0.88	1.05	0.71	0.67	0.67	0.89
Gd	3.57	3.88	3.82	3.73	3.44	4.05	3.56	3.59	3.62	3.94	4.53	3.28	2.96	3.03	3.79
Tb	0.54	0.61	0.63	0.61	0.57	0.61	0.52	0.63	0.59	0.61	0.65	0.53	0.49	0.49	0.65
Dy	3.51	3.96	3.88	3.73	3.34	3.98	3.44	3.66	3.89	3.82	3.98	3.42	2.93	3.23	3.96
Ho	0.74	0.83	0.82	0.74	0.68	0.85	0.70	0.78	0.74	0.78	0.78	0.69	0.56	0.64	0.84
Er	2.20	2.45	2.46	2.44	2.15	2.54	2.18	2.53	2.61	2.38	2.26	2.25	1.88	2.04	2.54
Tm	0.30	0.34	0.33	0.35	0.33	0.36	0.35	0.34	0.41	0.36	0.36	0.34	0.28	0.30	0.38
Yb	2.11	2.42	2.29	2.40	1.93	2.38	2.11	2.32	2.49	2.44	2.10	1.92	1.81	1.88	2.12
Lu	0.28	0.34	0.35	0.34	0.29	0.36	0.33	0.33	0.38	0.36	0.31	0.31	0.26	0.28	0.36
$(La/Yb)_{cn}$	4.73	5.34	4.92	4.00	5.80	4.88	4.76	5.04	4.84	4.70	7.58	5.45	4.95	5.23	5.89
$(La/Sm)_{cn}$	3.40	3.69	3.25	2.83	3.76	3.23	3.46	3.45	3.71	3.39	3.64	3.45	3.02	3.17	3.36
$(Gd/Yb)_{cn}$	1.40	1.33	1.38	1.29	1.47	1.41	1.40	1.28	1.20	1.34	1.78	1.41	1.35	1.33	1.48
$(Ce/Ce^*)_{cn}$	0.98	1.00	0.99	0.99	0.96	0.99	1.00	0.99	0.96	0.96	0.94	0.95	0.99	0.98	0.99
$(Eu/Eu^*)_{cn}$	0.81	0.89	0.66	0.84	0.81	0.78	0.85	0.72	0.81	0.78	0.76	0.72	0.73	0.70	0.76
Zr/Y	4.49	4.91	4.78	5.07	5.16	4.23	4.90	4.89	5.21	4.64	4.20	4.82	5.11	4.92	4.74
Ti/Zr	30.43	23.42	31.48	28.70	28.28	26.92	33.00	30.63	30.09	30.00	34.00	32.61	34.07	25.81	37.00
Nb/La	0.27	0.27	0.29	0.34	0.28	0.26	0.31	0.29	0.28	0.29	0.20	0.29	0.33	0.30	0.25
Lu/Yb	0.13	0.14	0.15	0.14	0.15	0.15	0.16	0.14	0.15	0.15	0.15	0.16	0.14	0.15	0.17
$(Nb/Nb^*)_n$	0.36	0.37	0.37	0.41	0.37	0.35	0.40	0.39	0.36	0.36	0.05	0.38	0.41	0.39	0.35
$(Ti/Ti^*)_n$	0.39	0.31	0.41	0.38	0.38	0.33	0.47	0.41	0.43	0.41	0.35	0.42	0.45	0.34	0.42
$(Zr/Zr^*)_n$	0.96	0.97	1.01	1.14	1.03	0.95	1.04	1.01	1.03	1.02	0.83	0.98	1.02	0.99	0.87

cn = chondrite normalized; n = primitive mantle normalized

6. U-Pb geochronology

Two additional basaltic samples (F1398/101 and F1398/57) collected from the Parauapebas Formation in Serra Norte, Carajás Province, were used for SHRIMP zircon U–Pb dating. Most zircon grains in these two samples have subhedral to anhedral crystal shapes, irregular surfaces, as well as common occurrence of fractures. The crystals vary in size from 100 μm to 300 μm and no inherited zircon crystal was observed. The majority of the grains are characterized by magmatic oscillatory zoning with high luminescence in the CL images (Fig. 10a, b); just one grain displayed no zoning (Fig. 10b).

Sample F1398/101 is dominated by small subhedral zircon grains (50–100 μm) with subrounded to prismatic edges. Only seven spots on well-shaped magmatic zircon grains were analyzed. Thorium and U contents are 18–206 ppm and 29–204 ppm, respectively, with Th/U ratios of 0.62–1.04. The seven analyses are basically concordant and form a single group with a Concordia age of 2749 ± 6.5 Ma (MSWD = 0.71, Fig. 10a, Table 2), which is interpreted as the crystallization age of the basalt. This age is similar to that reported by Gibbs et al. (1986), Wirth et al. (1986) and Olsewisk et al. (1989) and confirms that the basaltic lava sequence of the Parauapebas formation formed earlier than 2.77 Ga.

The sample from the lower lava (Fig. 10b) was dated at 2745 ± 5 Ma (MSWD = 0.64), whose dated grains are more scattered and discordant. These data suggest that magmatism occurred in a very short time interval (up to 10 Ma) similar to the Phanerozoic Serra Geral LIP (Thiede and Vasconcelos, 2010), which should be better investigated in future work.

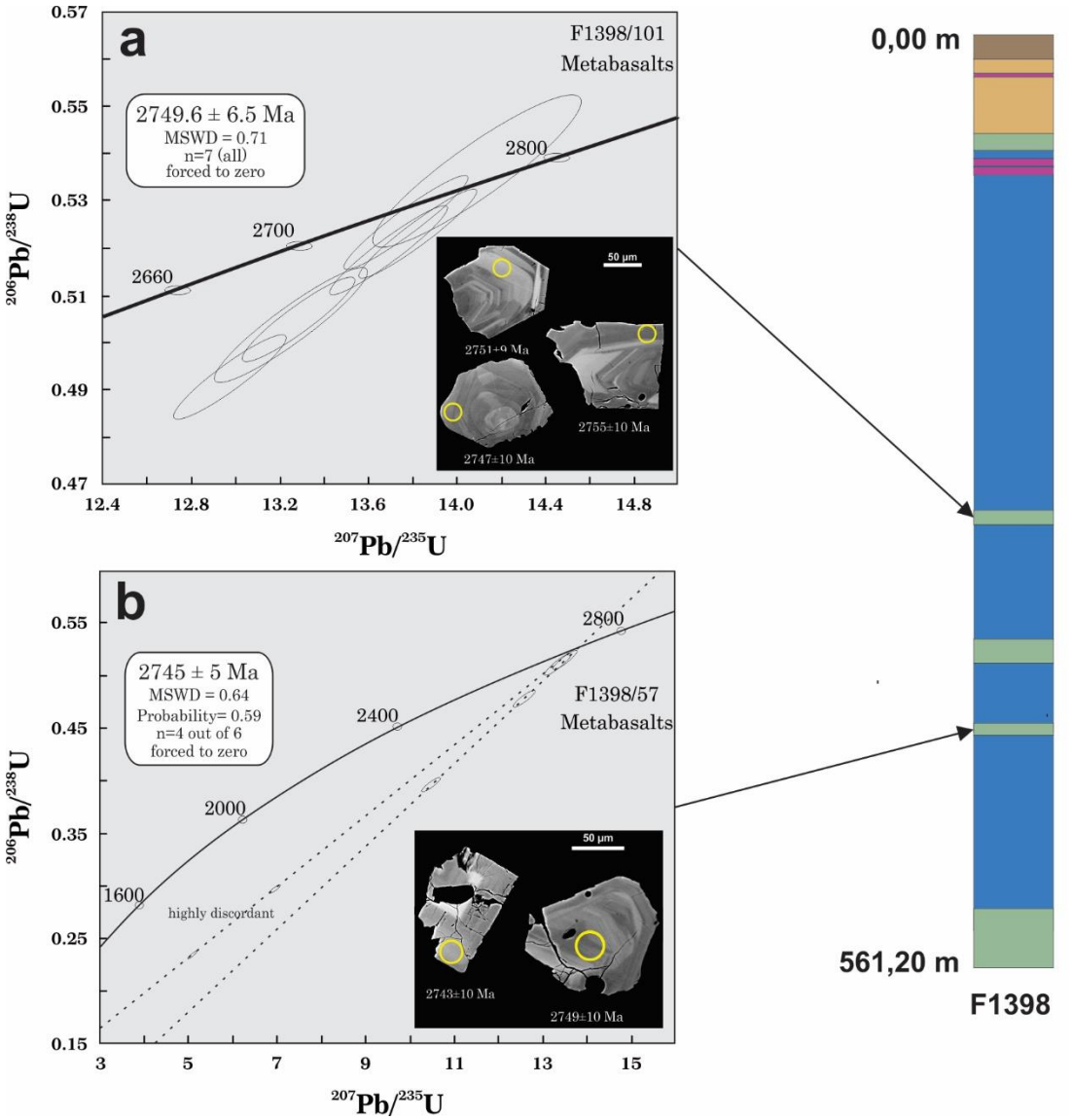

Figure 10. *SHRIMP U-Pb dating diagrams and cathodoluminescence images for the basalts from Parauapebas Formation and samples location within F1398 drill core log: a) Concordia diagram for sample F1398/101, showing a crystallization age of 2749.6 ± 6.5 Ma; b) Discordia diagram for sample F1398/57, defining discordia line with an upper intercept age of 2745 ± 5 Ma. The drill core legend is the same of figure 2.*

Table 2

SHRIMP U-Pb zircon data for Parauapebas Formation basalt sample F1398/101 and F1398/57.

Spot Name	U (ppm)	Th/U	Ages (common-Pb corrected, Ma)								
			$^{208}Pb/^{232}Th$	1σ (%)	$^{207}Pb/^{206}Pb$	±1σ	$^{206}Pb/^{238}U$	±1σ	$^{208}Pb/^{232}Th$	±1σ	Discordant (%)
F1398/101: basalt from Parauapebas Formation											
322D.1-1	135	0.91	.1413	1.8	2743	10	2720.8	34.6	2652	47	1
322D.1-2	29	0.64	.1424	3.0	2747	19	2773.2	50.6	2690	78	-1
322D.1-3	57	0.62	.1329	2.3	2750	15	2626.2	39.0	2541	64	4
322D.1-4	120	0.77	.1374	1.9	2755	10	2709.9	35.1	2597	48	2
322D.1-5	170	0.70	.1257	1.8	2751	9	2581.2	32.6	2370	43	6
322D.1-6	156	0.73	.1339	1.9	2749	10	2632.6	33.5	2499	51	4
322D.1-7	204	1.04	.1382	1.7	2752	8	2696.1	33.2	2605	43	2
F1398/57: basalt from Parauapebas Formation											
322F.1-1	133	3.71	0.0275	1.8	2749	10	2155.5	28.4	548	10	22
322F.2-1	137	0.58	0.1355	1.8	2743	10	2679.5	34.1	2520	50	2
322F.3-1	629	1.15	0.0657	1.5	2407	10	1358.9	17.4	1234	20	44
322F.4-1-3	389	0.92	0.1052	1.7	2745	9	2524.3	31.1	2016	34	8
322F.5.1	634	1.05	0.0835	1.5	2543	9	1682.4	21.2	1570	26	34
322F.6-1	67	0.66	0.1332	2.4	2737	16	2663.5	38.1	2528	60	3

Data in this table were calculated after ^{204}Pb corrections. The common Pb compositions were estimated from ^{204}Pb counting, assuming an isotopic composition of Broken Hill lead related to surface contamination (Nelson, 1997). All errors are 1 sigma (1σ).

7. Zircon mineral chemistry

Eight zircon grains were analyzed from two basaltic samples of the Parauapebas Formation F1398-101 (n=4) and F1398/57 (n=4). The major (Si, Zr and Hf) and some trace elements (including REE) abundances were in-situ analyzed at only one spot in each zircon grain, and the entire data is presented in Table 3. The two analyzed samples present Th/U ratios ranging from 0.35-1.12 (1398/101) and 0.72–1.35 (F1398/57). The Hf values are somewhat consistent for all samples ranging from 1.04 % to 1.39 % with a mean value of 1.15 %. The average values of main elements for the analyzed zircon grains are Yb = 53.38 ppm, Y = 212.41 ppm, U = 35.32 ppm, Th = 31.90, ZrO_2 = 65.08 % and SiO_2 = 33.58 %.

A criterion that has become commonly employed for distinguishing magmatic versus metamorphic zircon is the Th/U ratio. Specifically, zircon affected by metamorphic events shows considerably lower Th/U ratios (~0.1) (Hidaka et al., 2002; Rubatto, 2002). In contrast, most zircon of igneous origin have Th/U values typically within the 0.4–1.0 range (Hoskin et al., 2000; Hoskin and Schaltegger, 2003). Our zircon results (Table 3) show Th/U ratios higher than 0.3, revealing that none of the studied zircon grains have the characteristic Th/U signature of metamorphic origin and accordingly they are most plausibly magmatic. However, occurrences of high Th/U metamorphic and low Th/U magmatic zircons have been rarely reported (e.g., Hidaka et al., 2002).

Table 3

Mineral chemistry data of zircon grains for Parauapebas Formation basalt.

Sample	SiO_2 (%)	ZrO_2 (%)	Hf (%)	U (ppm)	Yb (ppm)	Y (ppm)	Th (ppm)	Dy (ppm)	Er (ppm)	Lu (ppm)	Pb (ppm)	U/Yb	Th/U
101-D_1-5	33.98	65.33	1.34	30.76	14.70	79.24	10.74	20.63	18.25	8.56	4.35	2.09	0.35
101-D_1-6	34.04	64.95	1.13	49.02	41.96	173.80	33.10	24.43	18.60	20.64	2.28	1.17	0.68
101-D_1-7	33.32	65.84	1.08	30.70	64.45	248.04	25.83	29.99	41.02	12.06	0.68	0.48	0.84
101-D_1-1	33.89	65.54	1.10	15.00	44.14	176.69	16.86	32.86	37.65	12.02	5.09	0.34	1.12
57-F_1-1	33.83	65.47	1.06	13.76	45.99	176.66	9.95	20.19	26.24	15.09	10.81	0.30	0.72
57-F_1-3	33.02	63.70	1.05	52.99	107.57	439.98	71.60	78.65	69.82	23.32	16.83	0.49	1.35
57-F_1-5	32.75	64.00	1.04	57.80	64.66	287.39	58.37	64.17	42.12	8.03	12.71	0.89	1.01
57-F_1-4	33.82	65.78	1.39	32.58	43.58	117.49	28.79	26.49	19.73	15.73	16.10	0.75	0.88

U/Yb ratios have been used to differentiate crustal zircon grains from those of oceanic origin. Grimes et al. (2007) note that zircons from different source regions have divergent U/Yb ratios, being rather low in ocean gabbros (0.18) and increasing to 1.07 in continental granitoids, and to 2.1 in kimberlite. These authors introduced a pair of discrimination diagrams based on the U/Yb ratios versus Hf and Y contents to distinguish between zircons derived from oceanic crust, continental crust, and mantle (kimberlite zircon megacrysts). Our zircons crystals plot in the continental zircon field (Fig. 11).

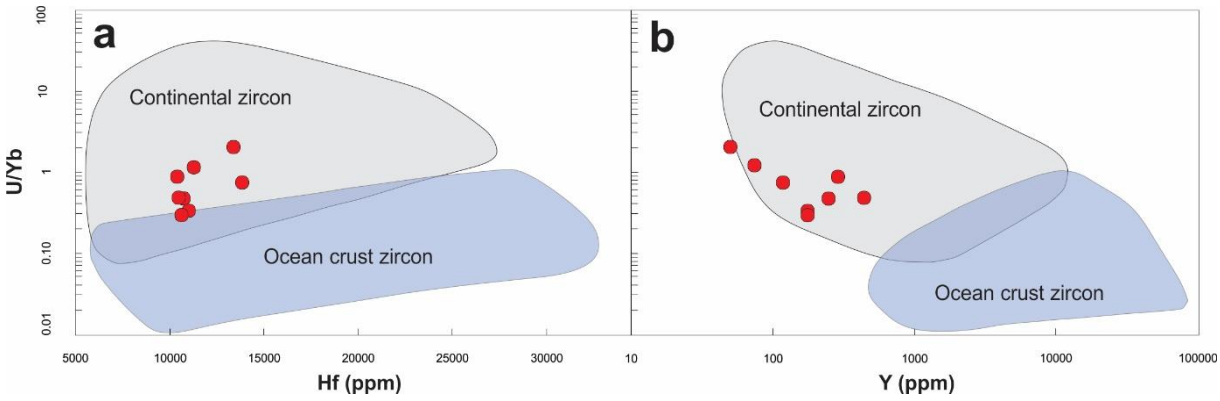

Figure 11. *Discriminant diagrams for zircon crystals from basalts of the Parauapebas Formation with continental and oceanic crust zircon fields defined by Grimes et al. (2007): a) U/Yb vs. Hf diagram; b) U/Yb vs. Y diagram.*

8. Sr and Nd isotopic data

The whole-rock Sr and Nd isotopic data are listed in Table 4. The initial isotopic ratios were calculated with the crystallization age of 2749 Ma based on the U–Pb ages of zircon grains from basalts published in this article.

All analyzed rocks (basalt samples) have $^{87}Sr/^{86}Sr(t)$ ratios varying from 0.726 to 0.729, variably negative initial εNd(t) (-1.53 to -4.11) (Fig. 12; 13a), display similar $^{147}Sm/^{144}Nd$ ratios, and render Nd model ages between 3.02 and 3.36 Ga. In the eNd(t) vs. $^{87}Sr/^{86}Sr(t)$ diagram (after Caro and Bourdon, 2010), the samples are located near the continental crust

field, except for the F1279/D sample (Fig. 12). An increase of the $^{87}Sr/^{86}Sr$ ratio could happen during subduction-related metamorphism or crustal contamination (Bebout, 2013). Given the high $^{87}Sr/^{86}Sr$ ratios, the relatively wide range of εNd(t) and Nd model ages higher than crystallization age (~2750 Ma), we consider that the primary magma must have experienced significant contamination by upper crustal rocks with low Nd isotopic values. The potential role of crustal contamination on the geochemistry of rocks from the Parauapebas Formation is discussed further.

Table 4

Sr and Nd isotopic data for the Parauapebas Formation rocks.

Sample	$^{87}Sr/^{86}Sr \pm 2E$	$^{87}Sr/^{86}Sr$ (t)	Nd ppm)	$^{147}Sm/^{144}Nd$	$^{143}Nd/^{144}Nd \pm 2E$	$\varepsilon_{Nd\ (0)}$	$\varepsilon_{Nd\ (2749)}$	T_{DM} (Ga)
F1100/172	0.72917 ± 4	0.726	36.252	0.1161	0.511100 ± 6	-30.0	-1.53	3.02
F1279/Z	0.73192 ± 4	0.729	23.04	0.1408	0.511416 ± 27	-23.8	-4.11	3.36
F1279/D	-	-	16.601	0.1337	0.511396 ± 23	-24.22	-1.95	3.16
F1398/151	0.73131 ± 4	0.728	14.525	0.1499	0.511638 ± 14	-19.5	-2.99	3.31

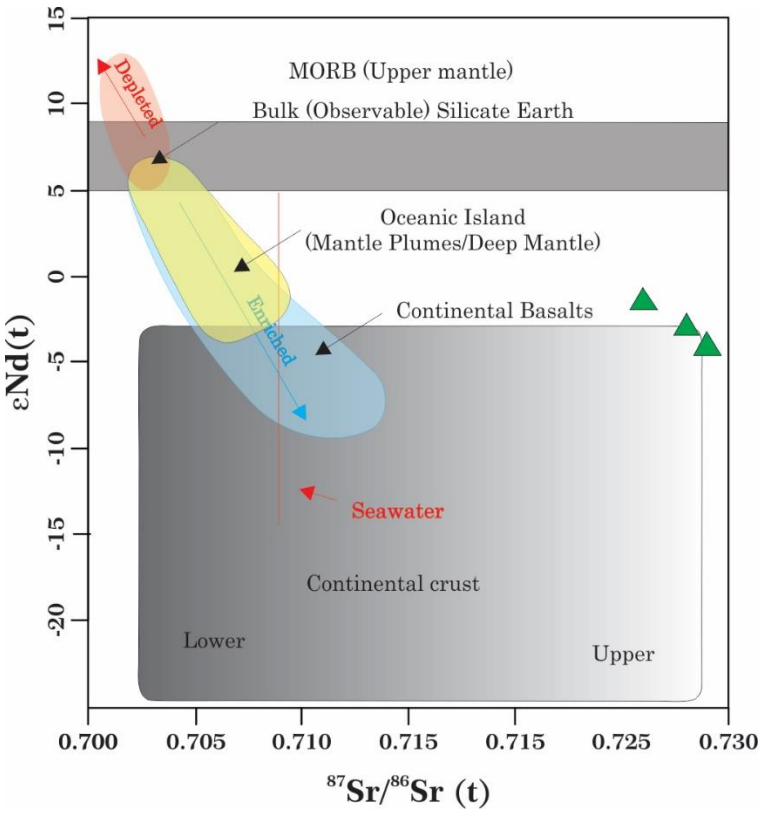

Figure 12. *εNd vs. 87Sr/86Sr (t) diagram (after Caro and Bourdon, 2010) for basalts samples from Parauapebas Formation.*

9. Discussion

9.1. Alteration and element mobility

The mobility of the major and trace elements during post-magmatic alteration is a critical concern in the study of Archean volcanic rocks (Ordóñez-Calderón *et al*., 2008; Polat and Hofmann, 2003; Polat *et al*., 2007, 2011). The volcanic rocks studied underwent moderate seafloor hydrothermal alteration and/or sub-greenschist facies metamorphism indicated by moderate LOI contents (1.77–4.40 wt.%) (Table 1), preservation of primary textures and minerals, absence of foliation, and minor replacement of the primary mineral assemblage (e.g., chloritization). It is essential to evaluate the effects of the secondary alteration on the geochemistry of the basalts accordingly before considering any petrogenetic and tectonic setting interpretations.

It is widely accepted that the concentration of HFSE (Nb, Ta, Th, Zr and Hf), REEs (mainly Gd-Lu) and some transition metals (Ni, V, Cr, Sc, Co) is not significantly changed during seafloor hydrothermal alteration and low-grade regional metamorphism (Ordóñez-Calderón *et al*., 2008; Polat and Hofmann, 2003; references therein). However, it is important for the mobility of each element to be tested since that even the immobile element may be mobilized under certain conditions (e.g. Hastie et al., 2007; Pearce, 1996). To test their mobility, we use correlation coefficients of Zr (one of the least mobile elements) versus other elements. Zr exhibits good correlations with some other elements such as HREEs, Th, Nb, Ta, Yb, U, and Hf, suggesting that these elements were relatively immobile during post-magmatic alteration. In addition, the absence of Ce anomalies, ranging from 0.90 to 1.10 (Table 1), are consistent with limited LREE mobility for the samples during secondary alteration (Polat and Hofmann, 2003). Therefore, the characteristics of these immobile elements in the studied basalts are considered useful for interpreting their original composition in this contribution.

9.2. Crustal contamination

Crustal contamination may modify the composition and isotopic character of the primary mantle derived magmas or even produce hybrid magmas that include a large proportion of crustal melt (Harris and Chaumba, 2001). High abundances of LREE, LILE (Rb, Th, U, K) and Pb, and strong depletion of Nb, Ta, and Ti are typical of contamination by crustal material (Taylor and McLennan, 1985) and this process can impart subduction-like signatures (e.g., negative Nb–Ti anomalies) and lead to the misidentification of contaminated continental intraplate basalts as arc related (Xia, 2014 and Wang *et al*., 2015). Therefore, it is pertinent to

determine the role, if any, that continental crust had in the formation of the volcanic rocks from the Parauapebas Formation before considering potential geodynamic models for the Grão-Pará basin.

Although it has been suggested that the Grão-Pará rocks exhibit evidence of crustal contamination (e.g., Gibbs et al., 1986; Olszewsky et al., 1989; Lobato et al., 2005a), the potential role of this contamination by either sub-continental lithospheric mantle, continental crust, or a combination of both on the geochemistry of the rocks throughout the Parauapebas Formation has not been assessed. The primitive mantle-normalized multi-element and chondrite-normalized REE diagrams from the Parauapebas Formation's volcanic rocks (Fig. 9a, b) show enrichment in LILE (Rb, Ba, Th, U, K) and Pb, depletion in some HFSE (Nb and Ti), and enriched LREE patterns. These trace element features are compared with the average of upper continental crust (Rudnick and Gao, 2003) as shown on Fig. 9a, b. This distribution of trace elements suggests that basaltic melts may have been modified by addition of crustal material. Additionally, the high Th content (>4.0 ppm) and Th–U positive anomaly indicate significant contamination with upper crustal materials (Rudnick and Gao, 2003). The very low Nb/La ratios (0.24 – 0.34) in all the samples (Fig. 13b) also argues the possibility of extensive contamination by upper crustal materials (Xia et al., 2014). This is further supported by the tight correlation observed between Nb/La and other geochemical indices of crustal contamination, such as εNd(t), La/Sm and SiO_2 (Fig. 13a, c, d). Furthermore, the high $^{87}Sr/^{86}Sr$ ratios, the relatively wide range of εNd(t) (−1.53 to −4.11) and Nd model ages between 3.02 and 3.36 Ga (Fig. 12; Table 4) provide additional evidence that the Parauapebas Formation`s primary magma must have experienced significant contamination of upper crustal rocks with low Nd isotopic values.

Accordingly, all the lines of evidence above indicate that the original mantle melt for the Parauapebas Formation's basalts was more likely contaminated by basement rocks (gneisses and migmatites), which could be those of the ca. 3.0 Ga Xingu Complex, probably during its ascent through the continental crust. Therefore, the arc-like features (e.g., HFSE depletion) that have been observed may have originated from contamination by crustal materials during the migration of the Parauapebas Formation`s magma rather than from a subduction modified magma source, although we cannot preclude the assimilation of the metasomatized subcontinental lithospheric mantle.

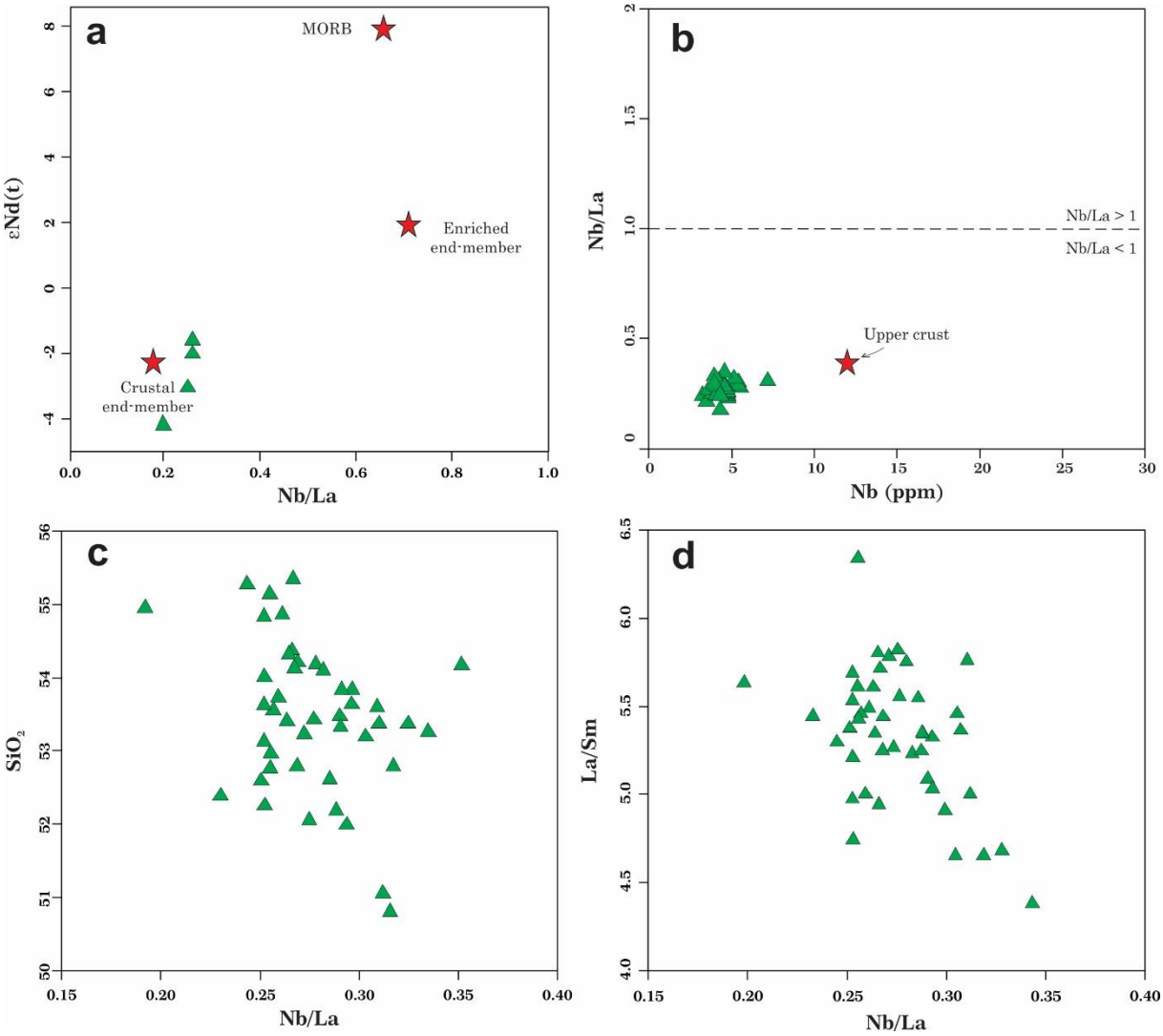

Figure 13. *Plots of some crustal contamination index for the Parauapebas Formation basalts: a) εNd (t) vs. Nb/La, MORB, enriched endmember and crustal endmember after Hawkesworth et al. (1984); b) Nb/La vs. Nb, data for average upper continental crust from Rudnick and Gao (2003); c) La/Sm vs. Nb/La; d) SiO2 vs. Nb/La.*

9.3. Tectonic setting

The tectonic setting of the volcano-sedimentary sequences of the Carajás Basin is highly debated. Some authors considered this extensive basaltic volcanism to be result from an intra-plate rifting of older continental crust (DOCEGEO, 1988; Gibbs et al., 1986; Macambira, 2003; Olszewski et al., 1989; Tavares, 2015), whereas others consider that the volcanism was formed in a subduction related environment (Lobato et al., 2005; Meirelles & Dardenne, 1991, Teixeira and Eggler, 1994; Zucchetti, 2007).

As we have shown, the geochemical characteristics of the Neoarchean Parauapebas Formation basaltic lavas demonstrate that it is more likely that they were contaminated by continental crust, although contamination by subduction-metasomatized sub-continental

lithospheric mantle must not be entirely ruled out. Regardless, both scenarios indicate the presence of continental lithosphere throughout the region at the time of emplacement of the Parauapebas' volcanic rocks. A continental setting is further supported by WDS zircon results that demonstrated that the analyzed zircon crystallized from a mantle-derived magmas emplaced into continental crust (Fig. 11). Intense seafloor hydrothermal alteration, presence of amygdaloidal vesicles in the basalts and their spatial association with BIF suggest a submarine environment.

As we have mentioned, the contamination by continental crust can impart subduction-type signatures (e.g., Nb and Ti depletion) and lead to incorrectly characterizing tectonic setting (Xia et al., 2014; Wang et al., 2015 and references therein). Hence, the use of some arc-like geochemical signatures to discriminate between continental intraplate basalts and arc basalts should be cautioned. For instance, when the geochemical diagrams using some sensitive trace elements, such as Th, Nb, Ta and Ti, as discriminating factors are utilized, the Parauapebas Formation's volcanic rocks (contaminated basalts) displace into the arc related basalts field [e.g., the Th/Yb vs. Nb/Yb diagram (Pearce, 2008); Fig. 14], leading to the misidentification of their tectonic setting

Therefore, it is very important for us to eliminate the effect of contamination of continental crust and to investigate how to correctly characterizing tectonic setting from Parauapebas Formation`s basalts. Some authors, as Xia et al. (2014) and Wang et al. (2015), explored this issue in others ancient continental basalts (eg. Siberian, Karoo, Deccan, Emeishan, and Basin and Range basalts) and propose some geochemical criteria to distinguish continental basalts from arc related ones. One of the main criteria cited is the use of discrimination diagrams that do not use these sensitive elements (e.g., Th, Nb, Ta and Ti), such as Zr/Y-Zr binary diagram (after Pearce and Norry, 1979).

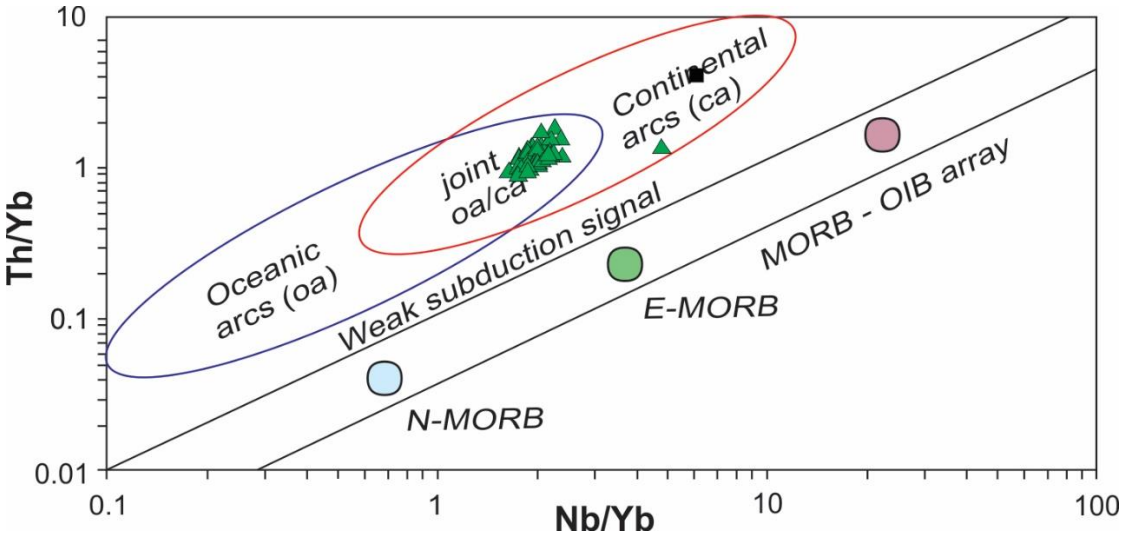

Figure 14. *Th/Yb vs. Nb/Yb diagram (Pearce, 2008) for Parauapebas Formation's basalts (see detailed discussion in the text). N-MORB: Normal mid-ocean ridge basalts, E-MORB: Enriched mid-ocean ridge basalts, OIB: Ocean island basalts. Black point represents average upper continental crust (Rudnick and Gao, 2003).*

Accordingly, we decided to use this suggested discrimination diagram (Zr/Y-Zr binary diagram) and FeO_T–MgO–Al_2O_3 triangular discrimination diagram (Pearce et al., 1977). The former diagram as a reference, and the latter for comparison. According to the Zr/Y-Zr diagram, most samples plot in the within-plate basalt's field (Fig. 15a), suggesting that the Parauapebas Formation's basalts were formed in an anorogenic tectonic setting. In the FeO_T–MgO–Al_2O_3 discrimination diagram, almost all samples also fall in the field of within-plate basalts (Fig. 15b), further supporting the nature of intraplate magmatism. Furthermore, their concentrations of incompatible trace elements are visibly higher than those of subduction-zone basalts, and their primitive mantle-normalized trace element distribution patterns without prominent Zr depletion and Sr enrichment (Fig. 9a) that distinguish them from the arc-related ones (Xia et al., 2014; Wang et al., 2015). Therefore, considering the geochemical features shown, these basalts were most likely formed in continental rifting, rather than in arc-like environment, formed earlier than 2.76 Ga.

However, the origin of a continental rift could not be linked only to a mantle plume event, but also may be linked to a transition from a collisional to post-collisional environment (Merle, 2011). In this latter case, the hypothesis of contamination by subduction-metasomatized sub-continental lithospheric during the orogenic event could be considered.

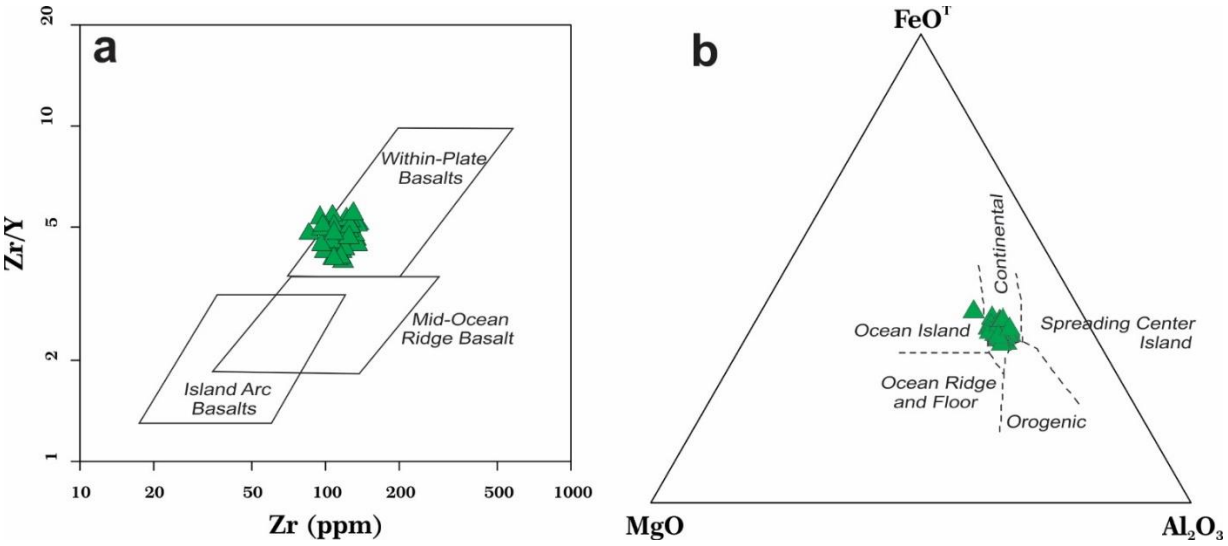

Figure 15. *Tectonic discriminant diagrams for the Parauapebas basaltic rocks: a) Zr/Y vs. Zr (after Pearce and Norry, 1979); b) MgO-FeOT-Al2O3 diagram (after Pearce et al., 1977) (see detailed discussion in the text).*

9.4. Geodynamic implications for Carajás Basin

Based on the geochemical, and petrological characteristics discussed above, the basaltic rocks of the Parauapebas Formation represent a magmatism formed in continental rift basin, which must have experienced significant contamination of upper crustal rocks. This rift basin likely formed in an extensional regime related to the post-orogenic setting following the collision between the Rio Maria and Carajás Domains in the passage from the Mesoarchean to the Neoarchean, as suggested by Tavares (2015). The following paragraphs will to debate this tectonic setting interpretation.

Some particular features that are common in "Archean rifts" around the world (Hartlaub et al., 2004), are very similar to those observed in the Carajás Basin, where the basalts of the Parauapebas Formation are deposited, such as the presence of old sialic basement, which imprints geochemical and isotopic signature of crustal contamination in the supracrustal sequences, as well as the bimodal nature of the volcanic packages. Furthermore, the stratigraphic sections are also very similar. From bottom upward, the stratigraphy in most Archean rifts is marked by basement rocks that are overlain by a sequence of continental to shallow-water sedimentary rocks. Pillowed to massive mafic volcanic rocks with a minor component of komatiitic, felsic volcanic and/or intrusive rocks and banded iron formation generally overlie the shallow-water sedimentary rocks. At the top, these rocks are overlain by a package of interbedded marine environment sedimentary and volcanic rocks (Hartlaub et al., 2004).

Previous studies consider that the Parauapebas Formation volcanism was formed in a subduction related environment (Lobato et al., 2005; Meirelles & Dardenne, 1991, Teixeira and Eggler, 1994; Zucchetti, 2007). They demonstrated that these volcanic rocks plot within a calc-alkaline/shoshonitic series field and an arc setting in various discrimination diagrams. As we have shown, this is happened because contamination by continental crust or lithosphere can impart subduction-like signatures (e.g., low Nb, low Ta and low Ti) and lead to the misidentification of contaminated continental intraplate basalts as arc related (Xia, 2014; Wang et al., 2015 and references therein).

As already mentioned, we consider that the basaltic volcanism from the Parauapebas Formation is a result of the rifting of older continental crust. Nevertheless, the hypothesis that this volcanism originated by shallow decompression mantle melting related to the opening of a back-arc continental basin in the Neoarchean (Lobato et al., 2005; Zucchetti, 2007) cannot be ruled out. One step ahead from the indication that extensive basaltic volcanism is a result from a rift-related setting, and therefore no associated to the back-arc continental environment, is the absence of arc-related plutonism in the assemblages from Neoarchean Carajás.

If the volcanism from the Parauapebas Formation, and consequently the Carajás Basin, originated from a continental rift process, then the question is whether the rift process may be linked to a mantle plume event or a transition from a collisional to post-collisional environment, followed by rifting. This latter is typically considered to result from delamination of lithospheric mantle and lower crust or slab breakoff (e.g. Rudnick and Gao, 2003) accompanied by upwelling of asthenospheric mantle. It is known that Rio Maria Domain collided with the Carajás Domain in the Mesoarchean (~2870 to 2830 Ma, Feio et al., 2013). Thus, we infer that the formation of this basin should be controlled by interactions between the Rio Maria and Carajás Domains, and therefore, the hypothesis of slab breakoff associated to this Mesoarchean orogeny is more likely. Due the generation of large mafic volcanism and A-type granites, it is known that this rift magmatism was expressive, associated with a considerable melting volume induced by underplating in the lower crust of mafic mantle magmas, as suggested by Feio et al. (2012).

It is widely accepted that the mafic-ultramafic layered complexes (e.g. Lago Grande, Luanga, Vermelho complexes), near the borders of the Carajás Basin, represent a major magmatic event coeval to the extensive basaltic volcanism of the Grão Pará Group (Machado et al., 1991; Ferreira Filho et al., 2007; Teixeira et al., 2015), and therefore associated to the same regional tectonic setting. These layered intrusions have Neoarchean ages (e.g., Machado

et al., 1991; Teixeira, 2013; Teixeira et al., 2015) that overlap with the ca. 2.75 Ga extensive basaltic magmatism of the Carajás Basin and were also contaminated by crustal material during the ascent and/or emplacement of the mafic-ultramafic magma (Ferreira Filho et al., 2007; Teixeira et al., 2015). Disregarding specific magma generation conditions, these results are consistent with a large volume of magma being transferred through continental crust in the Carajás Basin region (Teixeira et al., 2015). Ferreira Filho et al. (2007) and Teixeira et al. (2015) suggested that the mafic-ultramafic magmatism in Carajás is associated with intra-plate rifting of older continental crust, thus the layered intrusions could be related with a mantle upwelling and an incipient seafloor installation during rift process. This interpretation also argues that Carajás Basin originated from a continental rift process.

Based on the above features, the most possible setting for the formation of the Carajás Basin is the rift-related continental basin formed at ca. 2.75 Ga, and later closed possibly by collisional process. The rifting process is likely the result of a slab breakoff associated to a Rio Maria-Carajás Collision (Fig. 16) in the switch from compressional to extensional setting passage from the Mesoarchean to the Neoarchean. On the other hand, the exact time of the basin closure remains uncertain. Some authors interpreted the Neoarchean granites, intrusive into the Grão Pará Basin, as syntectonic and deformed during its emplacement and cooling at ~2.75 to ~2.73 Ga (Barros et al., 2009; Dall'Agnol et al., 2016), whereas Tavares (2015) interpreted as rift-related distensional intrusions which were deformed and metamorphosed at ~2.68–2.63 Ga, during the closure of the Carajás Basin.

In this scenario, the Carajás and Rio Maria domains (Fig. 16a) collided in the late stage of the Mesoarchean (Fig. 16b), thickening the lithosphere of the Carajás Province area and leading to a gravitational instability, which provided the driving force for the slab breakoff start (Fig. 16a). Following crustal thickening and subsequent slab breakoff (Fig. 16b), the asthenosphere upwelled and provided heat leading to partial melting of the lithospheric mantle (Fig. 16c). In the first stages of rifting (~2.76; Fig. 16c), the partial melting continued regionally, and parental magmas of mafic and ultramafic rocks were produced owing to decompression. Consequently, these magmas were emplaced along faults and formed the mafic rocks of the Parauapebas Formation and mafic-ultramafic layered complexes. Afterwards, in the course of rifting (Fig. 16d) occur the deposition of banded iron formations (Carajás Formation), bimodal magmatism, which occur concurrently beneath Carajás Formation, and A-type granitic magmatism. This latter resulted from partial melting of continental crust owing to the under-plating of mantle-derived magma.

Therefore, a switch from compressional to extensional setting in the passage from the Mesoarchean to the Neoarchean is suggested for the formation of the Carajás basin.

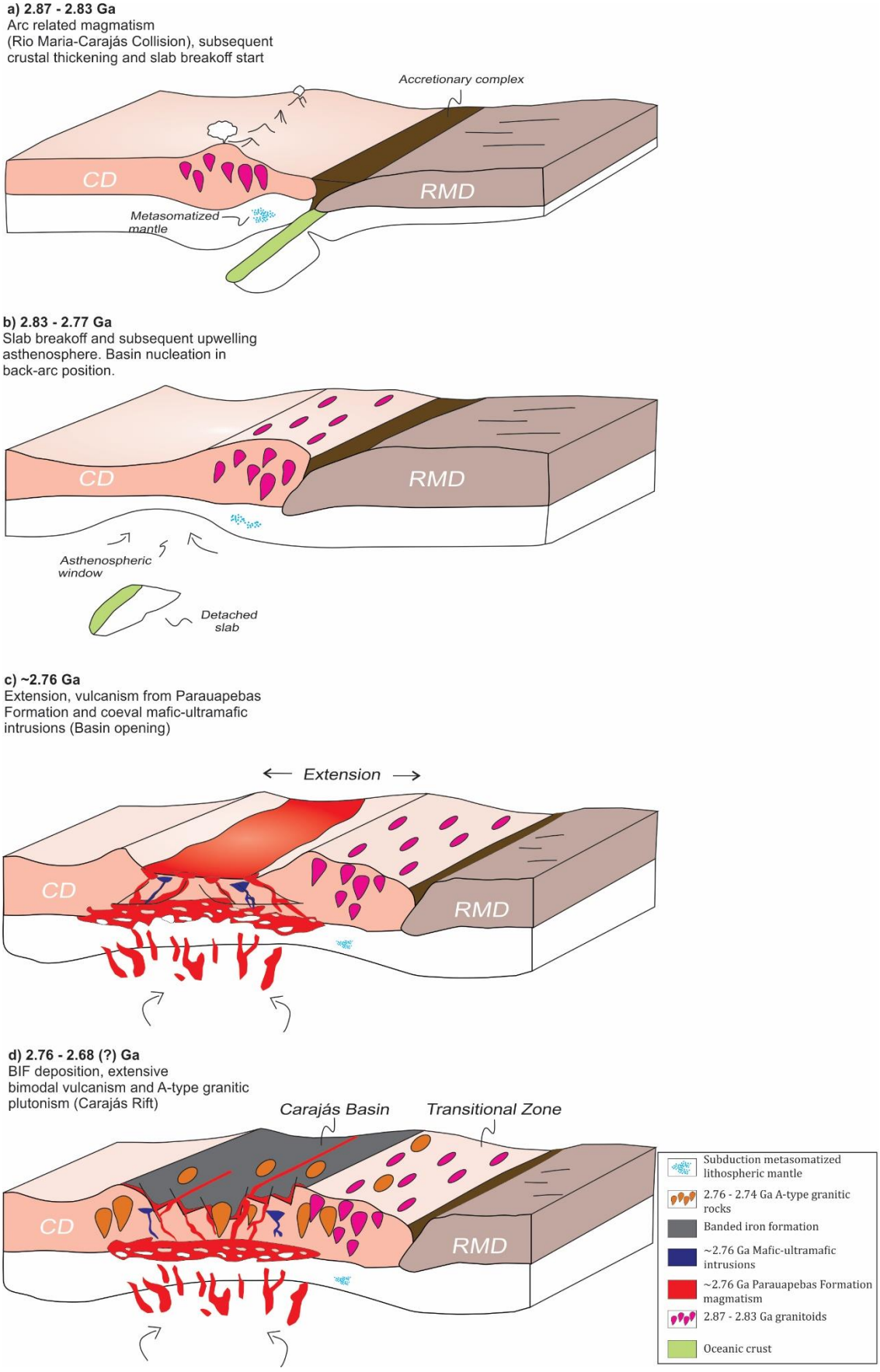

Figure 16. *Tectonic evolution model for the Carajás Basin. See text for detailed discussions.*

10. Conclusions

The following conclusions are drawn based on the petrographic, geochemical and isotopic characteristics of the mafic volcanic rocks of the Neoarchean (~ 2.75) volcano-sedimentary sequence of the Grão Pará Group:

1. The Parauapebas Formation basalts occur in extensive succession of massive or amygdaloidal lava flows with at least 370 m in thickness, which eleven cycles were identified by massive texture at the bottom and amygdaloidal and spilitization (seawater metasomatic alteration) zones at the top. Even though seafloor hydrothermal alteration processes and/or sub-greenschist metamorphism have affected these rocks, they still preserve their primary igneous textures and primary mineral assemblage. The primary igneous textures are largely amygdaloidal, intergranular and intersertal and rarely microporphyritic. The primary mineral assemblages consist predominantly of clinopyroxene and plagioclase (labradorite – andesine An_{40-55}) with minor quartz, K-feldspar, ilmenite, magnetite and rare pirite, titanite and zircon present as accessory minerals. Albite, chlorite, Fe-epidote, quartz and calcite are the main secondary minerals, being interpreted as products of seafloor hydrothermal alteration and/or sub-greenschist metamorphism.

2. SHRIMP zircon U–Pb dating constrains the Early Neoarchean crystallization ages of 2749 ± 6.5 and 2745 ± 5 Ma for mafic volcanic rocks. These ages are similar to the ages reported by Gibbs et al. (1996), Wirth et al. (1986) and Olsewisk et al. (1989) and confirm that the basaltic lava sequence of the Parauapebas formation formed earlier than 2.77 Ga.

3. The characteristics of Zr, Nb, Hf, Th, Ti, Y, Yb, LREE and HREE in the basalts are considered to be useful for interpreting their original composition, even though they underwent seafloor hydrothermal alteration, metamorphism and post metamorphic alteration.

4. Major and trace element geochemistry and Sr-Nd isotopic data suggest that the basaltic rocks were derived from the subcontinental lithospheric mantle affected by upper continental crustal components. The arc-like signatures observed, such as HFSE depletion, may have originated from crustal contamination during the migration of the Parauapebas Formation magma rather than a subduction modified magma source, although contamination by subduction-metasomatized sub-continental lithospheric mantle, previously modified in the Mesoarchean (Rio Maria-Carajás Collision), cannot be entirely ruled out.

5. The Parauapebas Formation basalts were most likely produced within a continental tectonic setting, rather than in a subduction environment. This basaltic volcanism is more plausible as a result from intra-plate rifting of older continental crust.

6. A switch from compressional to extensional tectonic setting in the passage from the Mesoarchean to the Neoarchean is suggested for the deposition of volcano-sedimentary sequences from the Carajás basin. It is formed in an extensional regime related to the continental rift setting at ca. 2.75 Ga and later closed possibly by colisional process at the Neoarchean. The rifting process could be associated to a slab breakoff related to a Rio Maria-Carajás Collision.

Acknowledgments

The authors would like to acknowledge the help of the Vale S.A. mining company and CNPq (Conselho Nacional de Desenvolvimento Científico), for supporting this work. Analytical facilities of the Instituto de Geociências of the Universidade de Brasília (UnB) provided additional support for this research. Pedro L. G. Martins held a scholarship from Coordenação de Aperfeiçoamento de Pessoal de Nível Superior (CAPES) and this study is part of his M.Sc. dissertation developed at the Instituto de Geociências (Universidade de Brasília).

References

Almeida, J.A.C., Dall'Agnol, R., Oliveira, M.A., Macambira, M.J.B., Pimentel, M.M., Rämö, O.T., Guimarães, F.V., Leite, A.A.S., 2011. Zircon geochronology and geochemistry of the TTG suites of the Rio Maria granite-greenstone terrane: implications for the growth of the Archean crust of Carajás Province, Brazil. Precambrian Research 187, 201–221.

Almeida, J.A.C., Dall'Agnol, R., Leite, A.A.S., 2013. Geochemistry and zircon geochronology of the Archean granite suites of the Rio Maria granite-greenstone terrane, Carajás Province, Brazil. Journal of South American Earth Sciences 42, 103–126.

Althoff, F.J., Barbey, P., Boullier, A.M., 2000. 2.8-3.0 Ga plutonism and deformation in the SE Amazonian craton: the Archean granitoids of Marajoara (Carajás Mineral province, Brazil). Precambrian Research 104, 187–206.

Araújo, O.J.B., Maia, R.G.N., João, X.S.J., Costa, J.B.S., 1988. A megaestruturação arqueana da Folha Serra dos Carajás. Congresso Latino Americano de Geologia, Belém-Brazil, Anais, pp. 324–338 (in Portuguese).

Araújo, O.J.B., Maia, R.G.N., 1991. Projeto especial mapas de recursos minerais, de solos e de vegetação para a área do Programa Grande Carajás; Subprojeto Recursos Minerais; Folha SB.22-Z-A Serra dos Carajás - Estado do Pará. DNPM/CPRM, Brasilia 136 pp. (in Portuguese).

Arndt, N.T., 1994. Archean komatiites. In: Condie, K.C. (Ed.), Archean Crustal Evolution. Elsevier, Amsterdam, pp. 11–44.

Barros, C.E.M., Sardinha, A.S., Barbosa, J.P.O., Macambira,M.J.B., 2009. Structure, petrology, geochemistry and zircon U/Pb and Pb/Pb geochronology of the synkinematic Archean (2.7 Ga) A-type granites from the Carajás Metallogenic Province, northern Brazil. The Canadian Mineralogist 47, 1423–1440.

Bédard H.D., Brouillette P., Madore L. & Berclaz A. 2003. Archean cratonization and deformation in the northern Superior Province, Canada: an evaluation of plate tectonic versus vertical tectonic models. Precambrian Research 127: 61-88.

Beisiegel, V.R., Bernardelli, A.L., Drummond, N.F., Ruff, A.W., Tremaine, J.W. 1973. Geologia e Recursos Minerais da Serra dos Carajás. Revista Brasileira de Geociências, 3: 215-242 (in Portuguese).

Cann, J.R., 1970. Rb, Sr, Zr and Nb in some ocean floor basaltic rocks. Earth Planet. Sci. Lett. 10, 7–11.

Dall'Agnol, R., Oliveira, M.A., Almeida, J.A.C., Althoff, F.J., Leite, A.A.S., Oliveira, D.C., Barros, C.E.M., 2006. Archean and Paleoproterozoic granitoids of the Carajás Metallogenic Province, eastern Amazonian craton. Symposium on Magmatism, Crustal Evolution, and Metallogenesis of the Amazonian Craton, Abstracts Volume and Field Trips Guide (150 pp.).

Dall'Agnol, R., Oliveira, D.C., Guimarães, F.V., Gabriel, E.O., Feio, G.R.L., Lamarão, C.N., Althoff, F.J., Santos, P.A., Teixeira, M.F.B., Silva, A.C., Rodrigues, D.S., Santos, M.J.P., Silva, C.R.P., Santos, R.D., Santos, P.J.L., 2013. Geologia do Subdomínio de Transição do Domínio Carajás – Implicações para a evolução arqueana da Província Carajás - Pará. SBG, Simpósio de Geologia da Amazônia 13. CDrom, Anais, Belém (in Portuguese).

Dall'Agnol, R., et al., Mineralogy, geochemistry, and petrology of Neoarchean ferroan to magnesian granites of Carajás Province, Amazonian Craton: The or..., Lithos (2016), http://dx.doi.org/10.1016/j.lithos.2016.09.032

Dardenne, M.A., Ferreira Filho, C.F., Meirelles, M.R., 1988. The role of shoshonitic and calc-alkaline suites in the tectonic evolution of the Carajás District, Brazil. Journal of South American Earth Sciences 1, 363–372.

DePaolo, D.J., 1981. Neodymium isotopes in the Colorado Front Range and implications for crust formation and mantle evolution in the Proterozoic. Nature 291, 193-197.

Dias, GS, Macambira, MB, Dall'Agnol, R, Soares, ADV, Barros, CEM, 1996, Datações de zircões de sill de metagabro: comprovação de idade arqueana da Formação Águas Claras, Carajás, Pará. In: Simpósio de Geologia da Amazônia, 5, Sociedade Brasileira de Geologia, Belém, pp. 376-378 (in Portuguese).

Dilek, Y., Furnes, H., 2011. Ophiolite genesis and global tectonics: geochemical and tectonic fingerprinting of ancient oceanic lithosphere. Geo.l Soc. Am. Bull. 123, 387–411.

Dilek, Y., Polat, A., 2008. Suprasubduction zone ophiolites and Archean tectonics. Geology 36, 431–432.

DOCEGEO - Rio Doce Geologia e Mineração, 1988. Revisão Litoestratigráfica da Província Mineral de Carajás. 35° Congresso Brasileiro de Geologia, Belém, Brasil, Anais, Sociedade Brasileira de Geologia, pp. 11–59 (in Portuguese).

Feio, GRL, Dall'Agnol, R, Dantas, EL, Macambira, MJB, Gomes, ACB, Sardinha, AS, Oliveira, DC, Santos, RD, e Santos, PA., 2012, Geochemistry, geochronology, and origin of the Neoarchean Planalto Granite suite, Carajás, Amazonian craton: A-type or hydrated charnockitic granites?. Lithos, 151: 57-73.

Feio, G.R.L., Dall'Agnol, R., Dantas, E.L., Macambira, M.J.B., Santos, J.O.S., Althoff, F.J., Soares, J.E.B., 2013. Archean granitoid magmatism in the Canaã dos Carajás area: implications for crustal evolution of the Carajás province, Amazonian craton, Brazil. Precambrian Research 227, 157–185.

Ferreira Filho, C.F., Cançado, F., Correa, C., Macambira, E.M.B., Siepierski, L., Brod, T.C.J., 2007. Mineralizações estratiformes de EGP-Ni associadas a complexos acamadados em Carajás: os exemplos de Luanga e Serra da Onça. Publitec Gráfica & Editora, Contribuições à Geologia da Amazônia vol. 5, pp. 01–14 (in Portuguese).

Figueiredo e Silva, R.C.F. 2004. Caracterização petrográfica e geoquímica de jaspilitos e minérios de ferro dos depósitos N1, N4W, N4E e N5E, Província Mineral Carajás, Pará: implicações para a mineralização de ferro. Unpublish, M.Sc. Thesis, Instituto de Geociências, Universidade Federal de Minas Gerais, 151 p (in Portuguese).

Figueiredo e Silva, R.C., Lobato, L.M., Rosière, C.A., 2008. A hydrothermal origin for the jaspilite-hosted giant Sierra Norte deposits in the Carajás Mineral Province, Para State, Brazil. Rev. Econ. Geol. 15, 255–290.

Furnes, H., de Wit, M., Staudigel, H., Rosing, M., Muehlenbachs, K., 2007. A vestige of Earth's oldest ophiolite. Science 315, 1704–1707.

Furnes, H., Rosing, M., Dilek, Y., de Wit, M., 2009. Isua supracrustal belt (Greenland) - a vestige of a 3.8 Ga suprasubduction zone ophiolite, and the implications for Archean geology. Lithos 113, 115–132.

Furnes, H., Dilek, Y., de Wit, M., 2015. Precambrian greenstone sequences represent different ophiolite types. Gondwana Research, v. 27, Issue 2, Pages 649-685.

Gabriel, E.O., Oliveira, D.C., Santos, M.S., 2014. Sanukitoides mesoarqueanos de Água Azul do Norte, Sul do Domínio Carajás: Novos dados e perspectivas. SBG, Congresso Brasileiro de Geologia 47. CDrom, Anais, Salvador (in Portuguese).

Galarza, M.A.; Macambira, M.J.B., 2002. Geocronologia e evolução crustal da área do depósito de Cu-Au Gameleira, Província Mineral de Carajás (Pará), Brasil. Revista do Instituto de Geociências da USP, 2:143-159 (in Portuguese).

Gibbs, A.K., Wirth, K.R., Hirata, W.K., Olszewski Jr., W.J., 1986. Age and composition of the Grão Pará Group volcanics, Serra dos Carajás. Revista Brasileira de Geociências 16, 201–211.

Gioia, S.M.C.L., Pimentel, M.M., 2000. The Sm-Nd isotopic method in the geochronology laboratory of University of Brasilia. An. Acad. Bras. Ciênc. 72, 219-245.

Grainger, C.J., Groves, D.I., Tallarico, F.H.B., Fletcher, I.R., 2008. Metallogenesis of the Carajás Mineral Province, Southern Amazon Craton, Brazil: varying styles of Archean through paleoproterozoic to neoproterozoic base and precious-metal mineralization. Ore Geol. Rev. 33, 451-489.

Grimes, C.B.; Jhon, B.E.; Kelemen, P.B.; Mazdab, F.K.; Wooden, J.L.; Cheadle, M.J.; Hangoj, K.; Scwartz, J.J.; 2007. Trace element chemistry of zircons from oceanic crust: A method for distinguishing detrital zircon provance. Geology 35, 643-646.Harker A. (ed.). 1909. The natural history of the igneous rocks. NewYork, Macmillan, 384 p.

Hartlaub, R.P., Heamana, LM, Ashton KE, Chacko T, 2004. The Archean Murmac Bay Group: evidence for a giant Archean rift in the Rae Province, Canada. Precambrian Research, 131: 345–372

Harris C., Chaumba JB (2001) Crustal contamination and fluid-rock interaction during the formation of the Platreef, northern limb of the Bushveld Complex, South Africa. J Petrol 42: 1321-1347.

Hastie, A.R., Kerr, A.C., Pearce, J.A., Mitchell, S.F., 2007. Classification of altered island arc rocks using immobile trace elements: development of the Th–Co discrimination diagram. J. Petrol. 48, 2341–2357.

Hidaka, H.; Shimizu, H.; Adachi, M.; 2002. U–Pb geochronology and REE geochemistry of zircons from Palaeoproterozoic paragneiss clasts in the Mesozoic Kamiaso conglomerate, central Japan: evidence for an Archean provenance. Chem. Geol. 187, 279–293.

Hirata, W.K. 1982. Geologia Regional. In: Bernardelli, A.L. (coord.), Província Mineral de Carajás – Pará: depósitos de ferro, manganês, cobre, ouro, níquel e bauxita. SBG, Simpósio de Geologia da Amazônia, 1, Belém, Anexo aos Anais, p. 9-20 (in Portuguese).

Hoskin, P.W.O.; Kinny, P.D.; Wyborn, D.; Chappell, B.W. 2000. Identifying accessory mineral saturation during differentiation in granitoid magmas: an integrated approach. J. Petrol. 41, 1365–1396.

Hoskin, P.W.O.; Schaltegger, U.; 2003. The composition of zircon and igneous and metamorphic petrogenesis. In: Hanchar, J.M., Hoskin, P.W.O. (Eds.), Zircon.: Reviews in Mineralogy and Geochemistry, 53. Mineralogical Society of America, Chantilly, Virginia, pp. 27–62.

Irvine, T.N., Baragar, W.R.A., 1971. A guide to the chemical classification of the common volcanic rocks. Can. J. Earth Sci. 8, 523–548.

Janoušek V., Farrow C.M., Erban V. 2006. Interpretation of whole-rock geochemical data in igneous geochemistry: introducing Geochemical Data Toolkit (GCDkit). J Petrol 47:1255–1259

Janoušek V., Farrow C.M., Erban V, Trubač J. 2011. Brand new Geochemical Data Toolkit (GCDkit 3.0)—is it worth upgrading and browsing documentation? (Yes!). Geol výzk Mor Slez 18:26–30

Jenner, F.E., Bennett, V.C., Yaxley, G., Friend, C.R.L., and Nebel, O., 2013. Eoarchean within-plate basalts from southwest Greenland: Geology, v. 41, p. 327–330.

Kusky, T.M., 2004. Epilogue: What if anything have we learned about Precambrian ophiolites and early Earth processes? In: Kusky T.M. (Ed.), Precambrian Ophiolites and Related

Rocks, Developments in Precambrian Geology, Vol. 13 (K.C. Condie, Series Editor), Elsevier B.V., Amsterdam, pp.727-637.

Lafon, J.M., Macambira, M.J.B., Pidgeon, R.T., 2000. Zircon U–Pb SHRIMP dating of Neoarchean magmatism in the southwestern part of the Carajás Province (eastern Amazonian Craton, Brazil). 30th International Geological Congress, Abstract Volume, CD-ROM.

LeBas, M.J., LeMaitre, R.W., Streckeisen, A., and Zanettin, B., 1986. A chemical classification of volcanic rocks based on the total alkali-silica diagram: Journal of Petrology, v. 27, p. 745-750.

Lindenmayer, Z.G., Laux, J.H., Teixeira, J.B.G. 2001. Considerações sobre a origem das Formações Ferríferas da Formação Carajás, Serra dos Carajás. Revista Brasileira de Geociências, 31: 21-28 (in Portuguese).

Lobato, L.M., Rosière, C.A., Silva, R.C.F., Zucchetti, M., Baars, F.J., Seoane, J.C.S., Rios, F.J., Pimentel, M., Mendes, G.E. e Monteiro, A.M., 2005, A mineralização hidrotermal de ferro da Província Mineral de Carajás - controle estrutural e contexto na evolução metalogenética da Província. In: Marini, J.O.; Queiróz, E.T.; Ramos, W.B. (eds.), Caracterização de distritos mineiros da Amazônia. DNPM-CT-Mineral-ADIMB, 25–92 (in Portuguese).

Ludwig, K.R., 2001. SQUID version 1.02 A geochronological Toolkit for Microsoft Excel. Berkley Geochronological Centre Special Publication 2, pp. 19.

Ludwig, K.R., 2003. User's manual for Isoplot 3.00: a geochronological toolkit for Microsoft Excel. In: Berkeley Geochronology Center Special Publication, pp. 1-70.

Macambira, J.B. 2003. O ambiente deposicional da Formação Carajás e uma proposta de modelo evolutivo para a Bacia Grão Pará. Unpublish, Ph.D. Thesis, Instituto de Geociências, Universidade Estadual de Campinas, 217p.

Macambira, M.J.B., Lafon, J.M., 1995. Geocronologia da Província Mineral de Carajás; Síntese dos dados e novos desafios. Boletim do Museu Paraense Emílio Goeldi 7, 263–287 (in Portuguese).

Machado, N., Lindenmayer, Z.G., Krogh, T.E., Lindenmayer, D., 1991. U–Pb geochronology of Archean magmatism and basement reactivation in the Carajás area, Amazon shield, Brazil. Precambrian Research 49, 329–354.

Meirelles, M.R., Dardenne, M.A. 1991. Vulcanismo basáltico de afinidade shoshonítica e ambiente de arco arqueano, Grupo Grão-Pará, Serra dos Carajás, Pará. Revista Brasileira de Geociências, 21: 41-50 (in Portuguese).

Monteiro, L.V.S., Xavier, R.P., Souza Filho, C.R., Moreto, C.P.N., 2014. Metalogenia da Província Carajás. In: ―Metalogenia das Províncias Tectônicas Brasileiras‖. Serviço geológico do Brasil- CPRM. 1 ed, 50p (in Portuguese).

Moreto, C.P.N., Monteiro, L.V.S., Xavier, R.P., Creaser, R.A., DuFrane, S.A., Melo, G.H.C., Delinardo da Silva, M.A., Tassinari, C.C.G., Sato, K., 2015. Timing of multiple hydrothermal events in the iron oxide–copper–gold deposits of the Southern Copper Belt, Carajás Province, Brazil. Mineralium Deposita 50, 517–546.

Mougeot, R., Respaut, J.P., Briqueu, L., Ledru, P., Milesi, J.P., Macambira, M.J.B., and Huhn S.B. 1996, Geochronological constrains for the age of the Águas Claras Formation (Carajás Province, Pará, Brazil). In: Congresso Brasileiro de Geologia, 39, Salvador, 1996. Anais. Salvador, SBG. 6:579-581.

Nelson, D.R., 1997. Compilation of SHRIM U–Pb zircon geochronology data, 1996. Geological Survey of Western Australia Record 1997/2. Geological Survey of Western Australia, Perth, 189 pp.

Nogueira, A.C.R., Truckenbrod, W., Costa, J.B.S., Pinheiro, R.V.L., 1994. Análise faciológica e estrutural da Formação Águas Claras, Pré-Cambriano da Serra dos Carajás. Simpósio de Geologia da Amazônia, Belém, Brasil, Resumos Expandidos, pp. 363–364 (in Portuguese).

Nogueira, A.C.R., Truckenbrod, W., Pinheiro, R.V.L., 2000. Storm and tide-dominated siliciclastic deposits of the Archean Águas Claras Formation, Serra dos Carajás, Brazil. 31st International Geological Congress, Rio de Janeiro, Brazil, Extended Abstracts, CD-ROM.

Oliveira, M.A., Dall'Agnol, R., Almeida, J.A.C., 2011. Petrology of the Mesoarchean Rio Maria suit and the discrimination of sanukitoid series. Lithos 137, 192–209.

Olszewski, W.J., Wirth, K.R., Gibbs, A.K., Gaudette, H.E., 1989. The age, origin, and tectonics of the Grão Pará Group and associated rocks, Serra dos Carajás, Brazil: Archean continental volcanism and rifting. Precambrian Research 42, 229–254.

Ordóñez - Calderón, J.C., Polat, A., Fryer, B.J., Gagnon, J.E., Raith, J.G., Appel, P.W.U., 2008. Evidence for HFSE and REE mobility during calc-silicate metasomatism, Mesoarchean (~3075 Ma) Ivisaartoq greenstone belt, southern West Greenland. Precambrian Res. 161, 317–340.

Pearce, J.A., 1996. A user's guide to basalt discrimination diagrams. In: Wyman, D.A. (Ed.), Trace element geochemistry of volcanic rocks: Applications for massive sulphide exploration. Geological Association of Canada Short Course Notes, 12, pp. 79–113.

Pearce, J.A., 2008. Geochemical fingerprinting of oceanic basalts with applications to ophiolite classification and the search for Archean oceanic crust. Lithos 100, 14–48.

Pearce, J.A., 2014. Geochemical fingerprinting of the Earth's oldest rocks. Geology 42, 175–176.

Pearce, J.A., Norry, M.J., 1979. Petrogenetic implications of Ti, Zr, Y and Nb variations in volcanic rocks. Contrib. Mineral. Petrol. 69, 33–47.

Pearce, J.A., Peate, D.W., 1995. Tectonic implications of the composition of volcanic arc magmas. Annu. Rev. Earth Planet. Sci. 23, 251–285.

Pearce, T.H., Gorman, B.E., and Birkett, T.C., 1977. The relationship between major element chemistry and tectonic environment of basic and intermediate volcanic rock: Earth and Planetary Science Letters, v. 36, p. 121-132.

Peate, D.W., Pearce, J.A., Hawkesworth C.J., Colley, H., Edwards, C.M.H., and Hirso, K., 1997. Geochemical variations in Vanuatu arc lavas: The role of subducted material and a variable mantle wedge composition: Journal of Petrology, v. 38, p. 523-526.

Polat, A., Hofmann, A.W., 2003. Alteration and geochemical patterns in the 3.7–3.8 Ga Isua greenstone belt, West Greenland. Precambrian Res. 126, 197–218.

Polat, A., Kerrich, R., 2001. Magnesian andesites, Nb-enriched basalts–andesites, and adakites from late Archean 2.7 Ga Wawa greenstone belts, Superior Province, Canada: implications for late Archean subduction zone petrogenetic processes. Contrib. Mineral. Petrol. 141, 36–52.

Polat, A., Hofmann, A.W., Rosing, M., 2002. Boninite-like volcanic rocks in the3.7–3.8 Ga Isua greenstone belt, West Greenland: geochemical evidence forintra-oceanic subduction zone processes in the Earth. Chem. Geol. 184,231–254.

Polat, A., Kusky, T., Li, J., Fryer, B., Kerrich, R., Patrick, K., 2005. Geochemistry of Neoarchean (ca. 2.55–2.50 Ga) volcanic and ophiolitic rocks in the Wutaishangreenstone belt, central orogenic belt, North China craton: implications for geodynamic setting and continental growth. Geol. Soc. Am. Bull. 117, 1387–1399.

Polat, A., Appel, P.W.U., Frei, R., Pan, Y., Dilek, Y., Ordóñez-Calderón, J.C., Fryer, B., Hollis, J.A., Raith, J.G., 2007. Field and geochemical characteristics of the Mesoarchean (~3075 Ma) Ivisaartoq greenstone belt, southern West Greenland: evidence for seafloor hydrothermal alteration in a supra-subduction oceanic crust. Gondwana Res. 11, 69–91.

Polat, A., Appel, P.W.U., Fryer, B., 2011. An overview of the geochemistry of Eoarchean to Mesoarchean ultramafic to mafic volcanic rocks, SW Greenland: implications for mantle depletion and petrogenetic processes at subduction zones in the early Earth. Gondwana Res. 20, 255–283.

Resende N.P., e Barbosa A.L.M., 1972, Relatório de Pesquisa de Minério de Ferro, Distrito Ferrífero da Serra dos Carajás, Estado do Pará. AMZA, Relatório Final de Pesquisa, v. 1, texto, 248 p, v. 2, mapas e seções geológicas, p. 119 (in Portuguese).

Ross, P.-S., Bedard, J.H., 2009. Magmatic affinity of modern and ancient sub-alkaline volcanic rocks determined from trace element discriminant diagrams. Can. J. Earth Science. 46, 823–839.

Rubatto, D., 2002. Zircon trace element geochemistry: partitioning with garnet and the link between U–Pb ages and metamorphism. Chem. Geol. 184, 123–138.

Rudnick, R.L., Gao, S., 2003. Composition of the continental crust. In: Rudnick, R.L. (Ed.), The Crust. Elsevier-Pergamon, Oxford, pp. 1–64.

Santos, J.O.S., Hartmann, L.A., Faria, M.S., Riker, S.R., Souza, M.M., Almeida, M.E. Mcnaughton, N.J., 2006. A compartimentação do Cráton Amazonas em províncias: avanços ocorridos no período 2000–2006. Simpósio de Geologia da Amazônia Belém. Resumos Expandidos vol. 9. SBG, CDrom, Belém (in Portuguese).

Santos, P.A., Teixeira, M.F.B., Dall'Agnol, R., Guimarães, F.V., 2013. Geologia, petrografia e geoquímica da associação Tonalito-Trondhjemito-Granodiorito (TTG) do extremo leste do subdomínio de transição, Província Carajás - Pará. Boletim do Museu Paraense Emílio Goeldi, Série Ciências da Terra 8 pp. 257–290 (in Portuguese).

Siepierski, L., 2016. Geologia, petrologia e potencial para mineralizações magmáticas dos corpos máfico-ultramáficos da região de Canaã dos Carajás, Província Mineral de Carajás, Brasil. Unpublish Ph.D. Thesis, Universidade de Brasília, p. 156 pp (in Portuguese).

Siepierski, L., Ferreira Filho, C.F., 2016. Spinifex-textured komatiites in the south border of the Carajás ridge, Selva Greenstone belt, Carajás Province, Brazil. Journal of South American Earth Sciences 66, 41–55.

Smithies, R.H., Champion, D.C., Van Kranendonk, M.J., Howard, H.M., Hickman, A.H., 2005. Modern-style subduction processes in the Mesoarchaean: geochemical evidence from the 3.12 Ga Whundo intraoceanic arc. Earth and Planetary Science Letters 231, 221-237.

Souza, S.Z., Dall'Agnol, R., Althoff, F.J., Leite, A.A.S., Barros, C.E.M., 1996. Carajás mineral province: geological, geochronological and tectonic constrasts on the Archean evolution of the Rio Maria Granite-Greenstone Terrain and the Carajás block. Symposium on Archean Terranes of South America Platform, Brasília, 1996, Extended abstracts. SBG, pp. 31–32.

Souza, Z.S., Potrel, H., Lafon, J.M., Althoff, F.J., Pimentel, M.M., Dall'Agnol, R., Oliveira, C.G., 2001. Nd, Pb and Sr isotopes of the Identidade Belt, an Archaean greenstone belt of the Rio Maria region (Carajás Province, Brazil): implications for the Archaean geodynamic evolution of the Amazonian Craton. Precambrian Research 109, 293–315.

Sun, S.-S., McDonough, W.F., 1989. Chemical and isotopic systematics of oceanic basalts: implications for mantle composition and processes. In: Saunders, A.D., Norry, M.J. (Eds.), Magmatism in the Ocean Basins. Geological Society Special Publication vol. 42, pp. 313–345.

Tavares, F.M., 2015. Evolução geotectônica do nordeste da Província Carajás. Unpublish, Ph.D. Thesis, Universidade Federal do Rio de Janeiro, p. 115 pp (in Portuguese).

Taylor, S.R., McLennan, S.M., 1985. The Continental Crust; Its composition and evolution; an examination of the geochemical record preserved in sedimentary rocks. Blackwell, Oxford. 312.

Teixeira, A.S., 2013. Geologia, Petrologia e Geocronologia do Complexo Acamadado Lago Grande: Evidencia para uma Suite Magmática Mineralizada a PGE na Província Carajás – Brasil. Unpublish, M.Sc. Thesis, Universidade de Brasília, Brazil, p. 108 pp (in Portuguese).

Teixeira, J.B.G., Eggler, D.H., 1994. Petrology, geochemistry, and tectonic setting of Archaean basaltic and dioritic rocks from the N4 iron deposit, Serra dos Carajás, Pará, Brazil. Acta Geologica Leopoldensia 17, 71–114.

Teixeira, A.S., Ferreira Filho, C.F., Giustina, M.E.S.D., Araujo, S.M., Silva, H.H.A.B., 2015. Geology, petrology and geochronology of the Lago Grande layered complex: evidence for a PGE-mineralized magmatic suíte in the Carajás Mineral Province, Brazil. Journal of South American Earth Sciences 64, 116–138.

Trendall, A.F., Basei, M.A.S., De Laeter, J.R., Nelson, D.R., 1998. SHRIMP zircon U–Pb constraints on the age of the Carajás Formation, Grão Pará Group, Amazon Craton. Journal of South American Earth Sciences 11, 265–277.

Vasquez, M.L., Carvalho, J.M.A., Sousa, C.S., Ricci, P.S.F., Macambira, E.M.B., Costa, L.T.R., 2008. Mapa Geológico do Pará em SIG. Brazilian Geological Survey - CPRM.

Wang, X.-C., Wilde, S.A., Xu, B., Pang, C.-J., 2015. Origin of arc-like continental basalts: Implications for deep-Earth fluid cycling and tectonic discrimination. Lithos 261, 5-45.

Winchester, J.A., Floyd, P.A., 1977. Geochemical discrimination of different magma series and their differentiation products using immobile elements. Chem. Geol. 20, 325–343.

Wirth K.R., Gibbs A.K., Olszewski W. 1986. U-Pb zircon ages of the Grão Pará Group and Serra dos Carajás Granite. Revista Brasileira de Geociências, 16: 195-200

Xia, L.-Q., 2014. The geochemical criteria to distinguish continental basalts from arc related ones. Earth-Science Reviews 139, 195–212.

Zuchetti, M., 2007. Rochas máficas do Supergrupo Grão Pará e sua relação com a mineralização de ferro dos depósitos N4 e N5, Carajás, PA. Unpublish. Ph.D. Thesis, Universidade Federal de Minas Gerais, Brazil, 165pp (in Portuguese).

CAPÍTULO IV – CONDERAÇÕES FINAIS

Os terrenos arqueanos são importantes registros dos primórdios da evolução da Terra e estudar estas porções antigas do planeta, como a Província Mineral de Carajás, é um grande e instigante desafio, devido à elevada complexidade em termos geológicos envolvida na sua história evolutiva. Tal complexidade geológica, relacionada a vários episódios de magmatismo, deformação, metamorfismo, metassomatismo e alteração hidrotermal durante sua evolução, dificulta o reconhecimento da estratigrafia e composição química original das sequências supracrustais presentes nestes terrenos. Além destas dificuldades comuns na maioria dos terrenos arqueanos, em regiões tropicais como o Brasil, dificuldades adicionais podem aparecer em razão da escassez de afloramentos e do estado de preservação das rochas que em várias ocasiões é bastante afetado pelo intemperismo.

Os resultados encontrados neste estudo para a Província Carajás, o maior e mais bem preservado segmento arqueano do Cráton amazônico, são de extrema valia por fornecer dados preciosos da dinâmica do planeta durante os seus primeiros anos de vida. As sequências vulcanossedimentares arqueanas carregam o registro dos diversos tipos de magmatismo ocorridos na Terra primitiva e, portanto, a determinação dos ambientes tectônicos envolvidos na formação destas sequências é fundamental para a compreensão geodinâmica da formação e amalgamação dos crátons arqueanos. A importância econômica deste terreno arqueano também deve ser destacada, tendo em vista que a Província Carajás, conhecida por hospedar numerosos depósitos de classe mundial (p. ex., Fe, Cu, Ni e Mn) é a mais importante província mineral do Brasil e uma das maiores do mundo.

Neste contexto, esta dissertação de mestrado contribuiu para uma melhor caracterização da sequência vulcanossedimentar do Grão Pará e para um melhor entendimento da evolução da Bacia Carajás, norte da Província Carajás. As principais conclusões a serem destacadas são:

- Os basaltos da Formação Parauapebas, principal unidade vulcânica da Bacia Carajás, ocorrem em sucessões de extensos derrames de lavas maciças e amigdaloidais com pelo menos 369 metros de espessura, nos quais foram identificados 11 ciclos marcados por bases maciças e topos com amígdalas e zonas de espilitização. Apesar de terem sido afetadas por alteração hidrotermal de fundo oceânico e/ou metamorfismo incipiente, estas rochas ainda preservam sua textura e mineralogia primária em diversas porções dos derrames. A texturas primária preservada é comumente intergranular ou intersertal e em alguns domínios microporfiríticos. Enquanto que a mineralogia primária essencial é composta por plagioclásio (An $_{40\text{-}55}$) e augita ($WO_{média}$ = 37,7 %; $EN_{média}$ = 41,3 %; $FS_{média}$ = 21,0 %) e os acessórios são titanita, ilmenita, pirita e magnetita. Quartzo e

álcali-feldspato ocorrem, em menor quantidade, ocupando os espaços intersticiais. A albita ($An_{0,5-8,4}$), clorita (brunsvgita), Fe-epidoto, quartzo e calcita ocorrem como fases secundárias, sendo interpretadas como produto de alteração hidrotermal de fundo oceânico e/ou metamorfismo incipiente.

- Os dados de SHRIMP U-Pb em zircão demonstram idades de cristalização magmática de 2749 ± 6,5 e 2745 ± 5 Ma para as rochas vulcânicas máficas. Estas idades são semelhantes à obtida por Gibbs *et al.* (1996), Wirth *et al.* (1996) e Olsewisk *et al*. (1996), o que confirma que a sequência vulcânica do Grupo Grão Pará se formou depois de 2,77 Ga.

- Os elementos traços Zr, Nb, Hf, Th, Ti, Y e Tb, e elementos terras raras para os basaltos são considerados imóveis neste trabalho e, portanto, representam a composição do magma original, sem ser alterados por processos secundários.

- Contaminação com crosta mais antiga é indicada pelos dados de εNd (T = 2,749) variavelmente negativos (-1.53 a -4.11), idades modelo T_{DM} entre 3.02 e 3.36 Ga, altos valores de Sr/Sr(t), enriquecimento relativo em LREE e Th, além de anomalias negativas de Nb e Ti. Entretanto, a contaminação do manto por fluidos derivados de zona de subducção, anteriormente modificado no Mesoarquenao (Colisão Rio Maria-Carajás), não pode ser descartada. As feições geoquímicas e isotópicas observadas nos basaltos são também comparáveis às características do conjunto de intrusões acamadadas de Carajás (p. ex., Complexo Luanga e Lago Grande), o que sugere que o vulcanismo basáltico da Formação Parauapebas e os complexos acamadados são coevos e podem terem sido gerados pelo mesmo evento tectônico, como proposto por Ferreira Filho *et al*. (2007).

- Os resultados obtidos nesta pesquisa indicam que os basaltos da Formação Parauapebas foram formados, preferencialmente, em um ambiente intraplaca continental sem influência de zonas de subducção. Embora, este vulcanismo possa ter sido originado pela abertura de uma bacia *back-arc* continental, a inexistência de rochas plutônicas típicas de ambiente de arcos magmáticos, contemporâneas com o magmatismo bimodal, não favorecem esta interpretação. A ausência de rochas típicas de crosta oceânica, indica que a abertura do *rift* não evoluiu até o surgimento dessa crosta e, portanto, a situação pode ser a atribuída à de um *rift* abortado, conforme sugerido por Macambira, 2003.

- A Bacia Carajás provavelmente foi formada em regime divergente relacionada a um ambiente do tipo *rift* intracontinental por volta de 2,75 Ga, fechada posteriormente por processos colisionais ocorridos, provavelmente, no Neoarqueano. O processo de rifteamento pode ser associado a um *slab breakoff* relacionado a um relaxamento da orogênese mesoarqueana (Colisão Rio Maria-Carajás) como sugerido por Tavares (2015).

REFERÊNCIAS BIBLIOGRÁFICAS

Almeida, J.A.C., Dall'Agnol, R., Oliveira, M.A., Macambira, M.J.B., Pimentel, M.M., Rämö, O.T., Guimarães, F.V., Leite, A.A.S., 2011. Zircon geochronology and geochemistry of the TTG suites of the Rio Maria granite-greenstone terrane: implications for the growth of the Archean crust of Carajás Province, Brazil. Precambrian Research 187, 201–221.

Almeida, J.A.C., Dall'Agnol, R., Leite, A.A.S., 2013. Geochemistry and zircon geochronology of the Archean granite suites of the Rio Maria granite-greenstone terrane, Carajás Province, Brazil. Journal of South American Earth Sciences 42, 103–126.

Althoff, F.J., Barbey, P., Boullier, A.M., 2000. 2.8-3.0 Ga plutonism and deformation in the SE Amazonian craton: the Archean granitoids of Marajoara (Carajás Mineral province, Brazil). Precambrian Research 104, 187–206.

Araújo, O.J.B., Maia, R.G.N., João, X.S.J., Costa, J.B.S., 1988. A megaestruturação arqueana da Folha Serra dos Carajás. In: Congresso Latino Americano de Geologia, Anais, Belém-Brazil, pp. 324-338.

Avelar VG, Lafon JM, Correia FC Jr, Macambira BEM, 1999. O magmatismo arqueano da região de Tucumã, Província Mineral de Carajás, Amazônia Oriental, Brasil: novos dados geocronológicos. Rev. Bras. Geociênc. 29: 453–460.

Barros, C.E.M., Sardinha, A.S., Barbosa, J.P.O., Macambira,M.J.B., 2009. Structure, petrology, geochemistry and zircon U/Pb and Pb/Pb geochronology of the synkinematic Archean (2.7 Ga) A-type granites from the Carajás Metallogenic Province, northern Brazil. The Canadian Mineralogist 47, 1423–1440.

Bédard H.D., Brouillette P., Madore L. & Berclaz A. 2003. Archean cratonization and deformation in the northern Superior Province, Canada: an evaluation of plate tectonic versus vertical tectonic models. Precambrian Research 127: 61-88.

Beisiegel, V.R., Bernardelli, A.L., Drummond, N.F., Ruff, A.W., Tremaine, J.W. 1973. Geologia e Recursos Minerais da Serra dos Carajás. Revista Brasileira de Geociências, 3: 215-242.

Bleeker, W., 2003. The Late Archaean Record, a Puzzle in ca. 35 Pieces. Lithos. 71 (2): 99–134

Brito Neves, BB, Cordani, UG, 1991. Tectonic evolution of South America during the Late Proterozoic. Precambrian Research, 53: 23-40.

CordaniI, U.G. & Brito Neves, B.B. 1982. The geologic evolution of South America during the Archean and Early Proterozoic. Rev. Bras. Geoc., 12: 78-88.

Cordani, U.G.; Tassinari, C.C.G.; Kawashita, K. 1984. A Serra dos Carajás como região limítrofe entre províncias tectônicas. Ciências da Terra, 9: 6-11.

Costa, J.B.S. & Hasui, Y. 1997. Evolução geológica da Amazônia. In: COSTA, M.L.C. & ANGÉLICA, R.S. (coords.) Contribuição à Geologia da Amazônia. Belém, SBG-NO, p.15-90.

Dall'Agnol, R, Teixeira, NP, Rämö, OT, Moura, CAV, Macambira, MJB, Oliveira, DC, 2005, Petrogenesis of the Paleoproterozoic, rapakivi, A-type granites of the Archean Carajás Metallogenic Province, Brazil. Lithos 80: 101–129.

Dall'Agnol, R., Oliveira, M.A., Almeida, J.A.C., Althoff, F.J., Leite, A.A.S., Oliveira, D.C., Barros, C.E.M., 2006. Archean and Paleoproterozoic granitoids of the Carajás metallogenetic province, eastern Amazonian craton. In: Dall'Agnol, R., Rosa-Costa, L.T., Klein, E.L. (Eds.), Symposium on Magmatism, Crustal Evolution, and Metallogenesis of the Amazonian Craton, Abstracts Volume and Field Trips Guide, p. 150. Belém, PRONEXUFPA/SBG-NO.

Dall'Agnol, R., Oliveira, D.C., Guimarães, F.V., Gabriel, E.O., Feio, G.R.L., Lamarão, C.N., Althoff, F.J., Santos, P.A., Teixeira, M.F.B., Silva, A.C., Rodrigues, D.S., Santos, M.J.P., Silva, C.R.P., Santos, R.D., Santos, P.J.L., 2013. Geologia do Subdomínio de Transição do Domínio Carajás – Implicações para a evolução arqueana da Província Carajás - Pará. SBG, Simpósio de Geologia da Amazônia 13. CDrom, Anais, Belém.

Dardenne, M.A., Ferreira Filho, C.F., Meirelles, M.R., 1988. The role of shoshonitic and calc-alkaline suites in the tectonic evolution of the Carajás District, Brazil. J. South Am. Earth Sci. 1, 363-372.

Dilek, Y., Polat, A., 2008. Suprasubduction zone ophiolites and Archean tectonics. Geology 36 (5), 431–432.

Dilek, Y., Furnes, H., 2011. Ophiolite genesis and global tectonics: geochemical and tectonic fingerprinting of ancient oceanic lithosphere. Geological Society of America Bulletin 123 (3/4), 387–411.

DOCEGEO e Rio Doce Geologia e Mineração, 1988. Revisão Litoestratigráfica da Província Mineral de Carajás. In: SBG-NNO (Ed.), 35º Congresso Brasileiro Geologia, Belém, Anais, pp. 11-59.

Feio, G.R.L., Dall'Agnol, R., 2012. Geochemistry and petrogenesis of the Mesoarchean granites from the Canaã dos Carajás area, Carajás Province, Brazil: implications for the origin of Archean granites. Lithos 154, 33-52.

Feio, G.R.L., Dall'Agnol, R., Dantas, E.L., Macambira, M.J.B., Santos, J.O.S., Althoff, F.J., Soares, J.E.B., 2013. Archean granitoid magmatism in the Canaã dos Carajás area: implications for crustal evolution of the Carajás province, Amazonian craton, Brazil. Precambrian Res. 227, 157-185.

Ferreira Filho, C.F., Cançado, F., Correa, C., Macambira, E.M.B., Siepierski, L., Brod, T.C.J., 2007. Mineralizações estratiformes de EGP-Ni associadas a complexos acamadados em Carajás: os exemplos de Luanga e Serra da Onça. Publitec Gráfica & Editora, Contribuições à Geologia da Amazônia vol. 5, pp. 01–14.

Figueiredo e Silva, R.C.F. 2004. Caracterização petrográfica e geoquímica de jaspilitos e minérios de ferro dos depósitos N1, N4W, N4E e N5E, Província Mineral Carajás, Pará: implicações para a mineralização de ferro. Dissertação de mestrado, Instituto de Geociências, Universidade Federal de Minas Gerais, 151 p.

Furnes, H., Dilek, Y., de Wit, M., 2015. Precambrian greenstone sequences represent different ophiolite types. Gondwana Research, v. 27, Issue 2, Pages 649-685.

Galarza, M.A.; Macambira, M.J.B., 2002. Geocronologia e evolução crustal da área do depósito de Cu-Au Gameleira, Província Mineral de Carajás (Pará), Brasil. Revista do Instituto de Geociências da USP, 2:143-159 (in Portuguese).

Gibbs, A.K., Wirth, K.R., Hirata, W.K., Olszewski Jr., W.J., 1986. Age and composition of the Grão Pará Group volcanics, Serra dos Carajás. Rev. Bras. Geoc. 16, 201-211.

Gioia, S.M.C.L., Pimentel, M.M., 2000. The Sm-Nd isotopic method in the geochronology laboratory of University of Brasilia. An. Acad. Bras. Ciênc. 72, 219-245.

IBGE, 1999. Carta do Brasil ao Milionésimo digital. Rio de Janeiro, IBGE, SIG. Escala: 1:1.000.000.

Lafon, J.M., Macambira, M.J.B., Pidgeon, R.T., 2000. Zircon U–Pb SHRIMP dating of Neoarchean magmatism in the southwestern part of the Carajás Province (eastern

Amazonian Craton, Brazil). 30th International Geological Congress, Abstract Volume, CD-ROM.

Lemos V.P. & Villas R.N.N. 1983. Alteração supergênica das rochas básicas do Grupo Grão Pará. Implicações sobre a gênese do depósito de bauxita de N-5, Serra dos Carajás. Rev. Bras. Geociências, 13(3):165-177.

Lindenmayer, Z.G., Laux, J.H., Teixeira, J.B.G. 2001. Considerações sobre a origem das Formações Ferríferas da Formação Carajás, Serra dos Carajás. Revista Brasileira de Geociências, 31: 21-28.

Lobato, L.M., Rosière, C.A., Silva, R.C.F., Zucchetti, M., Baars, F.J., Seoane, J.C.S., Rios, F.J., Pimentel, M., Mendes, G.E. e Monteiro, A.M., 2005, A mineralização hidrotermal de ferro da Província Mineral de Carajás - controle estrutural e contexto na evolução metalogenética da Província. In: Marini, J.O.; Queiróz, E.T.; Ramos, W.B. (eds.), Caracterização de distritos mineiros da Amazônia. DNPM-CT-Mineral-ADIMB, 25–92.

Hasui, Y.; Haraly, N.L.E.; Schobbenhaus, C. 1984. Elementos geofísicos e geológicos da região amazônica: subsídios para o modelo geotectônico. In: Simpósio de geologia da Amazônia 2, Manaus. Anais, SBG-NO, p.129-148.

Hirata, W.K. 1982. Geologia Regional. In: Bernardelli, A.L. (coord.), Província Mineral de Carajás – Pará: depósitos de ferro, manganês, cobre, ouro, níquel e bauxita. SBG, Simpósio de Geologia da Amazônia, 1, Belém, Anexo aos Anais, p. 9-20.

Huhn, S.R.B., Santos, A.B.S., 1988. O terreno granito-greenstone da região de Rio Maria-Sul do Para. In: Amaral, A.F., Ledsham, E.J., Gouveia, J.L., Martins, F. (Eds.), SBG-NNO, 35º Congresso Brasileiro de Geologia. Belém, Anais, vol. 35, pp. 1438-1452.

Huhn, S.R.B., Santos, A.B.S., Amaral, A.F., Ledshan, E.J., Gouveia, J.L., Martins, L.P.B., Montalvão, R.G.M., Costa, V.G. 1988. O terreno "granito-greenstone" da região de Rio Maria – sul do Pará. In: SBG, Congresso Brasileiro de Geologia, 35, Belém, Anais, 3: 1438-1452

Huhn, S.R.B., Souza, C.I. de J., Albuquerque, M.C., Leal, E.D., Brustolin, V. 1999. Descoberta do depósito de Cu (Au) Cristalino: geologia e mineralização associada – Região da Serra do Rabo – Carajás – Pará. In: SBG, Simpósio de Geologia da Amazônia, 6, Manaus, Boletim, p. 140-143

Huston D.L, Pehrsson, S., Eglington, B.M., & Zaw, K., 2010. The geology and metallogeny of volcanic hosted massive sulfide deposits: Variations through geologic time and with tectonic setting. Economic Geology, v. 105, p. 571−591.

Jenner, F.E., Bennett, V.C., Yaxley, G., Friend, C.R.L., and Nebel, O., 2013. Eoarchean within-plate basalts from southwest Greenland: Geology, v. 41, p. 327–330, doi:10.1130/G33787.1.

Macambira, J. B. 2003. O ambiente deposicional da Formação Carajás e uma proposta de modelo evolutivo para a Bacia Grão-Pará. Tese de Doutorado. Campinas, Unicamp, 214p

Macambira, M.J.B., Lancelot, J. 1996. Time constraints of the Archean Rio Maria crust, Southeastern Amazonian Craton, Brazil. Int Geol Rev, 38: 1134–1142

Machado, N., Lindenmayer, Z.G., Krogh, T.E., Lindenmayer, D., 1991. U–Pb geochronology of Archean magmatism and basement reactivation in the Carajás area, Amazon shield, Brazil. Precambrian Research 49, 329–354.

Meireles, E.M., Hirata, W.K., Amaral, A.F., Medeiros Filho, C.A., Gato, W.C. 1984. Geologia das folhas Carajás e Rio Verde, Província Mineral de Carajás, Estado do Pará. In: SBG, Congresso Brasileiro de Geologia, 33, Rio de Janeiro, Anais, 5: 2164-2174.

Meirelles, M.R. 1986. Geoquímica e petrologia dos jaspilitos e rochas vulcânicas associadas, Grupo Grão-Pará, Serra dos Carajás - PA. Brasília. 150 p. (Dissertação de Mestrado, IG/UnB).

Meirelles, M.R. & Dardenne, M.A. 1991. Vulcanismo basáltico de afinidade shoshonítica em ambiente de arco arqueano, Grupo Grão-Pará, Serra dos Carajás-Pará. Revista Brasileira de Geociências, 21:41-50.

Nogueira, A.C.R., Truckenbrod, W., Costa, J.B.S., Pinheiro, R.V.L., 1994. Análise faciológica e estrutural da Formação Águas Claras, Pré-Cambriano da Serra dos Carajás. Simpósio de Geologia da Amazônia, Belém, Brasil, Resumos Expandidos, pp. 363–364.

Nogueira, A.C.R., Truckenbrod, W., Pinheiro, R.V.L., 2000. Storm and tide-dominated siliciclastic deposits of the Archean Águas Claras Formation, Serra dos Carajás, Brazil. 31st International Geological Congress, Rio de Janeiro, Brazil, Extended Abstracts, CD-ROM.

Oliveira, M.A., Dall'Agnol, R., Almeida, J.A.C., 2011. Petrology of the Mesoarchean Rio Maria suit and the discrimination of sanukitoid series. Lithos 137, 192–209.

Olszewski, W.J., Wirth, K.R., Gibbs, A.K., Gaudette, H.E., 1989. The age, origin, and tectonics of the Grão-Pará Group and associated rocks, Serra dos Carajás, Brazil: Archean continental volcanism and rifting. Precam. Res. 42, 229-254.

Pinheiro RVL & Holdsworth RE. 2000. Evolução tectonoestratigráfica dos sistemas transcorrentes Carajás e Cinzento, Cinturão Itacaiúnas, na borda leste do Craton Amazônico, Pará. Rev. Bras. Geoc., 30(4): 597-606.

Rosière C.A., Baars F.J., Seoane J.C.S, Lobato. L.M., Silva L.L.da, Souza S.R.C.de, Mendes G.E. 2006. Structure and iron mineralisation of the Carajás Province. Applied Earth Science: IMM Transactions section B, 115: 126-133.

Santos, JOS, 2003. Geotectônica dos Escudos das Guianas e Brasil-Central, in Geologia, Tectônica e Recursos Minerais do Brasil (eds: L A Bizzi, C Schobbenhaus, R M Vidotti e J H Gonçalves), pp 169-226 (Companhia de Pesquisa e Recursos Minerais: Brasília).

Santos, J.O.S., Hartmann, L.A., Faria, M.S., Riker, S.R., Souza, M.M., Almeida, M.E. Mcnaughton, N.J., 2006. A compartimentação do Cráton Amazonas em províncias: avanços ocorridos no período 2000–2006. Simpósio de Geologia da Amazônia Belém. Resumos Expandidos vol. 9. SBG, CDrom.

Siepierski, L., Ferreira Filho, C.F., 2016. Spinifex-textured komatiites in the south border of the Carajás ridge, Selva Greenstone belt, Carajás Province, Brazil. Journal of South American Earth Sciences 66, 41–55.

Smithies, R.H., Champion, D.C., Van Kranendonk, M.J., Howard, H.M. and Hickman A.H., 2005. Modern-style subduction processes in the Mesoarchean: geochemical evidence from 3.12 Ga Whudo intracratonic arc: Earth and Planetary Science Letters, v. 231, pp. 221-237.

Souza, Z.S., Potrel, H., Lafon, J.M., Althoff, F.J., Pimentel, M.M., Dall'Agnol, R., Oliveira, C.G., 2001. Nd, Pb and Sr isotopes of the Identidade Belt, an Archaean greenstone belt of the Rio Maria region (Carajás Province, Brazil): implications for the Archaean geodynamic evolution of the Amazonian Craton. Precambrian Research 109, 293–315.

Tassinari, C.C.G.; Bettencourt, J.S.; Geraldes, M.C.; Macambira, M.J.B.; Lafon, J.M. 2000. The Amazonian Craton. In: CORDANI, U.G.; MILANI, E.J.; FILHO, A.T.; CAMPOS, D.A. (eds.) Tectonic Evolution of South America. Rio de Janeiro, 31º International Geological Congress, SBG. p. 41-95.

Tassinari, C.C.G., Macambira, M.J.B., 2004. A evolução tectônica do Cráton Amazônico. In: Mantesso-Neto, V., Bartorelli, A., Carneiro, C.D.R., Brito Neves, B.B. (Eds.), Geologia do Continente Sul-Americano: Evolução da Obra de Fernando Flávio Marques de Almeida, pp. 471–485.

Tavares, F.M., 2015. Evolução geotectônica do nordeste da Província Carajás. Tese de doutorado, Universidade Federal do Rio de Janeiro, p. 115 pp.

Teixeira, A.S., Ferreira Filho, C.F., Giustina, M.E.S.D., Araujo, S.M., Silva, H.H.A.B., 2015. Geology, petrology and geochronology of the Lago Grande layered complex: evidence for a PGE-mineralized magmatic suíte in the Carajás Mineral Province, Brazil. Journal of South American Earth Sciences 64, 116–138.

Teixeira, J.B.G., Eggler, D.H., 1994. Petrology, geochemistry, and tectonic setting of Archaean basaltic and Dioritic rocks from the N4 iron deposit, Serra dos Carajás, Pará, Brazil. Acta Geol. Leopoldensia 17, 71-114.

Teixeira W, Tassinari CCG, Cordani UG, Kawashita K (1989) A review of the geochronology of the Amazonian Craton: tectonic implications. Precamrian Res 42: 213–227

Trendall, A.F., Basei, M.A.S., De Laeter, J.R., Nelson, D.R., 1998. SHRIMP zircon U–Pb constraints on the age of the Carajás Formation, Grão Pará Group, Amazon Craton. Journal of South American Earth Sciences 11, 265–277.

Van Kranendonka M. J., Ivanica T. J., Wingatea M. T. D., Kirklanda C. L., Wychea S., 2013. Long-lived, autochthonous development of the Archean Murchison Domain, and implications for Yilgarn Craton tectonics. Precambrian Research 229 (2013) 49–92.

Vasquez, M.L., Carvalho, J.M.A., Sousa, C.S., Ricci, P.S.F., Macambira, E.M.B., Costa, L.T.R., 2008. Mapa Geológico do Pará em SIG. CPRM.

Wirth K.R., Gibbs A.K., Olszewski W. 1986. U-Pb zircon ages of the Grão-Pará Group and Serra dos Carajás Granite. Revista Brasileira de Geociências, 16: 195-200.

Zuchetti, M., 2007. Rochas máficas do Supergrupo Grão Pará e sua relação com a mineralização de ferro dos depósitos N4 e N5, Carajás, PA (Tese de doutorado Nº 7). Universidade Federal de Minas Gerais, Brasil, p. 165.

ANEXO – FICHA PETROGRÁFICAS REPRESENTATIVAS